LORAN-C PHASELAG INVESTIGATION

DAVID WELLS
DEREK A. DAVIDSON

March 1983

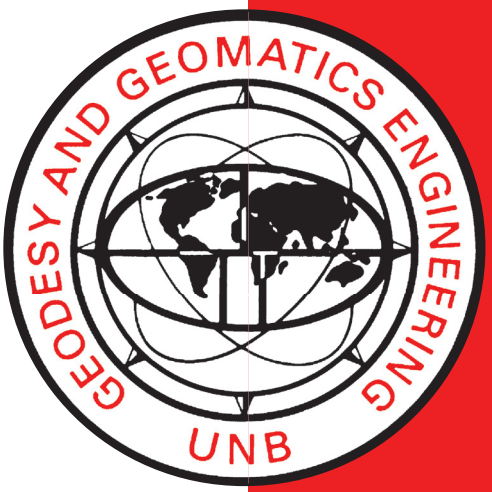

TECHNICAL REPORT
NO. 96

PREFACE

In order to make our extensive series of technical reports more readily available, we have scanned the old master copies and produced electronic versions in Portable Document Format. The quality of the images varies depending on the quality of the originals. The images have not been converted to searchable text.

LORAN-C

PHASE LAG INVESTIGATION

by

David E. Wells

Derek A. Davidson

Department of Surveying Engineering
University of New Brunswick
P.O. Box 4400
Fredericton, N.B.
Canada
E3B 5A3

March 1983

PREFACE

This is the final report of work performed under a contract number OAE82-00037 entitled, "LORAN-C Phaselag Investigation", funded by the Bedford Institute of Oceanography. The Scientific Authority for this contract was R.M. Eaton.

Part of the work contained herein was funded by a strategic research grant entitled "Marine Geodesy", from the Natural Sciences and Engineering Research Council of Canada.

Much insight into the application of stochastic modelling and least-squares prediction was gained during a six months' visit to UNB of Prof. Dr. Ing. Heribert Kahmen, from the University of Hanover. While not directly concerned with the studies involved in this contract, his work is relevant to the general problem of ASF prediction. A report on this topic is included as Appendix IV to this report.

TABLE OF CONTENTS

LIST OF TABLES

LIST OF FIGURES

CHAPTER 1

INTRODUCTION

In order to use LORAN-C measurements for positioning, the phaselag of the low radiofrequency wave must be taken into account. In particular, to produce accurate LORAN-C lattices for hydrographic charts, the phaselag must be accurately predicted in the lattice computations. In order to develop adequate phaselag prediction models for latticing hydrographic charts along the Atlantic coast of Canada, a series of special LORAN-C calibration cruises have been held to collect data on which to base such a model.

This report summarizes the results of a project whose objectives were to

(a) assemble a consistent data base from existing LORAN-C calibrations. This data base should enable the verification of chart lattices and the production of correction diagrams, and the improvement of the model used to predict phaselags.

(b) Study improved techniques for predicting LORAN-C phaselags.

Let us introduce definitions of the basic quantities dealt with in this report. Phaselags are the difference in phase between the real LORAN-C wave and a reference wave travelling at a specified constant velocity. The constant velocity used can be the vacuum speed of light, taken in this work to be 299 792.5 km/s. The real wave is not travelling in a vacuum, having an atmosphere through which to travel. At the LORAN-C frequency of 100 KHz the earth over which the wave travels also has a retardation effect. Assumptions can be made of an over-water path, and standard atmospheric conditions [Brunavs, 1977; Gray, 1980] to model a travelling wave. The difference between this over-water wave and the real wave is known as the

additional secondary factor (ASF). The real wave should still, in general, lag behind the modelled over-water wave since the real wave is slowed down by unmodelled land effects. If land slows the real wave, then the ASF will be positive.

Observed ASFs are the difference between an actual LORAN-C observation at a known (calibration) point, and a model of that observation assuming an over-water travel path between the LORAN transmitters and the calibration point. Predicted ASFs are the difference between a modelled LORAN-C observation which incorporates the land path, using Millington's method [Bigelow, 1965], and a model of the same LORAN-C observation which assumes an all over-water travel path. Residual ASFs are observed minus predicted ASFs. The better the ASF predictions, the closer the residual ASFs should be to zero.

Chapter 2 of this report summarizes the Atlantic Canada LORAN-C calibration data base, and how it is organized and formatted. An outline is given of the FORTRAN programs which can access this data base.

Chapter 3 considers LORAN-C ASF prediction. The observed ASFs are shown and described. The assumptions used to predict ASFs are described, and residual ASF results are described.

Chapter 4 presents the conclusions from this work, and recommendations for future work.

CHAPTER 2

LORAN-C ASF DATA BASE

Development of the LORAN-C ASF data base consisted of four steps:

(a) Cataloguing the calibration data available.

(b) Developing the data base format.

(c) Assessing and verifying the observations to be placed in the data base.

(d) Preparing software to be used in conjunction with the data base.

In this chapter we describe the work done on each of these steps.

2.1 Catalogue of LORAN-C ASF Data

LORAN-C calibration cruises carried out in the Atlantic region are listed in Table 2.1. Other Canadian calibration data has been collected on land, and in other areas, such as around Vancouver Island, and Lakes Huron, Erie, and Ontario. This project concentrated on the Atlantic region calibration cruise data, which involves the largest amount of data, and would allow checks on the consistency of both the data and ASF prediction models.

2.2 LORAN-C ASF Data Base Format

One of the main parts of this project has been to compile a consistent data base of the available observations. This data base is a sequentially accessed set of files, with a format capable of being used for time difference (TD) observations, as well as for time of arrival (TOA) observations. The format has been chosen to make the data base convenient for data verification, further ASF prediction research, chart lattice

	Year		Ship	Area	Main Observation Type	Fix Method	LORAN Stations	Data Points
1	1978	297 300	NARWHAL	Fundy	TOA	MRS	9930 MXY 9960 X	718
2	1978	302 303	NARWHAL	Halifax	TOA	MRS	9930 MXY 9960 X	223
3	1978	304 304	NARWHAL	Chedabucto	TOA	MRS	9930 MXY 9960 X	80
4	1978	309 312	NARWHAL	PEI	TD	Sextant	5930 X Y	336
5	1978	310 313	NARWHAL	Northumberland.S			NOT YET AVAILABLE	
6	1978	314 314	NARWHAL	St. Mary's Bay	TOA	MRS	9930 MXY 9960 X	0
7	1978	297 300	NARWHAL	Fundy	TOA	MRS	9960 MWX 9930 Y	664
8	1978	302 303	MARWHAL	Halifax	TOA	MRS	9960 MWX 9930 Y	229
9	1978	304 307	NARWHAL	Chedabucto	TOA	MRS	9960 MWX 9930 Y	669
10	1978	310 313	NARWHAL	Northumberland.S			NOT YET AVAILABLE	
11	1978	314 314	NARWHAL	St. Mary's Bay	TOA	MRS	9960 MWX 9930 Y	70
12	1979	304 310	MAXWELL	Mahone Bay	TOA	MRS	9960 MWX 7930 Z	1555
13	1980	110 117	MAXWELL	Fundy	TOA	MRS	5930 MXY 9960 M	1136
14	1980	157 164	BAFFIN	Fortune Bay	TD	MRS	5930 X Y	93
15	1980	193 196	MAXWELL	Placentia	TOA	MRS	5930 MXY 9960 X	545
16	1980	294 299	PANDORA	Canso Bay	TOA	MRS	5930 MXY 9960 X	1062
17	1980	302 302	PANDORA	Halifax	TOA	MRS	5930 MXY 9960 M	258

TABLE 2.1

LORAN-C ASF Cruises in Atlantic Canada

production and lattice checking. Access programs to this data base have been produced and both data and accompanying programs have been designed to be easily transferable between different types of computers.

The data base is composed of a number of files of 80 column fixed length records. Each file contains data for a convenient area and date, and is such that the same methods were used for all data points within the file. Typically, one cruise is given in one file, but, for example, the October 1980 cruise covered two specific areas: Canso Bay and Halifax. In this case each area is allocated its own file. Similarly, different observation types in the same cruise would dictate different files on the data base.

The first file in the data base is a header file, giving an index to the cruise files, notes on the observations including any necessary corrections, information on the ASF computation used, the LORAN-C stations, and the cruise files data format. Appendix I lists this header file and contains details of the data format, which need not be reproduced here.

The LORAN-C data base can be stored on a magnetic tape with the first file being the header file, and the cruise files following consecutively as given in the index on the header file. This information can be distributed as requested in any of the standard magnetic tape densities (typically 800 or 1600 bpi) and either of the two standard character formulations, ASCII or EBCDIC.

2.3 LORAN-C Observations

All available data covering the Atlantic region has been compiled in the data base. This involves cruises which used both TOA and TD observations between 1978 and 1980. It has, however, been TOA data which has been used at the primary stages of the investigation to derive and check

models for predicting ASF. This is because TOA observations allow separation of the ASF attributed to the two wave travel paths from the master station and the respective secondary stations to the receiver position. Since the two wave paths can have entirely different characteristics, more can be learned about the ASF by considering the two paths separately. The TD data can then be used to check and verify the ASF prediction models produced using the TOA data.

An assesment of the TOA data in the data base is provided in Chapter 3, supported by the plots in Appendices II and III.

2.4 ASF Computer Programs

In parallel with producing a data base of the LORAN-C calibration data, computer programs have been prepared. This has mainly involved converting programs written at the Bedford Institute of Oceanography, which run on the BIO CDC computer, so that they will also run on the IBM computer at UNB. This includes software to predict ASF using Johler's formula [Johler et al., 1956], and using Brunavs' polynomial approximation of Johler's formula [Brunavs, 1977]. Programs using Millington's method [Bigelow, 1965] have also been prepared, including the use of a digitized coastline to determine the land-sea boundaries, and thus enable the derivation of a predicted ASF with over-land paths. It is these predicted ASFs which have been compared with the observed ASFs to indicate the validity of various conductivity models.

CHAPTER 3

LORAN-C ASF PREDICTION

3.1 Observed ASF

Observed additional secondary factor (ASF) values derived from TOA measurements made during the 1979 and 1980 field seasons are plotted in Appendix II. This chapter gives a cruise-by-cruise summary of the ASFs produced by the LORAN-C stations observed on each of these cruises. The cruise numbers refer to Table 2.1. Figure 3.1 shows the general area of each cruise.

Cruise 12: MAXWELL, Mahone Bay

Seneca Transmitter

A varied land and sea path of approximately 550 nautical miles. ASF range = 4.40 to 6.50 microseconds. Recovery effect is generally shown. Some values not consistent with adjacent values.

Caribou Transmitter

A varied land and sea path of approximately 230 nautical miles. ASF range = 2.50 to 4.50 microseconds. Recovery effect is shown.

Nantucket Transmitter

Approximately 500 nautical miles of seawater, although to the northern area may contain land path effects. ASF range = -0.20 to 1.10 microseconds. There should not be negative values, but these negative values are in the accuracy range of $\pm$ 0.30 microseconds.

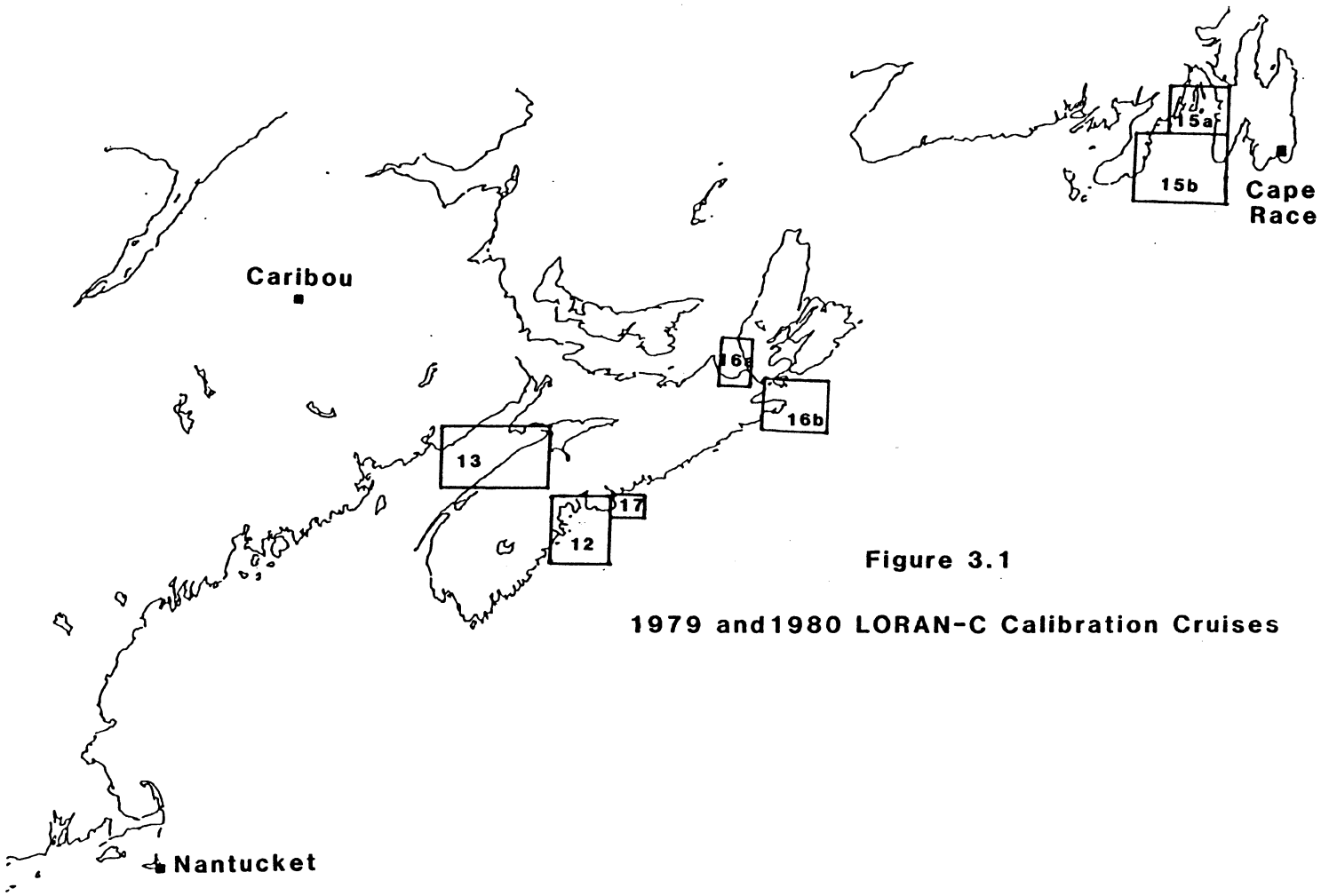

Figure 3.1

1979 and1980 LORAN-C Calibration Cruises

Cruise 13: MAXWELL, Fundy Bay

Caribou Transmitter

Approximately 130 nautical miles of land, and up to 30 miles of sea. ASF range 1.70 to 2.50 microseconds. Recovery effect is shown: 2.13 to 1.70 microseconds across the Bay.

Nantucket Transmitter

Approximately 320 nautical miles of seawater path, except some points to the south which may have land path effects. ASF range -0.30 to +0.90. The higher values are to the south which will experience land path effects. The negative values reflect the fix accuracy.

Cape Race Transmitter

A varied land and sea path of approximately 550 nautical miles. ASF range 2.40 to 3.00 microseconds. No apparent recovery effect.

Cruise 15: MAXWELL, Placentia

Caribou Transmitter

A complicated land and sea path of approximately 550 nautical miles. ASF range 1.30 to 2.00 microseconds.

Nantucket Transmitter

Overwater path of approximately 700 nautical miles, although the Nova Scotia shoreline may give land path effects. ASF range -0.60 to +0.40.

Cape Race Transmitter

A complicated land and sea path of approximately 70 nautical miles. ASF range 0.80 to 1.10.

Cruise 16: PANDORA, Canso Bay

Caribou Transmitter

A complicated 320 nautical mile land and sea path. ASF range +1.80 to +3.70 microseconds. Higher values show where the paths involve more land. Adjacent points differ by up to 0.75 microseconds.

Nantucket Transmitter

A path of approximately 500 nautical miles, with completely over-water paths to the south. ASF range -0.50 to +1.60. The higher values show where the paths traversed land. Adjacent points often differ by up to 0.70 microseconds.

Cape Race Transmitter

350 nautical miles of mainly sea path, but complicated effects of Cape Breton except for the south of the area. ASF range +0.30 to +1.50. The higher numbers are to the north, showing the effect of passing over the land. Adjacent points often differ, but to within 0.30 microseconds.

Cruise 17: PANDORA, Halifax

Caribou Transmitter

A 250 nautical mile path involving land, the 30 mile Bay of Fundy and approximately 80 miles of Nova Scotia. ASF range +3.50 to +3.70. The recovery effect is shown.

Nantucket Transmitter

Approximately 370 nautical miles of sea water path, although the Nova Scotia coastline may introduce some effects. ASF range 0.40 to 0.50 microseconds.

Cape Race Transmitter

Approximately 500 nautical miles of sea water path, but complicated by passing over, or parallel to, 150 miles of the Nova Scotia coastline. ASF range close to 1.20 microseconds. Approximately the same value throughout the area, which should be the case if far from passing over a coastline.

3.2 Predicted ASF

The computed ASFs have been derived using Millington's method [Bigelow, 1965] and Brunavs' [1977] approximating polynomial. Values of conductivity are then assumed for the land and sea paths. A sea conductivity of 4.0 mho/m has been used, and, for initial investigation into the cruise data, a land conductivity has been used of 0.0015 mho/m.

The header file section "Phase Lag Computation", Appendix I, contains details of the constants assumed in the formulation:

atmospheric refractivity, N = 338

vertical lapse factor of the atmosphere, α = 0.75

permittivity of the land E_2 = 15.0

permittivity of sea water E_2 = 81.0

3.3 Residual ASF

Residual ASF values corresponding to each of the observed values plotted in Appendix II were computed by subtracting the corresponding predicted ASF values (computed as in Section 3.2). The results are plotted in Appendix III.

Initially all predicted ASFs were derived assuming all land has a conductivity (σ_ℓ) of 0.0015 mho/m. In some cruise areas it was considered that further insight could be obtained if a different land conductivity value was considered. For these areas conductivity values of 0.001 or 0.002 mho/m were used to compute residual ASFs, and the results are plotted in Appendix IV. The units of observed and residual ASF discussed here are microseconds.

Cruise 12: MAXWELL, Mahone Bay

Seneca Transmitter

(σ_ℓ = 0.0015) In general the residuals are good, reducing observed ASFs of 4.00 to residuals of 0.10. The inconsistent values, however, are still present at about 2.50.

Caribou Transmitter

(σ_ℓ = 0.0015) Good reduction of 2.50 observed ASF to -0.11 residual ASF. A line to the northeast of the cruise area gives anomalies of 1.45, suggesting poor fixing since all transmitters have problems along this line.

Nantucket Transmitter

(σ_ℓ = 0.0015) Good reductions of approximately 1.00 observed ASF to 0.00 residual ASF. Similar to the other transmitters, part of the line to the northeast of the area shows anomalies.

Cruise 13: MAXWELL, Fundy Bay

Caribou Transmitter

(σ_ℓ = 0.0015) The residual ASFs are reduced from approximately 2.0 to the range -0.40 to 0.13. The eastern part of the cruise shows the best results, being approximately zero.

(σ_ℓ = 0.002) Using a land conductivity of 0.002 mho/m reduces the western part of the cruise to approximately zero. This suggests that the west of New Brunswick has a land conductivity of about 0.002, while the eastern paths have land conductivities of about 0.0015. These estimates are for land between Caribou and the cruise area, and do agree quite well with the results of Brunavs [1980] where he gives the southwest of New Brunswick as having 0.002 mho/m conductivity, and areas to the east with 0.001 mho/m. It is possible that the areas of 0.001 and 0.002 give results similar to a single value of 0.0015. One should, however, be cautious in giving these conclusions as the observation differences between the different conductivity values (i.e., -0.30 to 0.00, and 0.00 to +0.20) are within the quoted accuracy limits of the field work.

Nantucket Transmitter

(σ_ℓ = 0.0015) The northwest area of the cruise is over water: observed and residual ASFs are the same at approximately -0.20. The southwest area of the cruise has observed ASFs of about 0.20 reduced to about -0.20. The northeast area of the cruise reduces 0.75, 1.00 to -0.15, 0.03.

(σ_ℓ = 0.002) A higher land conductivity has minimal effect in the southwest area of the cruise (adding +0.06 to some residuals). In the northeast area the longer overland path of northern Nova Scotia

reduces the absolute value of residual from ≃ -0.15 to ≃ -0.03. These variations are well within the accuracy limits of 0.30.

Cape Race Transmitter

(σ_ℓ = 0.0015) Observed ASFs are in the range 2.30 to 3.00, with the lower values to the south. Residual values are about 0.90 to the north, and 0.20 to the south. The corrections in all areas are thus the same.

(σ_ℓ = 0.001) The lower conductivity reduces the residual ASFs by approximately 0.20, thus improving the results, giving residuals of about 0.70 to the north, and 0.00 to the south.

Cruise 15: MAXWELL, Placentia

Caribou Transmitter

(σ_ℓ = 0.0015) Observed ASFs of 2.00 to 1.50 are reduced to -0.30 to -0.50. It is possible an offset of -0.4 exists in the observations, or that a land conductivity of 0.002 should be implied on the landpath, which traverses central New Brunswick, Prince Edward Island, and the Burin Peninsula of Newfoundland.

Nantucket Transmitter

(σ_ℓ = 0.0015) This transmitter gives problems in this cruise, from observed ASFs of ≃ -0.30 giving residual ASFs of about -0.76. The overwater path (residuals and observed) ASFs are about -0.70, sugesting an offset of this magnitude. The long range from this transmitter could make an atmospheric scale error of 0.40 (see Appendix V, Kahmen [1982]).

Cape Race Transmitter

(σ_ℓ = 0.0015) Observed ASFs are reduced from the range 1.00, 1.60 to the range 0.10, 0.30. The ranges involved are short, being approximately 60 nautical miles.

Cruise 16: PANDORA, Canso Bay

Caribou Transmitter

(σ_ℓ = 0.0015) In general the residual ASFs are reasonable, being reduced from 1.9 to -0.4 north of the straits, and from 3.0 to 0.4 south of the straits. Adjacent points in the southern area do show possible fix-related problems with up to 0.7 difference in residual ASF.

Nantucket Transmitter

(σ_ℓ = 0.0015) To the north of the Strait of Canso the ASFs are reduced from observed values of 1.5 to residuals of -0.30. The wave path for this area traverses Nova Scotia. To the south of the straits, some points have completely overwater paths, giving about -0.4 for both observed and residual ASF. In the parts of the southern area which have landpath effects, the observed ASFs are in the range of about -0.2 to 0.7. The lower numbers are in the areas which have the least landpath. The residuals have values in the range -0.2 to 0.0.

Cape Race Transmitter

(σ_ℓ = 0.0015) North of the Strait of Canso observed ASF values of about 1.4 are reduced to residual ASF values of about 0.2. South of the straits there are some anomalous points, but generally observed ASFs of about 0.6 are reduced to about 0.0.

Cruise 17: PANDORA, Halifax

Caribou Transmitter

(σ_ℓ = 0.0015) Observed ASFs in the range 3.8 to 3.10 are reduced to residual ASFs in the range 0.9 to 0.6.

(σ_ℓ = 0.001) The lower conductivity value gives residual ASFs in the range 0.3 to 0.1.

Nantucket Transmitter

(σ_ℓ = 0.0015) The south of this area has an overwater path, giving observed and residual ASFs of about 0.35. The paths which experience some land have observed ASFs of about 0.5 reduced to about 0.45. This suggests a possible offset of +0.4.

Cape Race Transmitter

(σ_ℓ = 0.0015) Observed ASFs of about 1.2 are reduced to residual ASFs of about 0.6.

(σ_ℓ = 0.001) The increased conductivity has some effect reducing the residual ASF to about 0.5. There may be problems due to the paths travelling parallel to the Nova Scotia coastline giving effects which are not modelled. Alternatively, there may be an offset in the observations.

CHAPTER 4

CONCLUSIONS AND RECOMMENDATIONS

4.1 Results

A data base of LORAN-C calibration cruises within the Maritimes has been produced. A header file (Appendix I) is the first file, describing the contents and format of the cruise files. Each cruise, or specific area within a cruise, then forms a file within the data base.

Observed ASFs have been produced for all the 1979 and 1980 TOA cruises. Plots have also been produced giving the residual between the observed and predicted ASFs. The predicted ASFs were derived using an assumed homogeneous conductivity of 0.0015 mho/m for land.

Progress has been made in improving the model used to predict ASF. Some insight has been gained into the anomalous effect at low conductivities. Literature searches have revealed indications that the effective surface impedence technique may be more useful to use than Millington's method, when modelling variations in conductivity along the propagation paths. We consider these two topics in the following sections.

4.2 Investigation of the Low Conductivity Problem

Johler's [1956] model for ASF includes an anomalous effect at conductivities lower than 0.001 mho/m: the LORAN-C wave is modelled as gaining speed as conductivity decreases (the phaselag becomes smaller with decreasing conductivity). This is probably not the physical situation [CRPL, 1977]. There are two recognized possible causes for this problem: numerical integration of series formulae needed for Johler's equation [Brunavs, 1977], and the restriction of using a constant permittivity for

land paths.

Some consideration has been given to using lower land permittivity values, since Schelkunoff [1963, p. 29] indicates values other than the standard 15.0 electrostatic units (esu).

Land Surface Type	Quartz	Sand	Dry Soil	Wet Soil	Sea Water
Permittivity	4.5	10.0	10.0	30.0	78.0

TABLE 4.1

Permittivity Values (in esu) for Various Surface Types.

Johler used 15.0 as land permittivity. Using 4.5 reverses the anomalous trend.

	Conductivity (mho/m)		
Permittivity	0.01	0.001	0.0001
30	1242.2	2311.8	2010.2
15	1242.9	2377.7	2221.4
4.5	1243.3	2424.1	2485.3

TABLE 4.2

Johler's Model for Phaselag with Varying Permittivity. Table shows phaselag in metres at 1000 km.

More work is required to investigate the effect of the series formulae in Johler's algorithm, and to give more conclusive results on variations in the assumed land conductivity and permittivity.

Johler's series formulation may not be the optimum method: it was developed prior to the widespread use of modern electronic computers. One

stage in Johler's formulation involves the transformation of Watson [Bremmer, 1949, p. 31 et seq] which leads to the residue series. The need for this stage in the algorithm development should be evaluated.

4.3 Effective Impedence Calculation of Phase Lag

Millington's method is an empirical way of modelling inhomogeneous propagation paths, using several solutions of the wave equation in each of which the path is considered to have different but homogeneous propagation properties. It is based on the premise that it is easier to perform several solutions of the homogeneous wave equation than one solution of the inhomogeneous wave equation.

Information obtained from Dana [1982, personal communication] and the CRPLi Technical News Announcement [1977], indicates that it is now possible to use computer numerical integration techniques to solve the inhomogeneous wave equation. One such solution is called the effective impedence method. It does not give anomalous results at low conductivities, and can be adapted to small real time computers. This method does, however, have errors in the near field [Dana, 1982, personal communication]. Brunavs [1978] produced computer programs based on this approach, although he used it to model the phaselag variations based on terrain variations. It is considered that future work into the LORAN-C phaselag should include an investigation of the effective impedence technique.

4.4 Conclusions and Recommendations for Future Work

The 1979 and 1980 observed ASFs in the LORAN-C data base show

(a) the offshore phase recovery effect [Gray, 1980],

(b) phase retardation when wave paths pass over land,

(c) some observational inaccuracies, generally within $\pm$ 0.30 microseconds.

RECOMMENDATION 1: The 1978 TOA cruise data (not available in time for this report) should be investigated using plotted ASFs.

RECOMMENDATION 2: TOA cruise data obtained more recently than 1980 should be added to the data base and investigated using plotted ASFs.

RECOMMENDATION 3: Once an ASF prediction model has been developed which fits the TOA observed ASF data (see Recommendations 9 and 10 below), the TD cruise data should be investigated using a similar approach, plotting observed and residual ASF differences.

RECOMMENDATION 4: LORAN-C calibration data collected by van on land be added to the data base, and investigated using plotted ASFs.

RECOMMENDATION 5: LORAN-C calibration data collected on the Pacific coast and Great Lakes region should be added to the data base, and investigated using plotted ASFs.

It is considered that some of the fix errors may be due to using the NAD27 coordinate system, with its corresponding scale distortions. If the WGS72 coordinate system had been used at least a possible source of error could have been eliminated.

RECOMMENDATION 6: Consideration be given to converting the data base coordinate system from NAD27 to WGS72.

The computer programs used in the current phase lag model are large and time consuming. This includes the programs which find the land/sea boundaries on a wave path, evaluate the polynomial approximation of Johler's

formulae, and compute the phaselag using Millington's method. On an IBM 370, 2.5 minutes of CPU time are needed to search for land and sea sections for only 80 observations.

RECOMMENDATION 7: Further work should be done to improve the efficiency of the existing programs.

RECOMMENDATION 8: The existing data base and software should be installed on the HP-1000 computer now on order for the Surveying Engineering Department at UNB.

The standard land impedence model used so far (permittivity everywhere constant at 15 esu, conductivity homogeneous over an area at some value best fitting the observed data) appears to have two limitations:

(a) For low conductivity regions (such as the Newfoundland/Labrador area) the permittivity should also be lower, as seen from Tables 4.1 and 4.2.

(b) Predicted ASF values based on this standard impedence model do not represent the actual impedence as well as a model in which variations in conductivity and permittivity over a region can be accommodated. One simple approach is to define boundaries of small regions within which the conductivity (or permittivity) is homogeneous, and then to empirically fit the impedence values within these boundaries so that predicted ASFs agree with the observed ASF values over the entire calibration area. An impedence model of this type developed by Brunavs [1978] appears to be capable of modelling some of the residual ASF variations in Appendix III.

RECOMMENDATION 9: Further investigation should be carried out into regional impedence models, based on this data base, with a view to removing the low conductivity anomalous behaviour, and to reduce the residual ASF values.

RECOMMENDATION 10: The effective impedence technique of modelling inhomogeneous propagation should be investigated as an alternative to Millington's method.

After these improvements to the impedence modelling have been made, the remaining residual ASF values may or may not contain some spatial trend. This question is discussed in Appendix IV.

RECOMMENDATION 11: Techniques be developed so that residual ASF data series can be studied to determine whether a significant spatial trend remains.

REFERENCES

Bigelow, H.W. (1965). "Electronic surveying: Accuracy of electronic positioning systems." International Hydrographic Review, Vol. 6, pp. 77-112.

Bremmer, H. (1949). Terrestrial Radio Waves. Elsevier Publishing Company,

Brunavs, P. (1977). "Phase lags of 100 KHz radiofrequency ground wave and approximte formulas for computation." Canadian Hydrographic Service Internal Report.

Brunavs, P. (1978). "Investigation of ground factors affecting phase of LORAN-C east coast areas. Part I. Terrain Effect." Canadian Hydrographic Service Internal Report.

Brunavs, P. (1980). "Predicted versus observed phase lags of LORAN-C Maritime inshore areas." Canadian Hydrographic Service Internal Report.

CRPLi (1977). "Fundamental restrictions in the use of conductivities for calculating LORAN-C secondary phase corrections." Colorado Research and Prediction Laboratory Technical News Announcement.

Dana, P. (1982). Personal communication, December.

Gray, D.H. (1980). "The preparation of LORAN-C lattices for Canadian Charts." The Canadian Surveyor, vol. 34, no. 3, pp. 277-295.

Johler, J.R., W.J. Kellar and L.C. Walters (1956). "Phase of the low radiofrequency ground wave." National Bureau of Standards Circular 573, U.S. Department of Commerce.

Schelkunoff, S.A. (1963). Electromagnetic Fields. Blaisdell Publishing Company.

APPENDIX I

LORAN-C Data Base Header File

```
10          LORAN C PHASE LAG INVESTIGATION DATA BASE  MARCH 1983
20          ------------------------------------------------------
30       THIS DATA BASE REPRESENTS PART OF THE WORK CARRIED OUT AT THE
40    UNIVERSITY OF NEW BRUNSWICK TO FULFILL CONTRACT NUMBER OAE82-00037
50    FOR THE BEDFORD INSTITUTE OF OCEANOGRAPHY. PART OF THE REQUIREMENTS
60    OF THIS CONTRACT WAS :
70       TO ASSEMBLE A CONSISTENT DATA BASE FROM EXISTING LORAN C CALIBRATION
80       OBSERVATION FOR USE IN
90       1. VERIFYING CHART LATTICES AND PRODUCING LORAN C CORRECTION
100         DIAGRAMS.
110      2  IMPROVING THE MODEL USED IN PREDICTING LORAN C PHASE LAGS.
120
130
140
150
160                              DATA BASE FILES
170                              ---------------
180      1                  HEADER FILE FOR DATA BASE
190      2 1978  296 300 NARWHAL  FUNDAY       TOA   MRS      9930 MXY 9960 X
200      3 1978  301 303 NARWHAL  HALIFAX      TOA   MRS      9930 MXY 9960 X
210      4 1978  304 307 NARWHAL  CHEDABUCTO   TOA   MRS      9930 MXY 9960 X
220      5 1978  309 312 NARWHAL  PEI          TD    SEXTANT 5930 X Y
230      6 1978  310 313 NARWHAL  NORTHUMBRLD.S              NOT YET AVAILABLE
240      7 1978  314 314 NARWHAL  ST MARY'S B. TOA   MRS      9930 MXY 9960 X
250      8 1978  296 300 NARWHAL  FUNDAY       TOA   MRS      9960 MWX 9930 Y
260      9 1978  301 303 NARWHAL  HALIFAX      TOA   MRS      9960 MWX 9930 Y
270     10 1978  304 307 NARWHAL  CHEDABUCTO   TOA   MRS      9960 MWX 9930 Y
280     11 1978  310 313 NARWHAL  NORTHUMBRLD.S              NOT YET AVAILABLE
290     12 1978  314 314 NARWHAL  ST MARY'S B. TOA   MRS      9960 MWX 9930 Y
300     13 1979  304 310 MAXWELL  MAHONE BAY   TOA   MRS      9960 MWX 7930 Z
310     14 1980  110 117 MAXWELL  FUNDAY       TOA   MRS      5930 MXY 9960 M
320     15 1980  157 164 BAFFIN   FORTUNE BAY  TD    MRS      5930 X Y
330     16 1980  193 196 MAXWELL  PLACENTIA    TOA   MRS      5930 MXY 9960 X
340     17 1980  294 299 PANDORA  CANSO BAY    TOA   MRS      5930 MXY 9960 X
350     18 1980  302 302 PANDORA  HALIFAX      TOA   MRS      5930 MXY 9960 M
360
370
380
390
400
```

CORRECTIONS TO OBSERVATIONS

TYPES OF OBSERVATION

THERE ARE TWO MAIN TYPES OF CRUISE IN THIS DATA BASE: THOSE WHICH INVOLVED TOA OBSERVATIONS, AND THOSE WHICH INVOLVED TD OBSERVATIONS. THE TOA CRUISES REQUIRED REDUCTIONS TO ACCOUNT FOR THE OFFSET AND RATE DIFFERENCE OF THE SHIP'S CLOCK TO THE CLOCK AT EACH LORAN C STATION. TD CRUISES DO NOT REQUIRE SUCH CORRECTIONS SINCE THEY DO NOT USED A SHIP-BOARD CLOCK. TOA OBSERVATIONS ARE REDUCED TO GIVE THE TD WHICH WOULD HAVE BEEN OBSERVED IF A TD RECEIVER HAD BEEN USED TO MAKE THE OBSERVATION. TOA OBSERVATIONS CANNOT BE DEDUCED FROM TD OBSERVATIONS.

CLOCK CORRECTION TO TOA OSERVATIONS

TOA OBSERVATIONS ARE CORRECTED FOR THE SHIP'S CLOCK OFFSET AND DRIFT FROM EACH LORAN C TRANSMITTER. THE CORRECTION IS APPLIED BY

RANGE = RANGE + A0 + (T0 - TIME OF OBS) * A1

UNITS	USEC	USEC	USEC	DAYS	USEC/DAY

CLOCK SYNCHRONISATION FOR TOA OBSERVATIONS

THE CALIBRATION POSITION FOR THE SHIP'S CLOCK IS AT THE BIO WHARF, WHICH HAS ACCEPTED STANDARD READINGS TO THE LORAN C STATIONS AS DERIVED BY JANUARY 1980. ALL THE CLOCK CORRECTIONS (A0, A1) THUS APPLY TO THE OBSERVATIONS TO PRODUCE THESE VALUES. IT HAS BEEN THE POLICY TO MAINTAIN THESE VALUES CONSISTANTLY IN ANY DATA OBSERVATION OR REDUTION. THERE ARE, HOWEVER, REVISED VALUES DATED JULY 1980, WHICH SHOULD BE USED IN ANY INVESTIGATION REQUIRING A BETTER ACCURACY.

STANDARD READINGS AT BIO WHARF, DATED JANUARY 1980

CARIBOU		1372.90	MICROSECONDS
NANTUCKET		2150.00	
CAPE RACE		2821.77	

REVISED VALUES BIO WHARF, DATED JULY 1980

CARIBOU	SUMMER	1372.92	MICROSECONDS
	WINTER	1372.39	
NANTUCKET		2149.97	
CAPE RACE		2822.03	

EG. TO OUR TOA DATA, AFTER CORRECTING FOR CLOCK A0 AND A1, FOR ALL CAPE RACE OBSERVATIONS A +0.26 USEC CORRECTION IS APPLIED.

THE CARIBOU SUMMER VALUE SHOULD BE USED FOR ALL OUR CRUISES TO DATE SINCE IT IS CONSIDERED THAT THE WINTER READING IS A CONSEQUENCE OF BELOW FREEZING CONDITIONS.

P CORRECTIONS

P CORRECTIONS ARE APPLIED TO TOA'S TO PRODUCE TD'S. THE TOA CLOCK CORRECTIONS ARE NOT APPLIED TO PRODUCE TD'S, INSTEAD THE P CORRECTIONS ARE APPLIED BY

RANGE = RANGE - OLD P CORRN + NEW P CORRN.

HYPERBOLIC CORRECTION

THE HYPERBOLIC CORRECTION IS APPLIED IN SUCH CASES AS WHEN THE STANDARD EMISSION DELAY HAS BEEN SET SUBSEQUENT TO THE TIME OF THE CRUISE. THE TD OBSERVATION IS THUS PRODUCED BY

TD = RANGE SLAVE - RANGE MASTER + HYPERBOLIC CORRN.

1000
1010
1020
1030 PHASE LAG COMPUTATION
1040 ---
1050
1060 PHASE LAG COMPUTATIONS ARE CARRIED OUT USING BRUNAVS' 'C' COEFFICIENT
1070 FORMAULA. (P. BRUNAVS 1977, 'PHASE LAGS OF 100 KHZ RADIOFREQUENCY
1080 GROUND WAVE AND APPROXIMATE FORMULAS FOR COMPUTATION'). THIS GIVES THE
1090 PHASE LAG IN METRES BETWEEN THE ACTUAL WAVE, AND 'A FICTITIOUS WAVE
1100 MOVING AT THE VACUUM VELOCITY, C=299 792.5 KM/S. THE PHASE LAG AT THE
1110 TRANSMITTER IS BY DEFINITION SET TO BE EQUAL TO 'PI' (1499.0M). THE
1120 VALUES GIVEN REPRESENT THE TOTAL PHASE LAG FOR A SMOOTH SPHERICAL
1130 EARTH, AND ACCOUNT FOR THE EFFECTS OF ATMOSPHERIC REFRACTIVITY (N=338),
1140 VERTICAL LAPSE FACTOR OF ATMOSPHERE ('ALPHA'=0.75), CURVATURE OF EARTH,
1150 GROUND IMPEDANCE AND THE INDUCTION FIELD. THE DIELECTRIC CONSTANT FOR
1160 LAND IS ASSUMED TO BE E2 = 15.0 AND FOR SEAWATER, E2 = 81.0.'
1170 FORMULA 'C' IS:
1180 P = C1 + C2*S + (C3*S + C4)*EXP(C5*S) + C6/(1 + C7*S + C8*(S**4))
1190 + 2.277/S
1200
1210 WHERE S...DISTANCE IN 100'S OF KM.
1220 P...PHASE LAG IN METRES
1230 C1..C8...THE POLYNOMIAL COEFFICIENTS, WHICH ARE FUNCTIONS
1240 OF CONDUCTIVITY.
1250 FOR SOME STANDARD CONDUCTIVITY VALUES OF SEA WATER AND LAND:
1260

MHO/M	E2	C1	C2	C3	C4	C5	C6	C7	C8
4.0	81.0	-111.0	98.53	-12.9	112.8	-0.254	0.0	0.0	0.0
0.002	15.0	402.7	195.13	48.8	-195.3	-0.508	-169.3	8.29	31.0
0.0015	15.0	492.5	202.13	54.3	-236.5	-0.457	-208.2	7.16	21.0
0.001	15.0	633.3	207.42	75.0	-299.4	-0.400	-271.4	6.30	13.0

1320
1330 WHERE APPLICABLE MILLINGTON'S METHOD HAS BEEN USED TO ACCOUNT FOR
1340 MULTIPLE CONDUCTIVITY PATHS BETWEEN THE TRANSMITTER AND THE SHIP.
1350
1360 OBSERVED ADDITIONAL SECONDARY FACTOR
1370 THE OBSERVED TOA ADDITIONAL SECONDARY FACTOR IS DEFINED AS THE
1380 OBSERVATION CORRECTED FOR CLOCK, AND BIO STANDARD SYNCHRONISATION,
1390 MINUS THE RANGE COMPUTED FROM THE INDEPENDENT FIX ASSUMING AN OVER
1400 WATER PATH. THE TD ASF IS SIMILARLY THE OBSERVED TOA, OR THE TOA WHICH
1410 WOULD HAVE BEEN OBSERVED IF A HYPERBOLIC RECEIVER HAD BEEN USED, MINUS
1420 THE TD COMPUTED USING THE INDEPENDENT FIX POSITION AND AN OVER WATER
1430 PATH.
1440
1450

```
1460                          LORAN C STATIONS ON NAD 27
1470                          --------------------------
1480
1490     820202 059 14   NORTH AMERICAN DATUM 1927
1500   M DANA, IND.          8970 39 51 07.48 -087 29 11.51    0     0.0    400
1510   W MALONE, FL.         8970 30 59 38.23 -085 10 09.06 1100 3355.06   800
1520   X SENECA, N.Y.        8970 42 42 50.74 -076 49 34.50 2800 3162.04   800
1530   Y BAUDETTE, MINN.     8970 48 36 49.65 -094 33 16.99 4400 3753.69   500
1540   M EJDE                7970 62 17 59.68 -007 04 26.71    0     0.0    400
1550   X BO                  7970 68 38 06.15  014 27 47.00 1100 4048.07   200
1560   W SYLT                7970 54 48 29.80  008 17 36.33 2600 4065.70   300
1570   Y SANDUR              7970 64 54 26.58 -023 55 21.75 4600 2944.52  1800
1580   Z JAN MAYEN           7970 70 54 52.61 -008 43 58.69 6000 3216.24   200
1590   M WILLIAMS LAKE       5990 51 57 59.21 -122 21 56.68    0     0.0    400
1600   X SHOAL COVE          5990 55 26 21.97 -131 15 12.86 1100 2343.63   400
1610   Y GEORGE              5990 47 03 48.82 -119 44 34.78 2700 1927.31  1200
1620   Z PORT HARDY, BC      5990 50 36 30.37 -127 21 22.84 4100 1266.59   400
1630   M ANGISSOQ            7930 59 59 18.16 -045 10 32.65    0     0.0   1000
1640   W SANDUR              7930 64 54 27.74 -023 55 28.22 1100 4068.09  1800
1650   X EJDE                7930 62 18 02.37 -007 04 34.22 2100 6803.84   400
1660   Z CAPE RACE           7930 46 46 32.62 -053 10 32.41 4300 5212.28  1800
1670   S BREVOORT N.W.T.     7930 63 20 22.24  -64 09 46.40 6100 3617.90   300
1680   M SENECA              9960 42 42 50.74 -076 49 34.50    0     0.0   1000
1690   W CARIBOU             9960 46 48 27.54 -067 55 39.35 1100 2797.18   350
1700   X NANTUCKET           9960 41 15 11.98 -069 58 40.51 2500 1969.92   300
1710   Y CAPE FEAR           9960 34 03 45.61 -077 54 47.20 3900 3221.62   700
1720   Z DANA                9960 39 51 07.48 -087 29 11.51 5400 3162.04   400
1730   M TOK                 7960 63 19 44.16 -142 48 23.36    0     0.0    400
1740   X NARROW CAPE         7960 57 26 23.03 -152 22 03.03 1100 2804.39   400
1750   Y SHOAL COVE          7960 55 26 21.97 -131 15 12.86 2600 3651.17   400
1760   M FALLON              9940 39 33 07.03 -118 49 52.23    0     0.0    400
1770   W GEORGE              9940 47 03 48.82 -119 44 34.78 1100 2796.90  1200
1780   X MIDDLETOWN          9940 38 46 57.49 -122 29 40.04 2700 1094.49   400
1790   Y SEARCHLIGHT         9940 35 19 18.32 -114 48 13.95 4000 1967.27   500
1800   M ST PAUL I.          9990 57 09 09.88 -170 14 59.81    0     0.0    300
1810   X ATTU                9990 52 49 45.05 -173 10 52.31 1100 3875.36   300
1820   Y PORT CLARENCE       9990 65 14 40.12 -166 53 14.47 2900 3069.02  1000
1830   Z NARROW CAPE         9990 57 26 20.21 -152 22 11.22 4300 3590.13   400
1840   M IWO JIMA            9970 24 48 04.10  141 19 29.00    0     0.0   1800
1850   W MARCUS ISLAND       9970 24 17 07.70  153 58 51.50 1100 4283.99  1800
1860   X HOKKAIDO            9970 42 44 37.0   143 43 09.06 3000 6684.99   400
1870   Y GESASHI             9970 26 36 24.99  128 08 56.21 5500 4463.23   400
1880   Z YAP                 9970 09 32 45.66  138 09 55.23 7500 5746.64  1500
1890   M SEMERI CRICHI       7990 38 52 20.61   16 43 05.96    0     0.0    200
1900   X LAMPEDUSA           7990 35 31 20.88   12 31 29.96 1100 1755.90   400
1910   Y KARGABARUN          7990 40 58 20.95   27 52 01.52 2900 3273.35   200
1920   Z ESTARTIT            7990 42 03 36.49    3 12 15.90 4700 3999.75   200
1930   M JOHNSTON IS.        4990 16 44 43.95 -169 30 31.20    0     0.0    300
1940   X UPOLO POINT         4990 20 14 49.16 -155 53 09.70 1100 4972.14   300
1950   Y KURE                4990 28 23 41.77 -178 17 30.20 2900 5253.14   300
1960   M MALONE, FL          7980 30 59 38.74  -85 10 09.30    0     0.0    800
1970   W GRANGEVILLE, LA     7980 30 43 33.02  -90 49 43.60 1100 1809.54   400
1980   X RAYMONDVILLE, TX    7980 26 31 55.01  -97 50 00.09 2300 4443.38   400
1990   Y JUPITER, FL         7980 27 01 58.49  -80 06 53.52 4300 2201.88   275
2000   Z CAROLINA BEACH, NC  7980 34 03 46.04  -77 54 46.76 5900 2542.72   550
2010   M CARIBOU, ME.        5930 46 48 27.54  -67 55 39.35    0     .0    350
2020   X NANTUCKET, MASS.    5930 41 15 11.98  -69 58 40.51 1100 2131.88   275
2030   Y CAPE RACE, NFLD.    5930 46 46 32.62  -53 10 32.41 2500 3754.93  1500
2040   M CAROLINA BEACH, NC  9930 34 03 46.04  -77 54 46.76 0000 0000.00   550
2050   W JUPITER, FL         9930 27 01 58.49  -80 06 53.52 1100 2695.57   275
2060   X CAPE RACE           9930 46 46 32.62 -053 10 32.41 2800 8389.55  1800
2070   Y NANTUCKET           9930 41 15 11.98 -069 58 40.51 4900 3541.27   300
2080   Z DANA                9930 39 51 07.48 -087 29 11.51 6500 3560.68   400
2090   GREAT LAKES           8970
2100   NORWEGIAN SEA         7970
2110   WEST COAST CANADIAN   5990
2120   NORTH ATLANTIC        7930
2130   NORTHEAST U.S.        9960
2140   GULF OF ALASKA        7960
2150   U.S. WEST COAST       9940
2160   NORTH PACIFIC         9990
2170   NORTHWEST PACIFIC     9970
2180   MEDITERRAEN SEA       7990
2190   CENTRAL PACIFIC       4990
2200   SOUTHEAST U.S.        7980
2210   CANADIAN EAST COAST   5930
2220   OLD US EAST COAST     9930
2230
2240
```

```
                        CRUISE FILES DATA FORMAT
                        ------------------------

THE CRUISE FILES ARE COMPOSED OF 80 COLUMN FIXED LENGTH RECORDS. EACH
FILE CONTAINS DATA FOR A CONVENIENT AREA AND DATE, AND IS SUCH THAT THE
SAME METHODS WERE USED FOR ALL DATA POINTS WITHIN THE FILE. TYPICALLY
ONE CRUISE IS GIVEN IN ONE FILE,BUT THE OCTOBER 1980 CRUISE HAS TWO
SPECIFIC AREAS: CANSO BAY AND HALIFAX, SO EACH AREA IS ALLOCATED A
FILE. SIMILARLY, DIFFERENT DIFFERENT OBSERVATION TYPES IN THE SAME
CRUISE WOULD DICTATE DIFFERENT DATA BASE FILES.

AS AN AID TO IDENTIFY RECORD TYPES WITHIN EACH CRUISE FILE, A CHARACTER
IS USED IN THE SECOND COLUMN  TO INDICATE THE TYPE OF INFORMATION ON
THE LINE:
          'O'  OBSERVATION FIRST RECORD, GIVING TIME, FIX POSITION,ETC.
          'D'  TD INFORMATION, EG TD ASF'S.
          'A'  TOA INFORMATION, EG TOA ASF'S.
          ' '  LEADER RECORDS GIVING INFORMATION FOR THE CRUISE FILE.

EACH FILE IS COMPOSED OF FOUR SECTIONS:
    1. INTRODUCTORY RECORDS, DESCRIBING THE DATA IN THE FILE.
    2. MIND FILE, THE CONTROL FILE USED TO DERIVE THE OBSERVATIONS.
    3. LORAN C STATIONS OBSERVED, COORDINATE SYSTEM AND EMMISION DELAYS
    4. OBSERVATION POINTS, OBSERVATIONS, TIME, ASF'S, FOR EACH POINT.

  1. INTRODUCTORY RECORDS.

1.1   IYEAR     YEAR OF CRUISE.
      ISTART    DAY OF THE FIRST OBSERVATION.
      IFIN      DAY OF THE LAST OBSERVATION.
      SHIP(3)   SHIP'S NAME, UP TO 14 CHARACTERS.
      AREA(5)   AREA OF CRUISE, UP TO 20 CHARACTERS.
     (IGRI(I), LORAN C CHAIN GROUP REPITITION INTERVAL (GRI).
      ISTN(I)) STATION # WITHIN GRI, 0=MASTER,1=FIRST SLAVE,...
      INDIC1   LORAN C OBSERVATIONS TYPE INDICATORS:  A = TOA,
      INDIC2                                          D = TD.
      NINTR    NUMBER OF RECORDS BEFORE OBSERVATION RECORDS.
      FORMAT   (2X,I4,2(I3,1X),3A4,5A4,4(1X,I4,1X,I1),1X,2A1,I2)

1.2   COMMEN(20) AN 80 CHARACTER COMMENT OF THE CRUISE.
      FORMAT   (20A4)

1.3   TDSTN(I,J) J=1,2 STATION #'S OF THE I'TH TD OBSERVATION, THE
                  STATION #'S ARE GIVEN IN VECTORS IGRI, ISTN, LINE 1.
      BIOSYN(4)  CORRECTIONS TO TOA'S FOR BEST SYNCH. AT BIO
      DSTH )
      DNTH )   LATITUDE AND LONGITUDE LIMITS OF CRUISE          DEGREES
      DWST )
      DEST )
      NPTS     NUMBER OF DATA POINTS IN CRUISE FILE.
      FORMAT   (2X,6I1,4F6.2,2F10.5,2F11.5,I6)

1.4   COND(9)  CONDUCTIVITIES USED TO PRODUCE ASF'S.
      FORMAT   (2X,9F8.5)
```

```
2800   2. MIND FILES: USED BY PROGRAM MSQSD TO PROCESS RAW MRS AND LORAN DATA
2810                  FILES INTO COMPARISON FILES. THIS FILE COULD NOT BE
2820                  USED DIRECTLY AS INPUT TO MSQSD SINCE ALL DATA HAS BEEN
2830                  SHIFTED TWO COLUMNS TO THE LEFT.
2840
2850         NAME     DEFINITION                                        UNITS
2860   2.1   INUM     NUMBER OF MRS STATIONS.
2870         MESAG    DESCRIPTIVE MESSAGE 32 CHARACTERS.
2880         RMRLO    DISTANCE         LORAN TO MRS ANTENAE.            METRES
2890         TMRLO    RELATIVE BEARING                                  DEGREES
2900         IMSTR    START OF MRS RAW DATA FILES.
2910         IMEND    END
2920         FORMAT   (1X,I2,1X,16A2,1X,F4.1,1X,F5.1,1X,I2,1X,I2)
2930
2940   2.2   ONE OR MORE CARDS FOR EACH MRS STATION.ONE A IS ALWAYS PRESENT
2950         WHILE ANY NUMBER OF B'S CAN BE PRESENT(0-# OF TRANSPONDER MOVES).
2960     A.  ITNAM    MRS STATION NAME     6 CHARACTERS.
2970         IDLA     STATION LATITUDE.                                 DEGREES
2980         IMLA                                                       MINUTES
2990         SLA                                                        SECONDS
3000         IDLO     STATION LONGITUDE.                                DEGREES
3010         IMLO                                                       MINUTES
3020         SLO                                                        SECONDS
3030     B.  ID1      START TIME FOR TRANSPONDER POSITION               DAYS
3040         IH1      AND CORRECTIONS.                                  HOURS
3050         IM1                                                        MINUTES
3060         ID2      END TIME FOR TRANSPONDER POSITION                 DAYS
3070         IH2      AND CORRECTIONS.                                  HOURS
3080         IM2                                                        MINUTES
3090         TCOR1    FIXED MRS CORRECTION.                             METRES
3100         TCOR2    RANGE DEPENDENT CORRECTION.                       FRACTION
3110         TRHO     RANGE CONTROL STATION TO TRANSPONDER.             METRES
3120         TTH      BEARING                                           DEGREES
3130         FORMAT   (1X,2(I4,2I3,1X),F5.1,1X,F8.5,1X,F4.1,1X,F5.1)
3140
3150   2.3   TIMES DURING WHICH DATA IS TO BE SKIPPED. A GIVES THE HEADER AND
3160         MUST BE PRESENT,WHILE B IS PRESENT FOR EACH PERIOD TO BE SKIPPED.
3170     A           HEADER OF ' SKIP TIMES' STARTING IN COLUMN 1
3180     B   ID1     START OF PERIOD TO BE SKIPPED.                    DAYS
3190         IH1                                                        HOURS
3200         IM1                                                        MINUTES
3210         ID2     END OF PERIOD TO BE SKIPPED.                      DAYS
3220         IH2                                                        HOURS
3230         IM2                                                        MINUTES
3240         FORMAT  (2(1X,I4,2I3))
3250
3260   2.4   LORAN C RECEIVED STATION INFORMATION. ONE A IS PRESENT, WITH ONE
3270         B FOR EACH PERIOD IN WHICH A DIFFERENT SET OF STATIONS WERE USED.
3280     A           HEADER ' LORAN DATA ' STARTING IN COLUMN 1
3290         DCO     MINIMUM COURSE CHANGE WHICH DENOTES THAT THE     DEGREES
3300                 FOLLOWING BLPD MINUTES OF DATA IS TO BE SKIPPED.
3310         DSP     SPEED CHANGE TO GIVE BLPD MINUTES SKIPPED.       KNOTS
3320         BLPD    NUMBER OF MINUTES OF DATA TO BE SKIPPED          MINUTES
3330                 IF THE OBSERVED COURSE OR SPEED INDICATES A COURSE
3340                 CHANGE BY BEING LARGER THAN DCO OR DSP RESPECTIVELY.
3350         CONW    WATER CONDUCTIVITY USED IN MSQSD ASF COMPUTATIONS. MHO/M
3360         CONL    LAND CONDUCTIVITY. NOT CURRENTLY USED BY MSQSD.    MHO/M
3370         IASTR   START AUSTRON FILE FOR CRUISE.
3380         IAEND   END AUSTRON FILE FOR CRUISE.
3390         FORMAT  (12X,2(F4.1,1X),2(F3.1,1X),F6.4,2(1X,I2) )
3400     B   ID1     START TIME FOR THIS LORAN STATION SET.            DAYS
3410         IH1                                                        HOURS
3420         IM1                                                        MINUTES
3430         ID2     END TIME FOR THIS LORAN STAION SET.               DAYS
3440         IH2                                                        HOURS
3450         IM2                                                        MINUTES
3460         IGRP(J) THE FOUR LORAN STATIONS RECEIVED, DESCRIBED       10 USEC
3470                 BY THE GROUP REPETITION INTERVAL,
3480         ISTN(J) AND THE STAION NUMBER WITHIN THAT CHAIN.1,2,3,..
3490                 EG MASTER IS ALWAYS #0, THE FIRST SLAVE IS #1..
3500         FORMAT  ( 1X,2(I4,2I3,1X), 4(1X,I4,I2) )
3510
```

```
2.5   SHIP BOARD LORAN CLOCK CORRECTION DATA. ONE HEADER LINE
      FOLLOWED BY ONE LINE FOR EACH CLOCK PERIOD.
  A           HEADER OF ' CLOCK DATA' STARTING IN COLUMN 1
  B   ID1     START TIME FOR THIS CLOCK CORRECTION.          DAYS
      IH1                                                   HOURS
      IM1                                                   MINUTES
      ID2     END TIME FOR THIS CLOCK CORRECTION.           DAYS
      IH2                                                   HOURS
      IM2                                                   MINUTES
     SYNC(I,J) FOUR CLOCK SYNCH. CORRECTIONS FOR EACH LORAN. USEC
               STATION. ((J=1,# STNS),I=1, # CLOCK PERIODS).
     SLOP(I,J) FOUR CLOCK SLOPE CORRECTIONS FOR THE STATIONS.USEC/DAY
      FORMAT   ( 1X,2(I4,2I3,1X), 8F6.3  )

2.6   P CORRECTION DATA, ONE HEADER LINE FOLLOWED BY TWO LINES
      FOR EACH P CORRECTION PERIOD: THE FIRST GIVING THE OLD
      CORRECTION TO BE TAKEN OUT; THE SECOND GIVING THE NEW
      CORRECTION TO BE APPLIED. (THERE NEED NOT BE ANY PERIODS).
  A           HEADER ' P CORRECTIONS' STARTING IN COLUMN 1.
  B   ID1     START TIME FOR CORRECTION PERIOD.              DAYS
      IH1                                                   HOURS
      IM1                                                   MINUTES
      ID2     END TIME FOR CORRECTION PERIOD.               DAYS
      IH2                                                   HOUR
      IM2                                                   MINUTES
    PCORO(I,J) FOUR OLD P CORRECTION, ONE FOR EACH          USEC
               TRANSMITTER. ((J=1,# TRANSM),I=1,# PERIODS).
      FORMAT   ( 1X,2(I4,2I3,1X);4F9.2)
  C PCORN(I,J) FOUR NEW P CORRECTIONS.                      USEC
      FORMAT   ( 23X,4F9.2 )

2.7   HYPERBOLIC CORRECTION DATA: ONE HEADER LINE FOLLOWED BY
      ONE LINE FOR EACH PERIOD OF HYPERBOLIC CORRECTION.
  A           HEADER ' HYPERBOLIC DATA' STARTING IN COLUMN 1.
  B   ID1     START TIME FOR HYPERBOLIC PERIOD.              DAYS
      IH1                                                   HOURS
      IM1                                                   MINUTES
      ID2     END TIME FOR HYPERBOLIC PERIOD.               DAYS
      IH2                                                   HOURS
      IM2                                                   MINUTES
    IDHYM(J)  STATION # AS GIVEN IN LORAN DATA, FIRST IS #1,
              SECOND IS #2, ETC. SINCE HYPERBOLICS FOR THIS DATA
              ARE FOR MASTER TO SLAVE PAIRS,THIS IS A MASTER.
    IDHYS(J)  STATION # AS GIVEN IN LORAN DATA FOR THE SLAVE OF
              THIS YPERBOLIC (MS) PAIR. (J=1,# OF HYPERBOLICS).
      FORMAT  (1X,2(I4,2I3,1X),4(2I1,1X),3(F5.2,1X),F5.2)

3     LORAN C STATIONS OBSERVED, EXTRACTED FROM LORDAT FILE.
3.1   HEADER  HEADER LINE FOR LORDAT FILE, INCLUDES DATUM.

3.2   STATIONS ALL STATIONS WITHIN EACH CHAIN OBSERVED, ONE LINE PER
               STATION, TO THE TOTAL STATIONS OF ALL OBSERVED CHAINS.

3.3   CHNAMS  NAMES OF ALL CHAINS OBSERVED.


4.    OBSERVATION POINT RECORDS.
      OBSERVATION POINTS ARE STORED IN TIME ORDER.

4.1   IDAY    OBSERVATION TIME DAY,
      IHR                    HOUR,
      MIN                    MINUTE.
      IDLAT   FIX POSITION: LATITUDE DEGREES,
      RMLAT                 LATITUDE MINUTES AND DECIMALS.
      IDLON                 LONGITUDE DEGREES,
      RMLON                 LONGITUDE MINUTES AND DECIMALS.
      FIX     FIX METHOD USED TO OBTAIN ABOVE POSITION.
      IHDG    HEADING COMPUTED FROM CONSECUTIVE FIX POSITIONS.
      ISPEED  SPEED COMPUTED FROM CONSECUTIVE FIX POSITIONS.
      TOA(4)  TOA'S OBSERVED.
      FORMAT  (1X,'0',I3,1X,2I2,I3,F7.3,I4,F7.3,A3,I4,I3,4F9.2)

4.2   TDOBS(3) TD OBSERVATIONS, OR DERIVED TD'S FROM TOA'S.
      TDASF(10) TD ASF, OBSERVED FOLLOWED BY COMPUTED ASF'S.
      FORMAT  (1X,'D',3F9.2,10F6.2)

4.3   TOAASF(13) TOA ASF, OBSERVED FOLLOWED BY COMPUTED ASF'S.
      FORMAT  (1X,'A',13F6.2)
```

APPENDIX II

PLOTS OF OBSERVED ASF

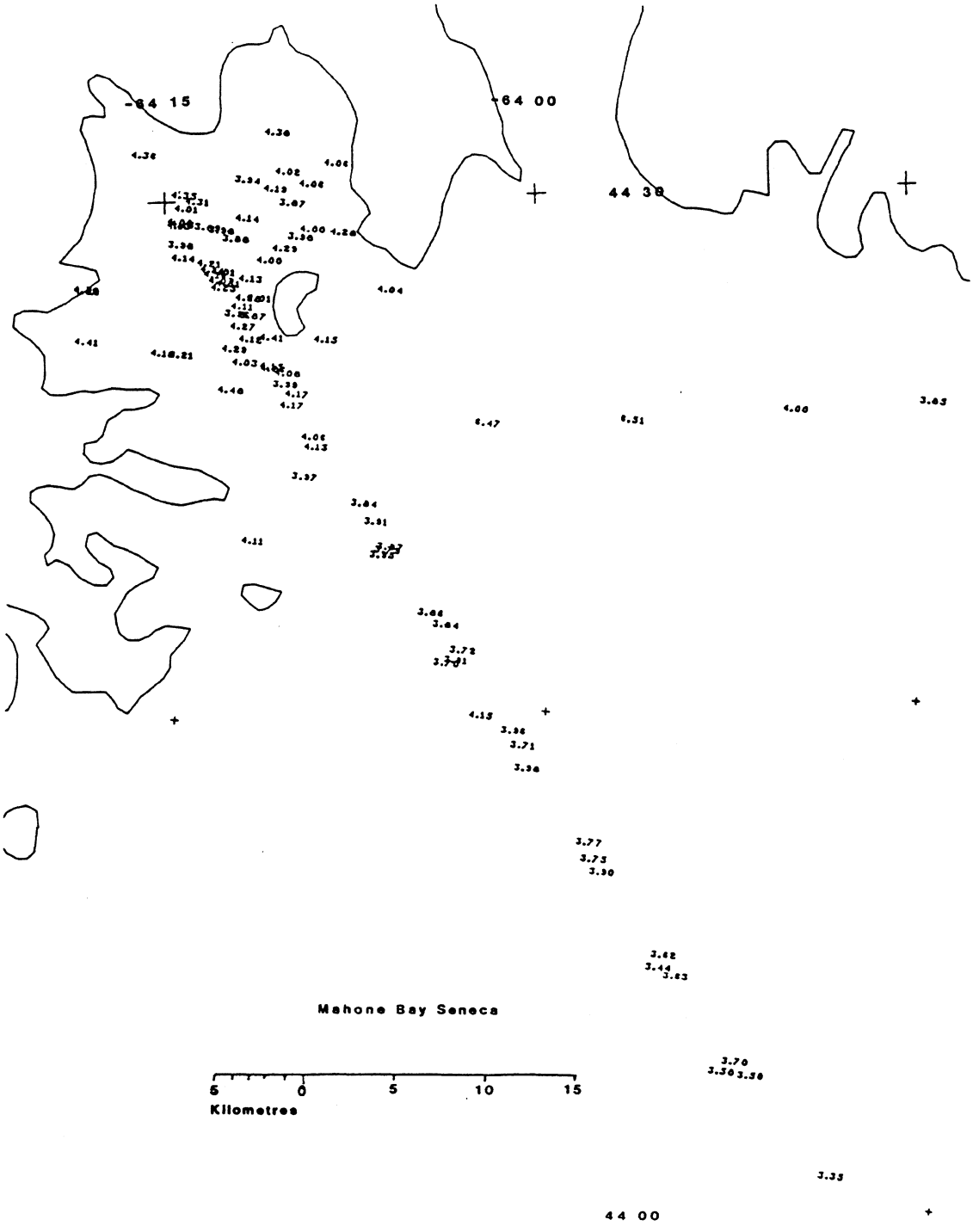
-64 15
-64 00
44 30
44 00
Mahone Bay Seneca
5 0 5 10 15
Kilometres

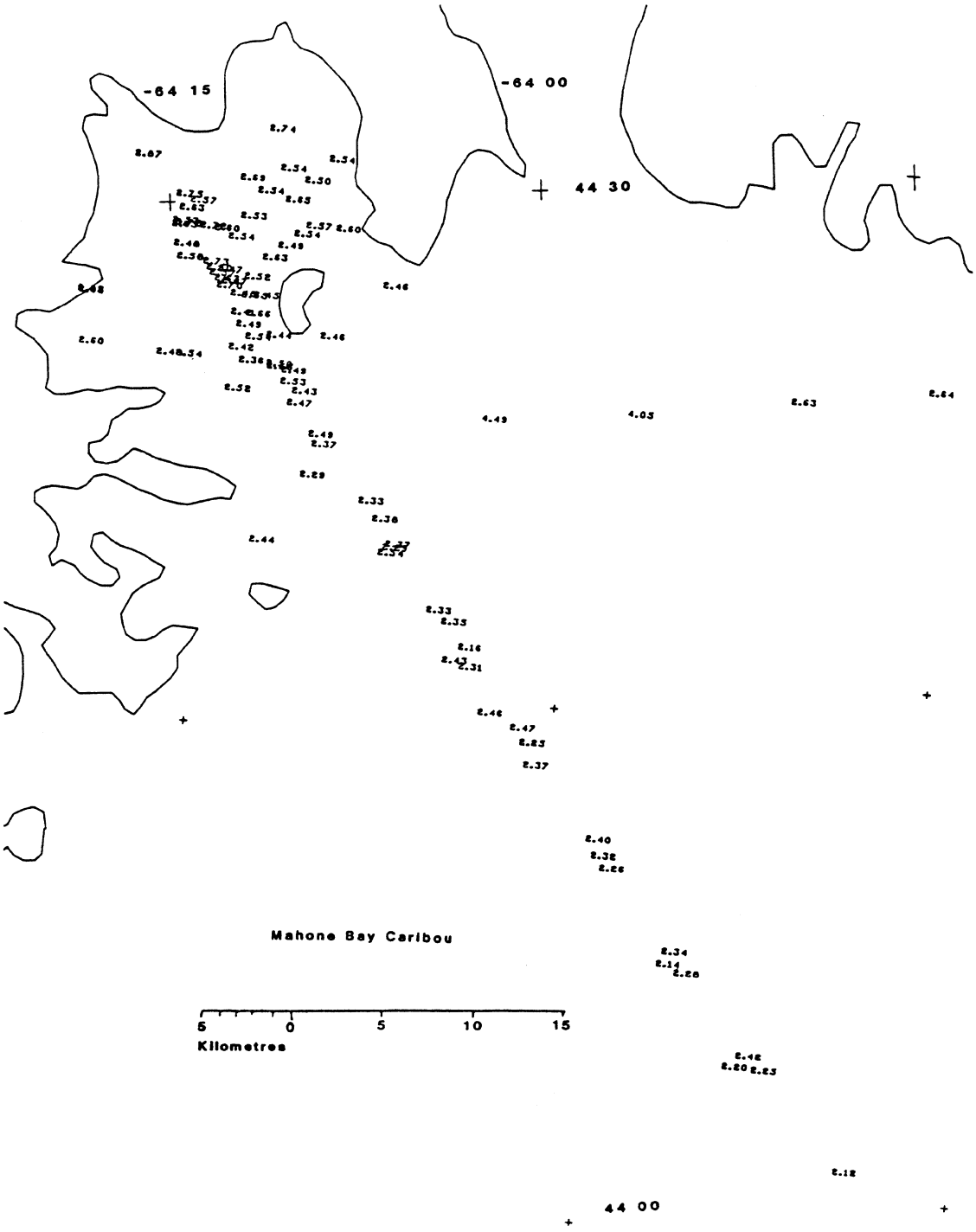
-64 15
-64 00
44 30
44 00
Mahone Bay Caribou
5 0 5 10 15
Kilometres

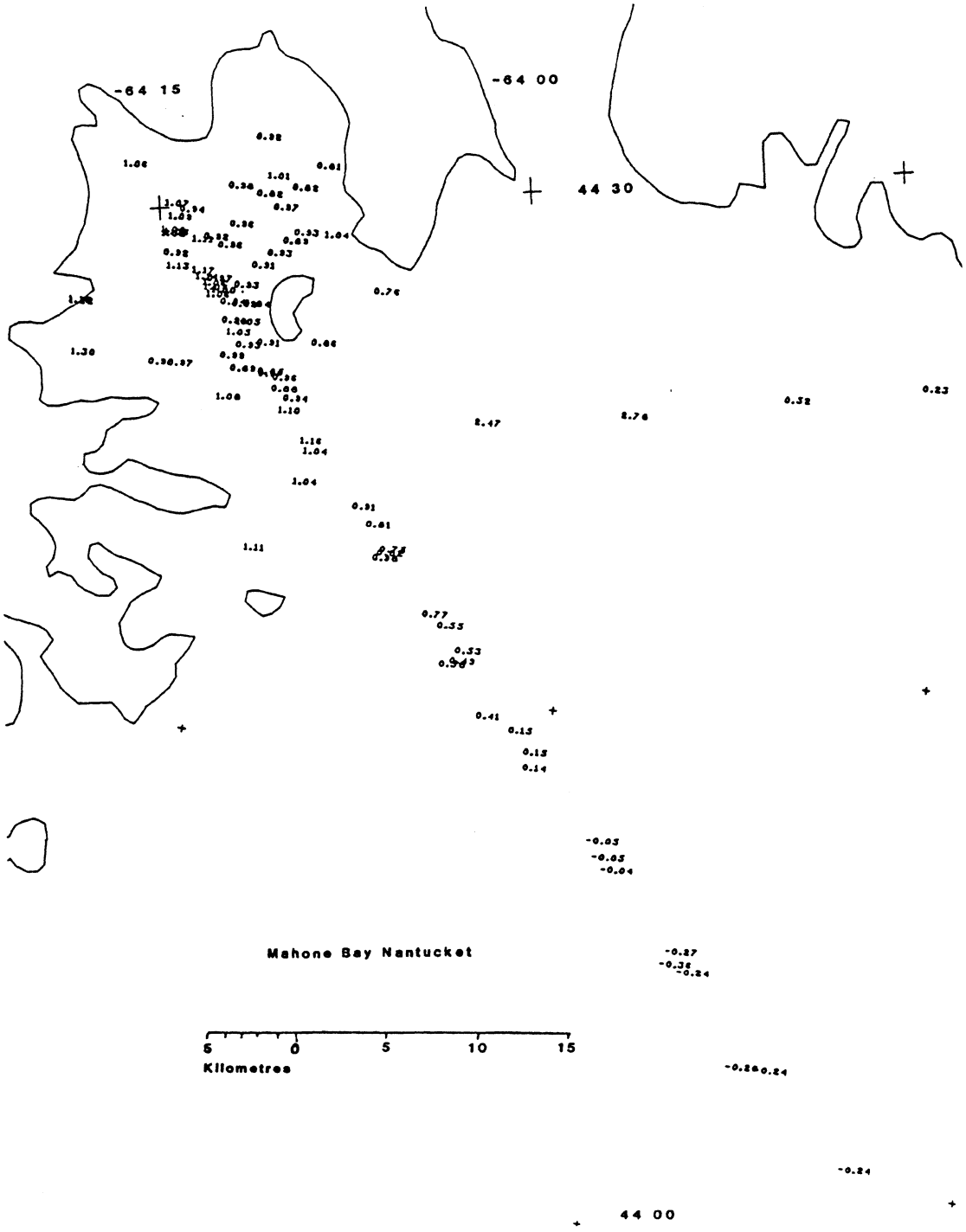
-64 15
-64 00
44 30
Mahone Bay
Nantucket
5 0 5 10 15
Kilometres
44 00

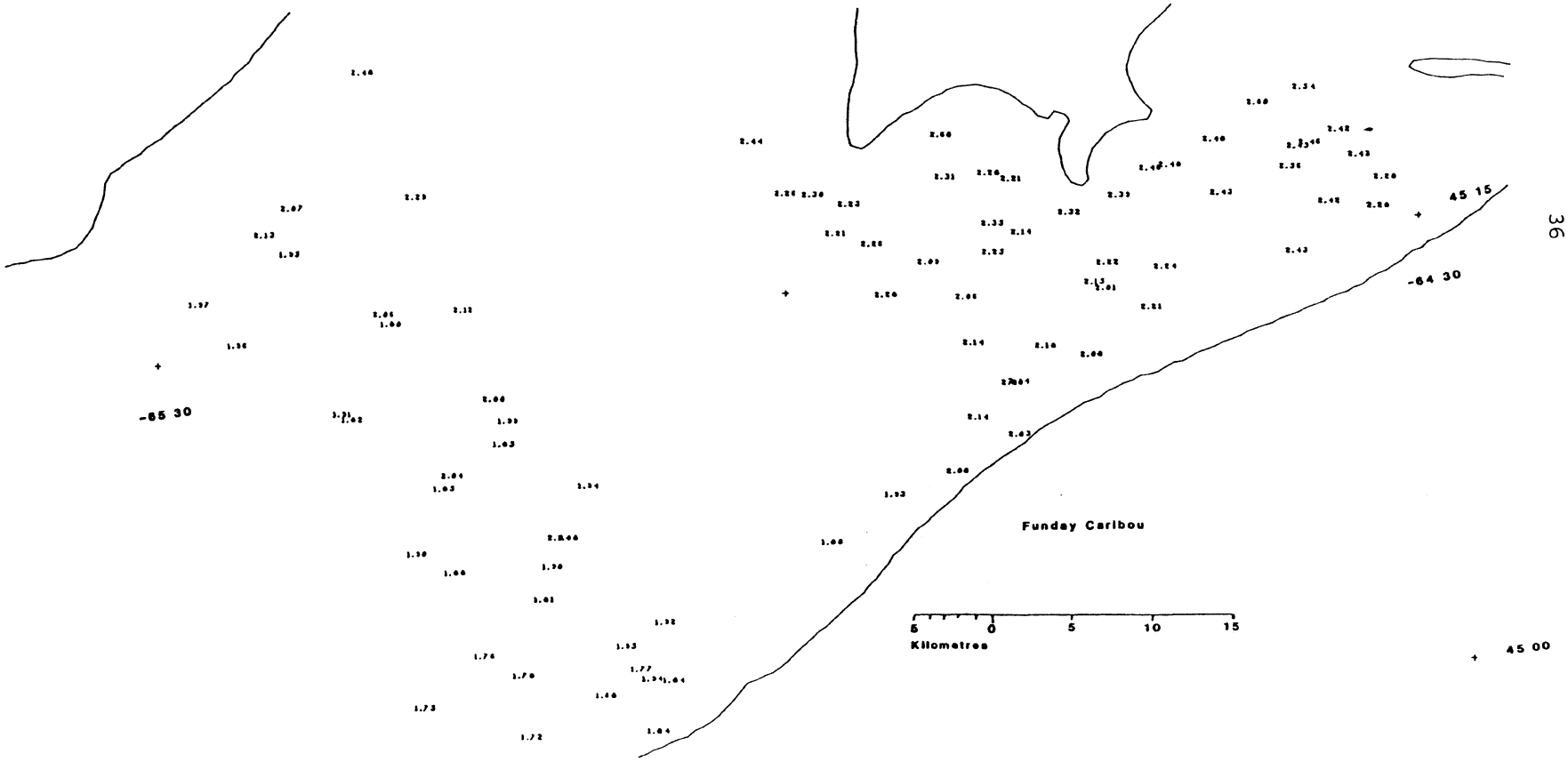
-65 30
-64 30
45 15
45 00
Funday Caribou
5 0 5 10 15
Kilometres

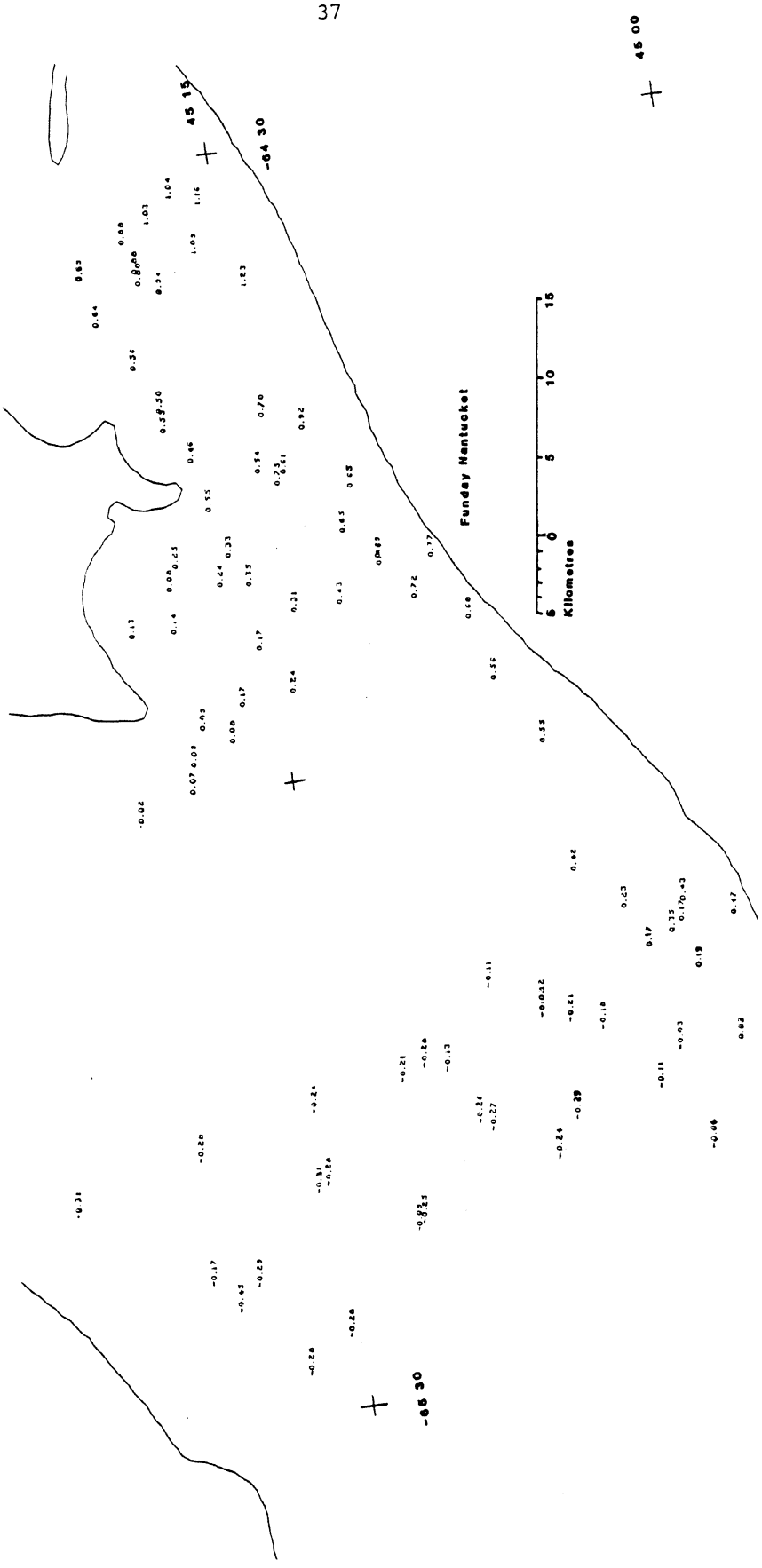
45 15
45 00
-64 30
-65 30
Fundy
Nantucket
0
5
10
15
Kilometres

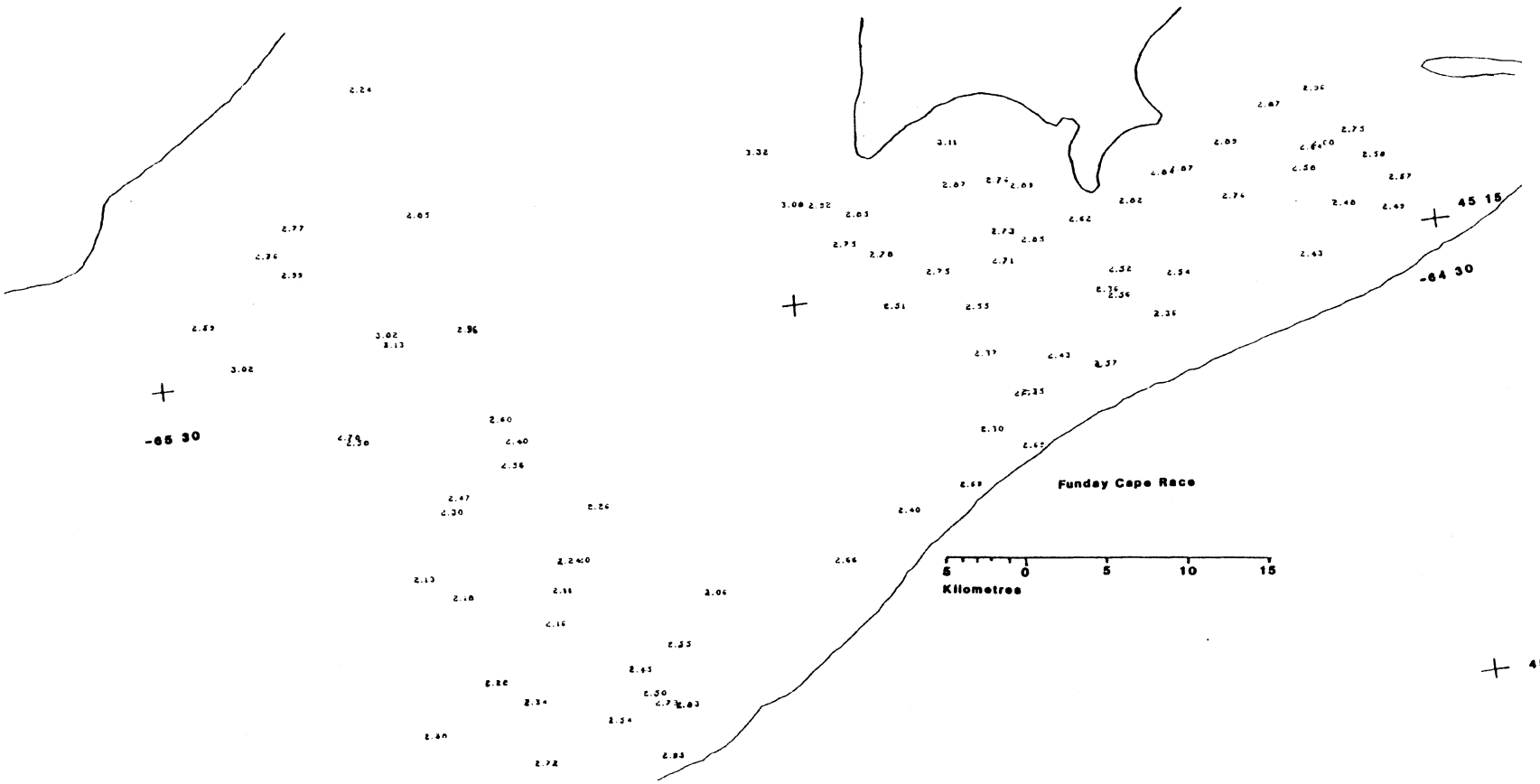
-65 30
-64 30
45 15
45 00
Funday Cape Race
5 0 5 10 15
Kilometres

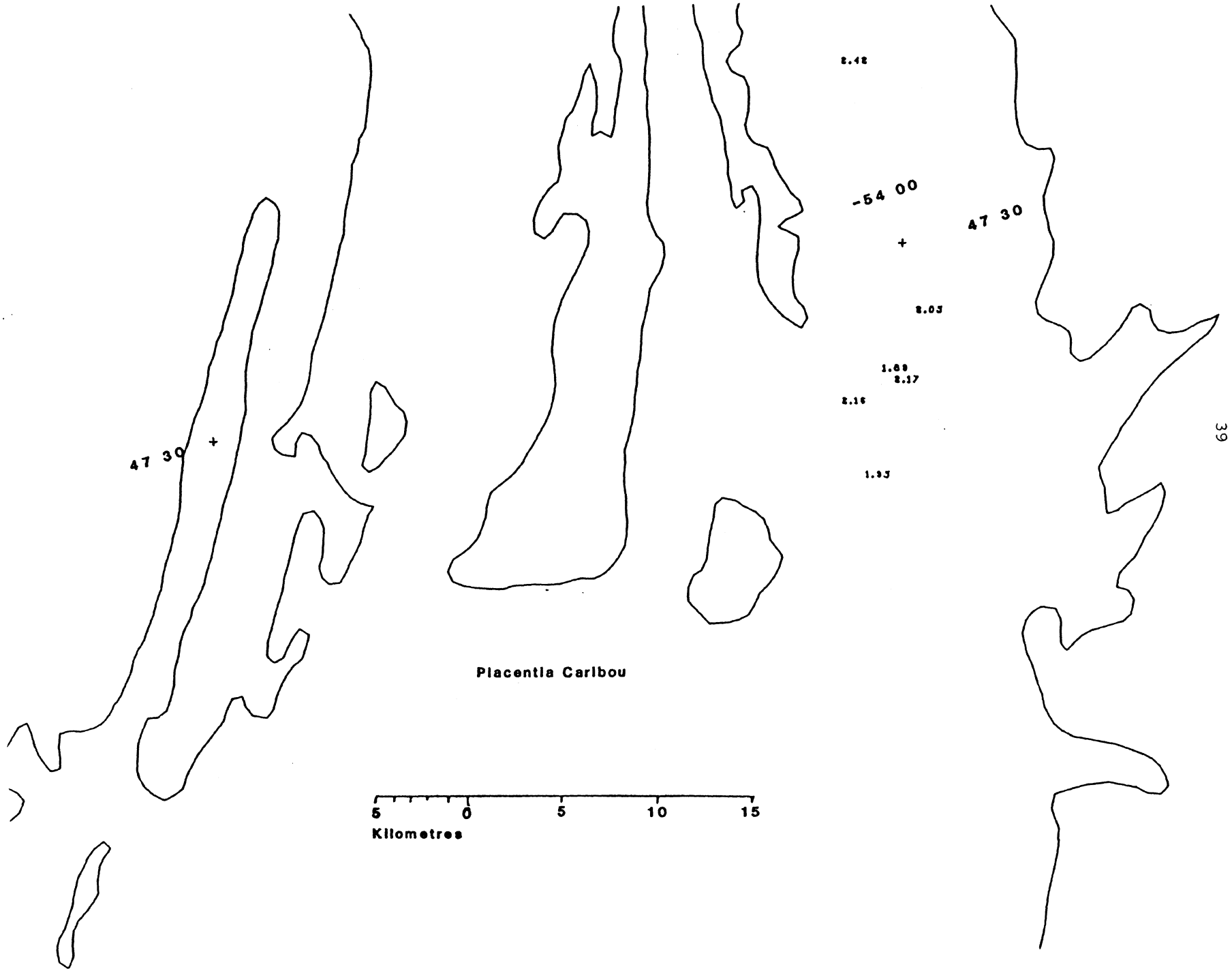
-54 00
47 30
47 30
Placentia Caribou
5 0 5 10 15
Kilometres

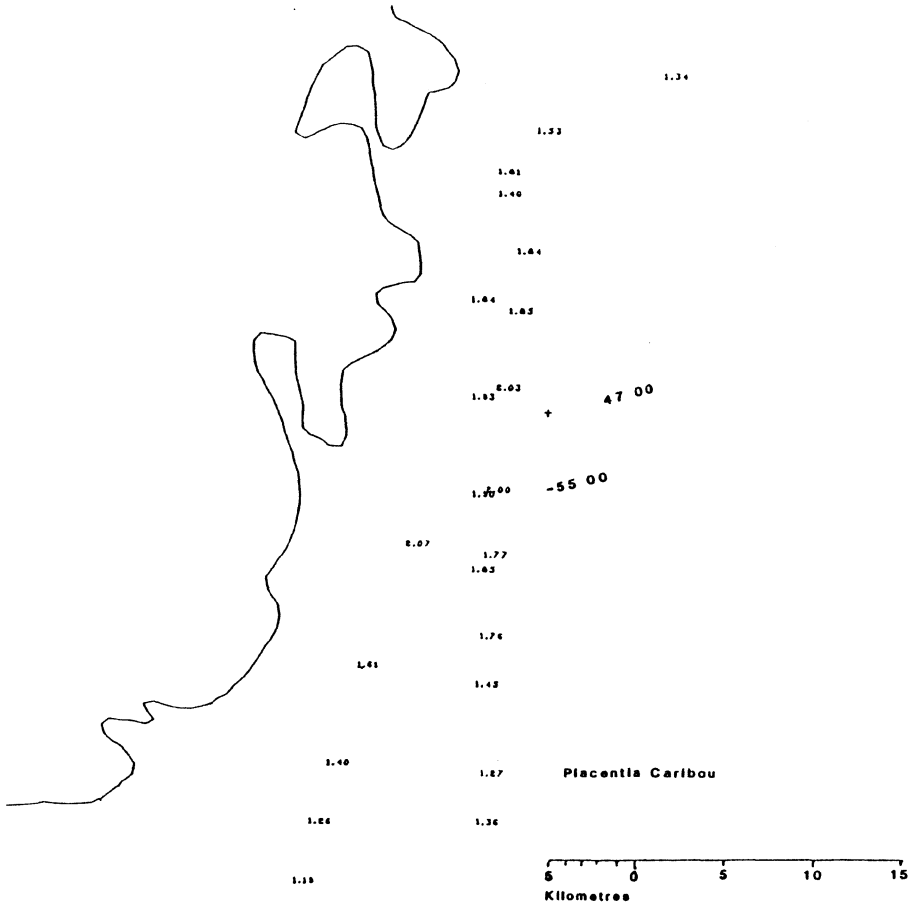
1.34
1.33
1.41
1.40
1.44
1.44
1.43
1.43
1.03
47 00
-55 00
1.00
1.07
1.77
1.63
1.76
1.61
1.43
1.40
1.87
Placentia Caribou
1.86
1.36
1.39
1.69
1.38
5 0 5 10 15
Kilometres

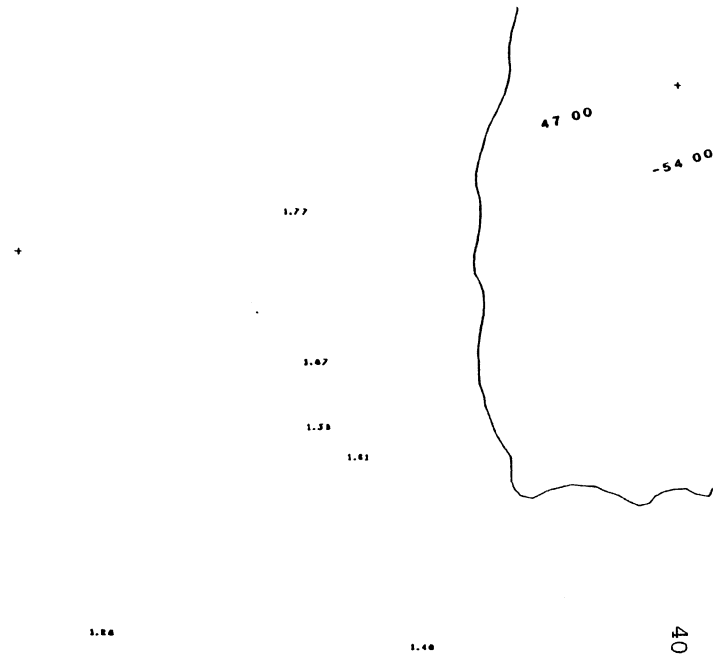
47 00
-54 00
1.77
1.67
1.58
1.61
1.86
1.48

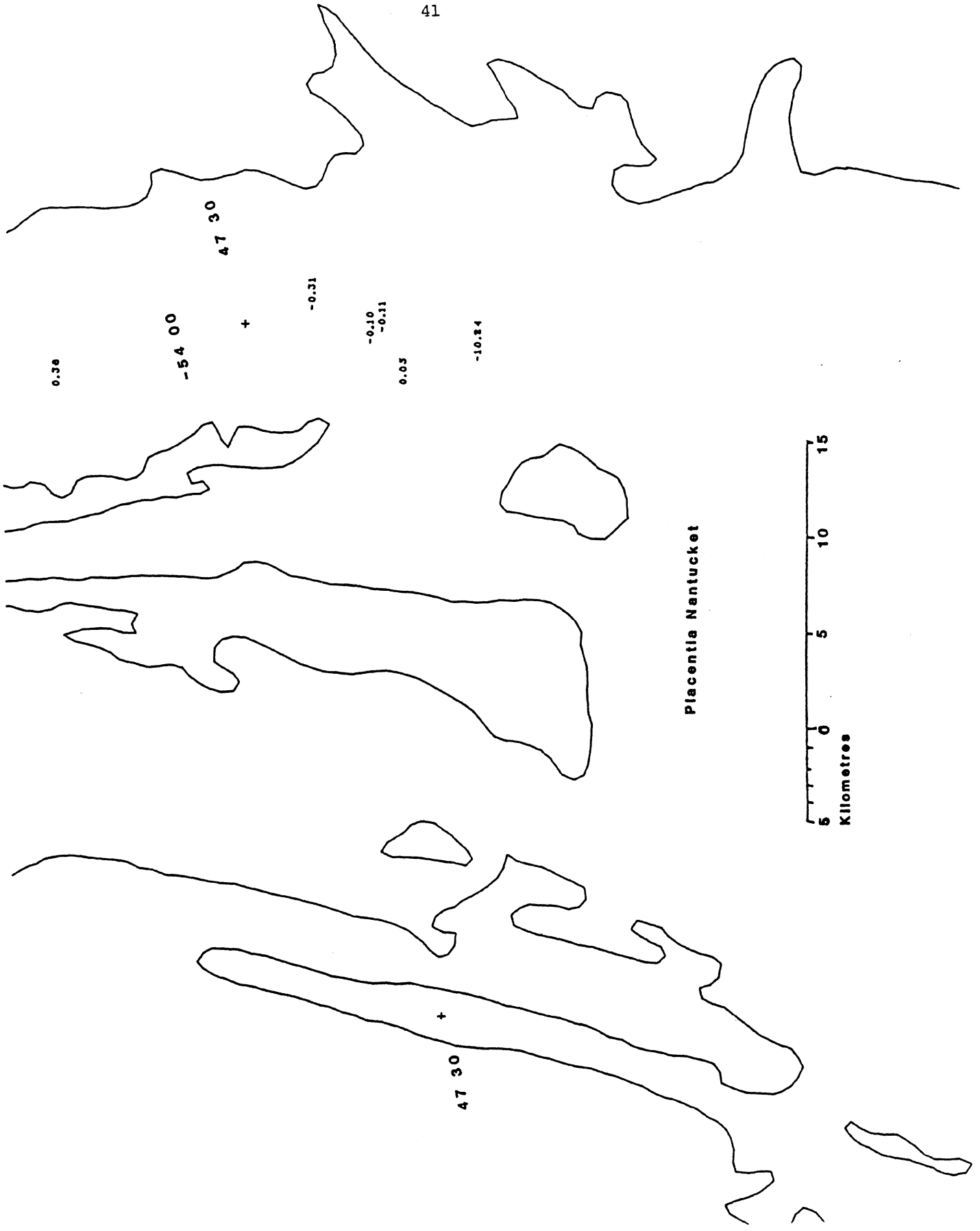
47 30
-54 00
47 30
0.38
-0.31
-0.10
-0.11
0.05
-10.24
Placentia Nantucket
5 0 5 10 15
Kilometres

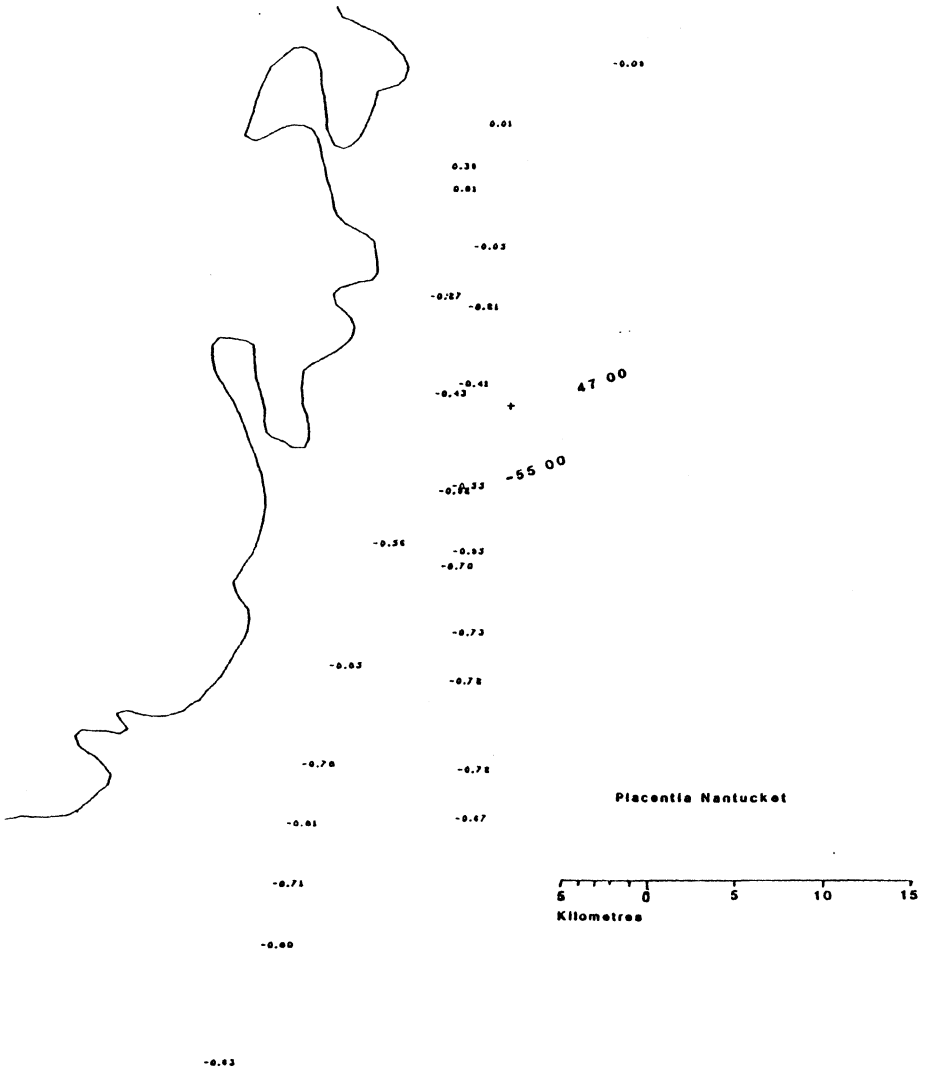
47 00
-55 00
Placentia Nantucket
5 0 5 10 15
Kilometres


47 00
-54 00

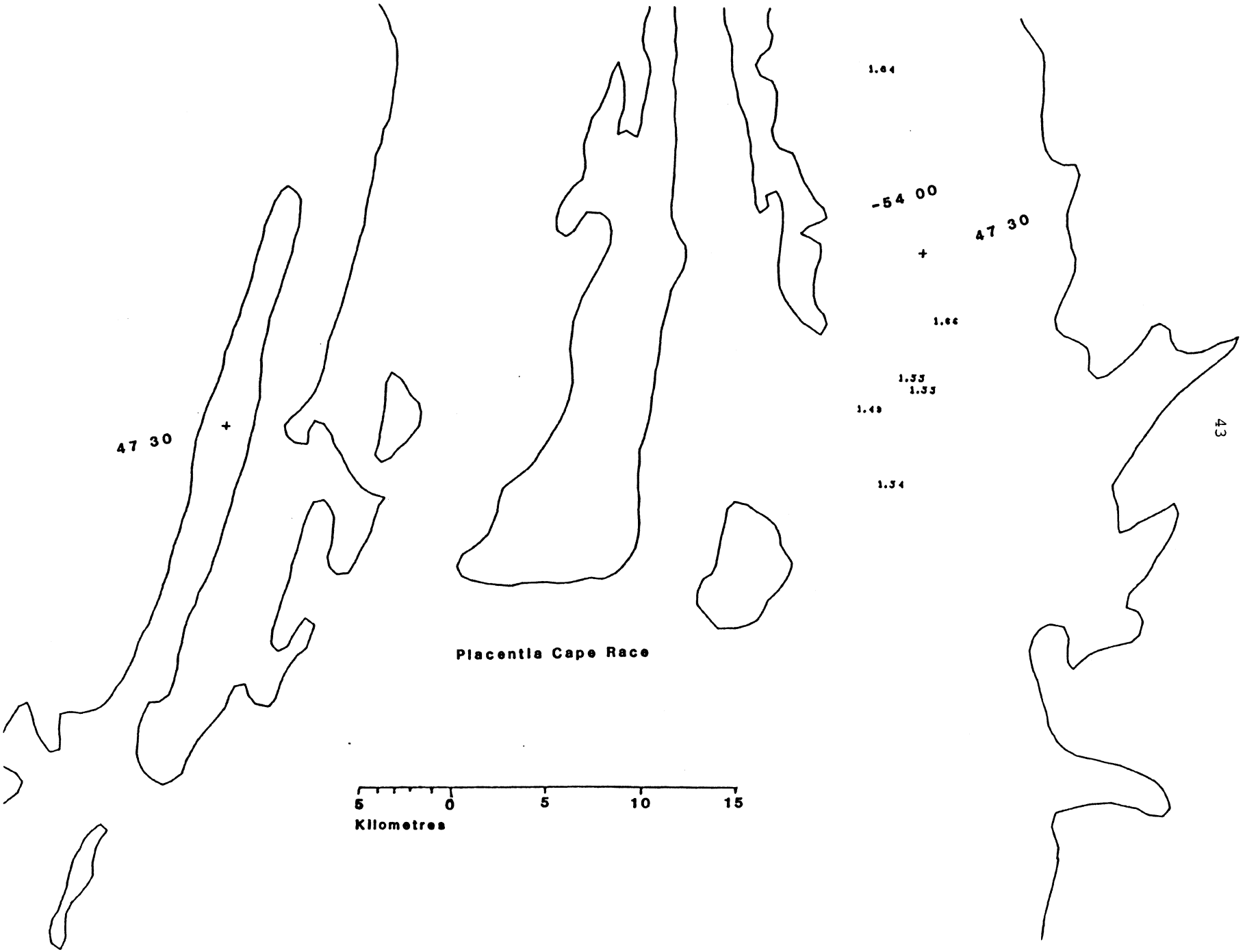
1.64
-54 00
47 30
1.66
1.55
1.55
1.48
1.54
47 30
Placentia Cape Race
5 0 5 10 15
Kilometres

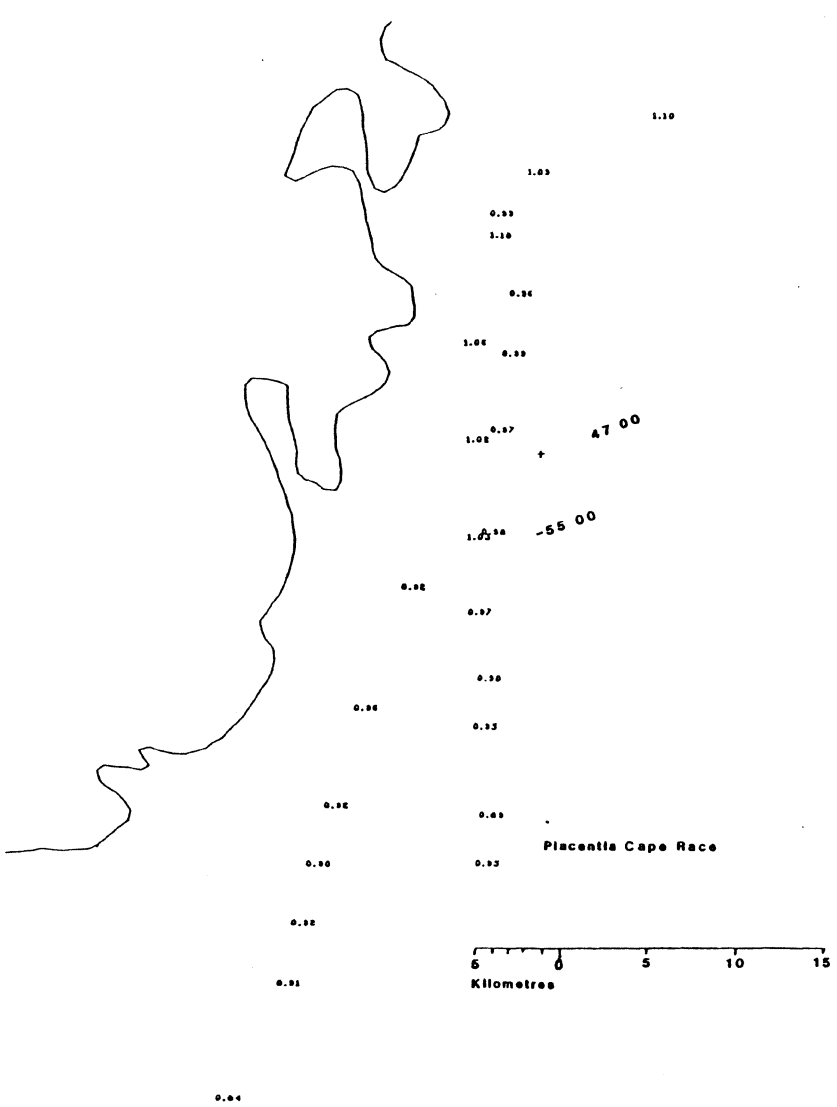
47 00
-55 00
Placentia Cape Race
5 0 5 10 15
Kilometres

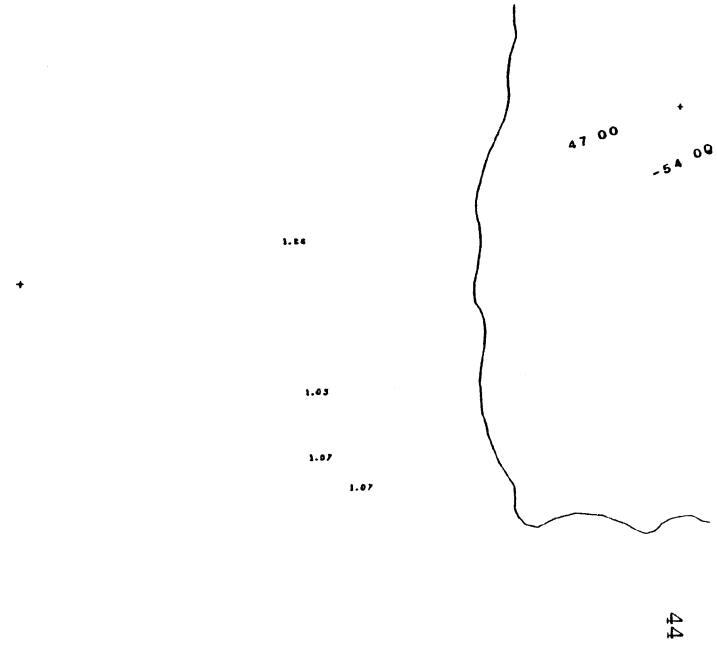
47 00
-54 00

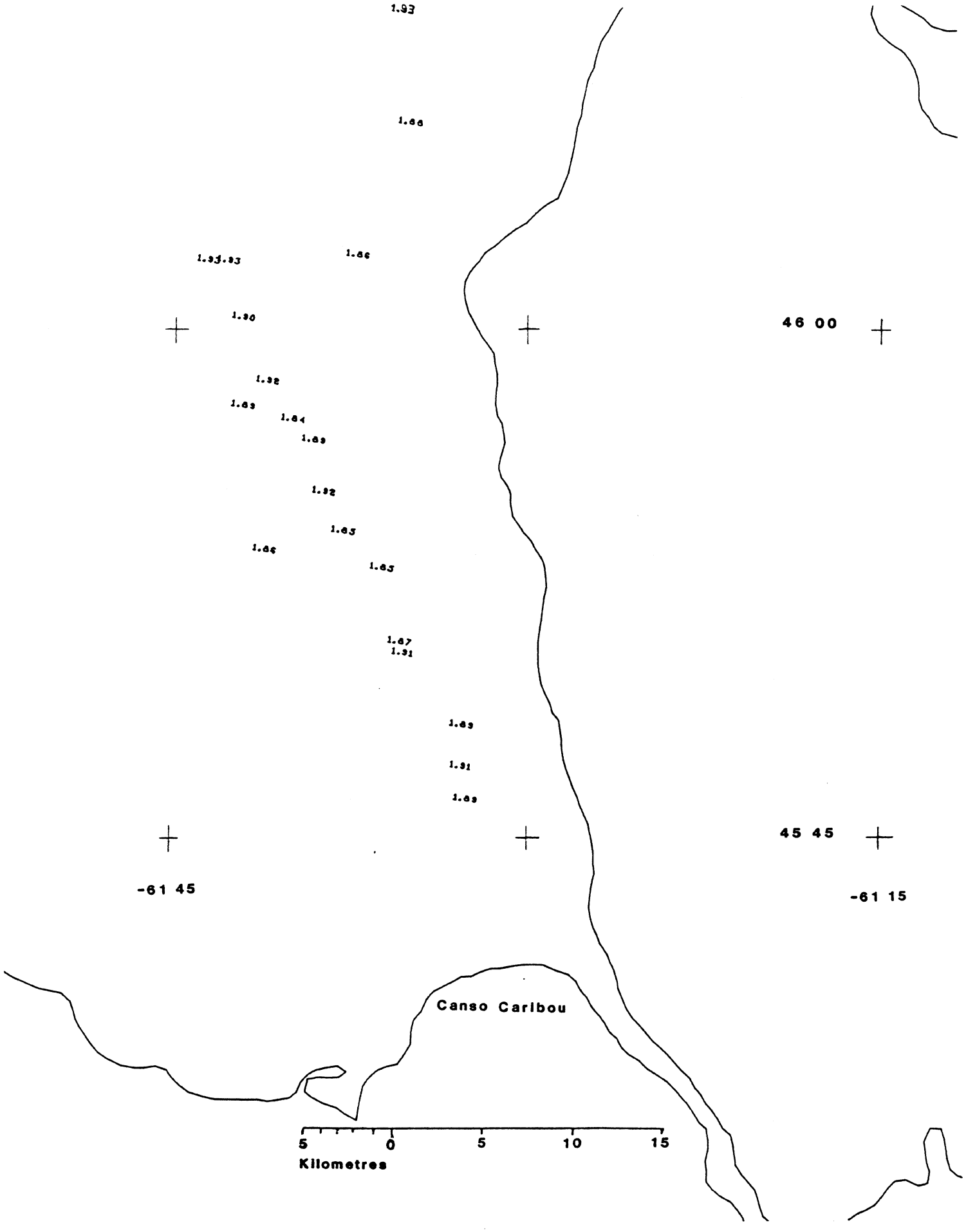
1.93
1.86
1.93 1.93
1.86
1.90
46 00
1.92
1.89
1.84
1.89
1.92
1.85
1.86
1.85
1.87
1.91
1.89
1.91
1.89
45 45
-61 45
-61 15
Canso Caribou
5 0 5 10 15
Kilometres

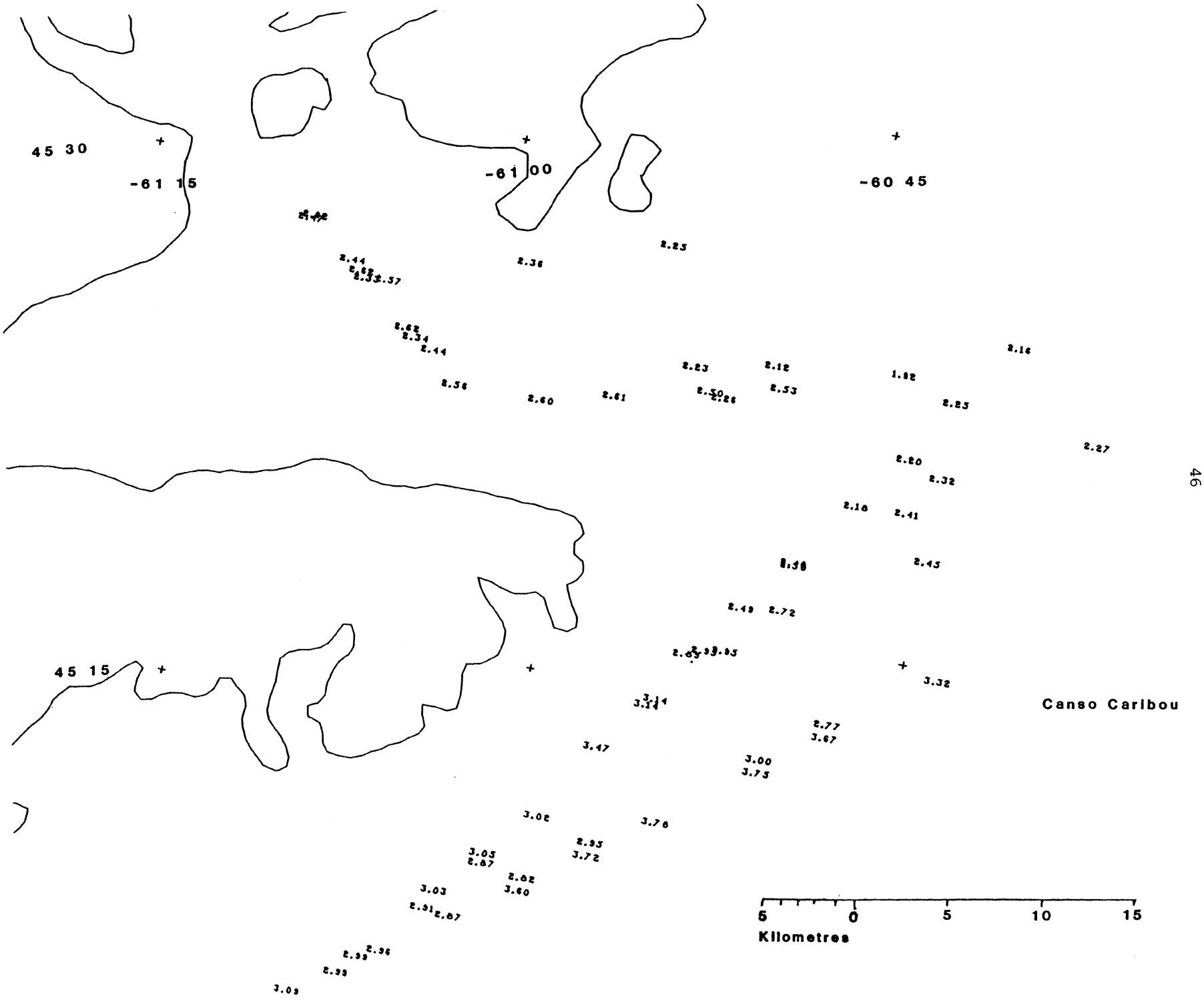
45 30
-61 15
-61 00
-60 45
45 15
2.42
2.44
2.62
2.32
2.37
2.36
2.23
2.62
2.34
2.44
2.56
2.60
2.61
2.50
2.26
2.23
2.12
2.53
1.82
2.16
2.25
2.27
2.20
2.32
2.16
2.41
2.38
2.43
2.49
2.72
2.99
2.85
3.32
3.14
3.47
2.77
3.67
3.00
3.75
3.02
3.76
2.95
3.72
3.05
2.87
2.82
3.60
3.03
2.91
2.87
2.96
2.93
2.93
3.03
Canso Caribou
5
0
5
10
15
Kilometres

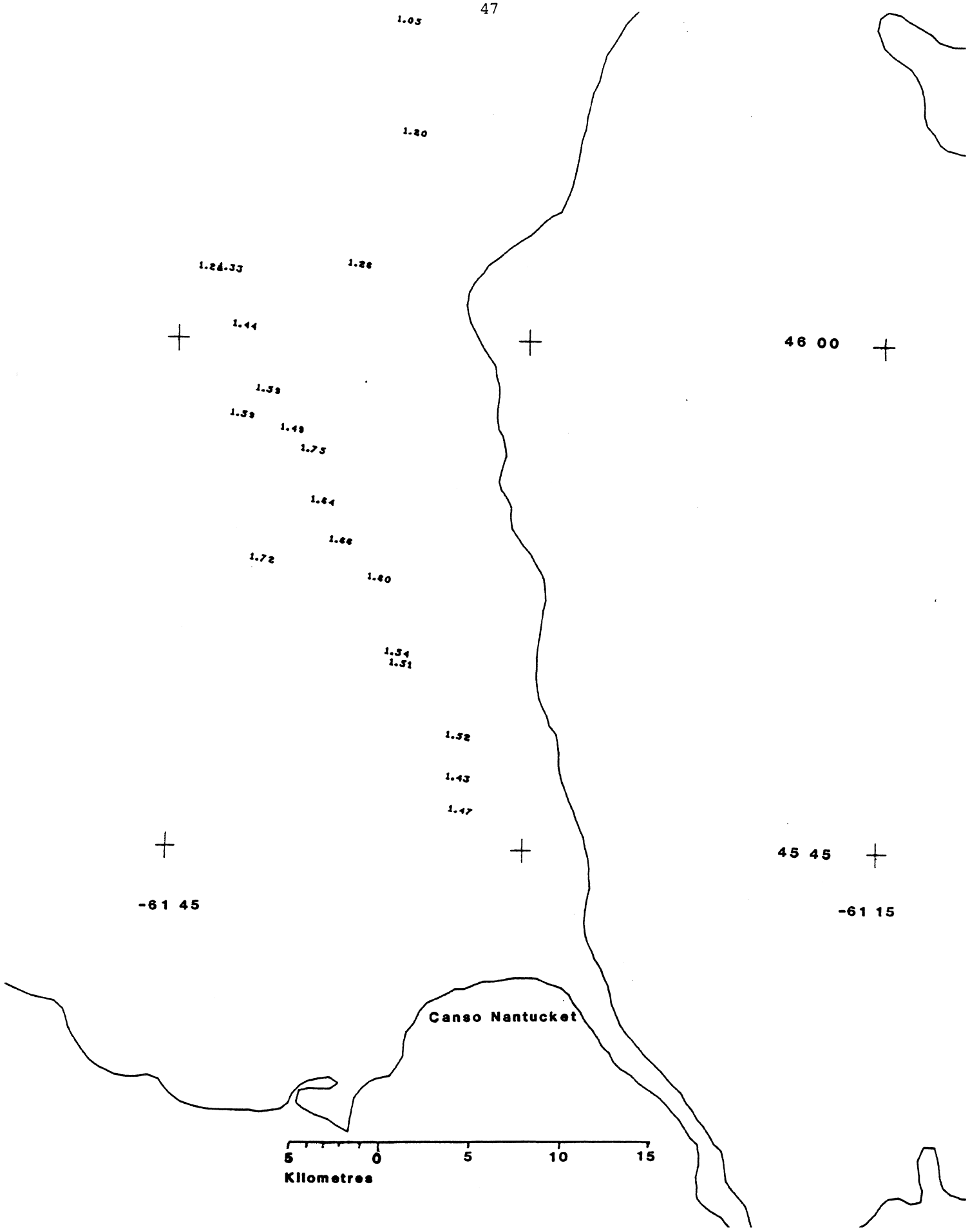
1.03
1.20
1.24 1.33
1.26
1.44
46 00
1.39
1.38
1.48
1.75
1.64
1.66
1.72
1.60
1.54
1.51
1.52
1.43
1.47
45 45
-61 45
-61 15
Canso Nantucket
5 0 5 10 15
Kilometres

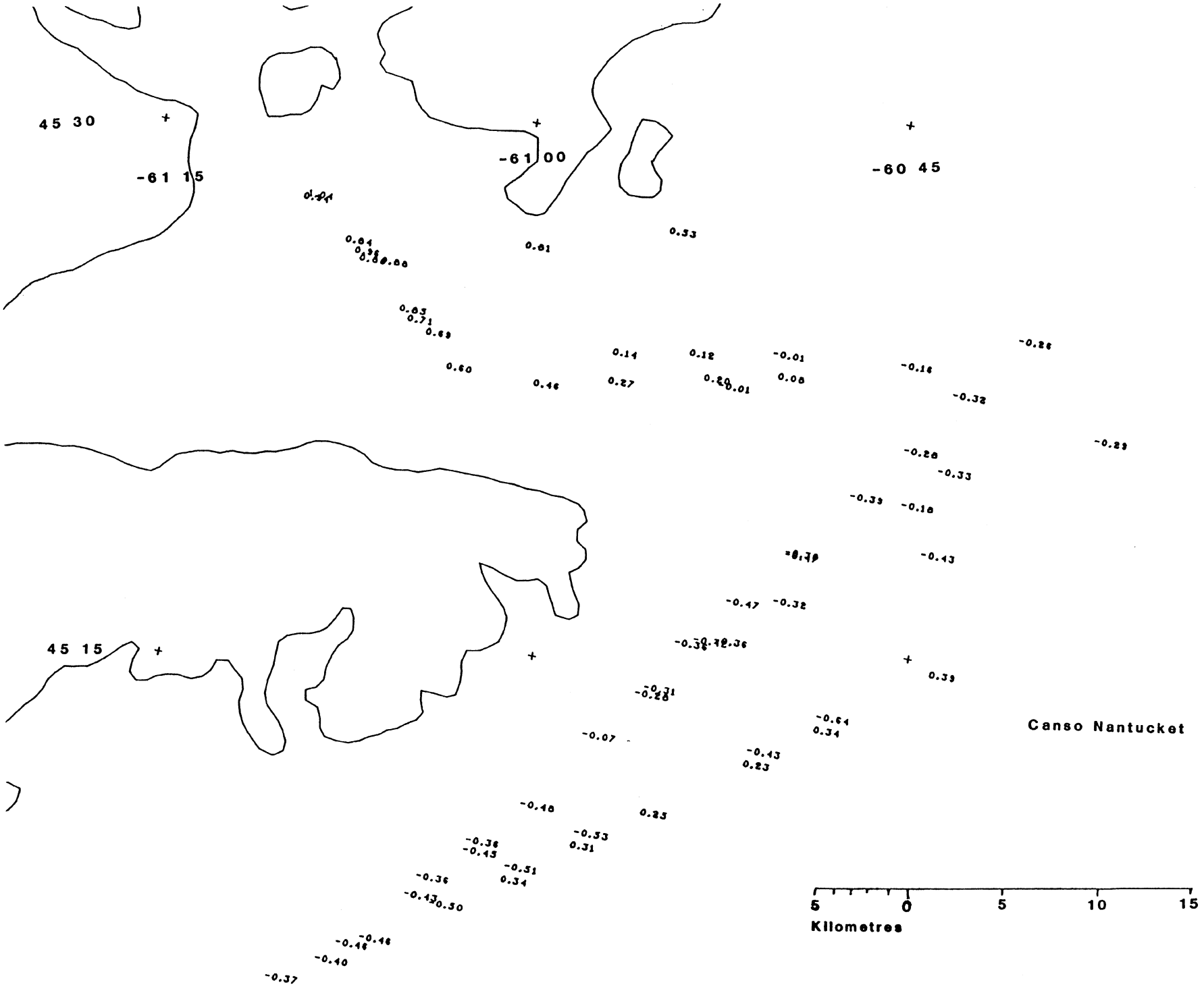
45 30
-61 15
-61 00
-60 45
45 15
0.33
0.61
0.63
0.71
0.69
0.60
0.46
0.14
0.12
-0.01
0.27
0.01
0.08
-0.16
-0.26
-0.32
-0.23
-0.28
-0.33
-0.39
-0.18
-0.43
-0.47
-0.32
0.39
-0.64
0.34
-0.07
-0.43
0.23
-0.48
0.23
-0.53
0.31
-0.36
-0.43
-0.51
0.34
-0.36
-0.43
0.30
-0.46
-0.40
-0.37
Canso Nantucket
5 0 5 10 15
Kilometres

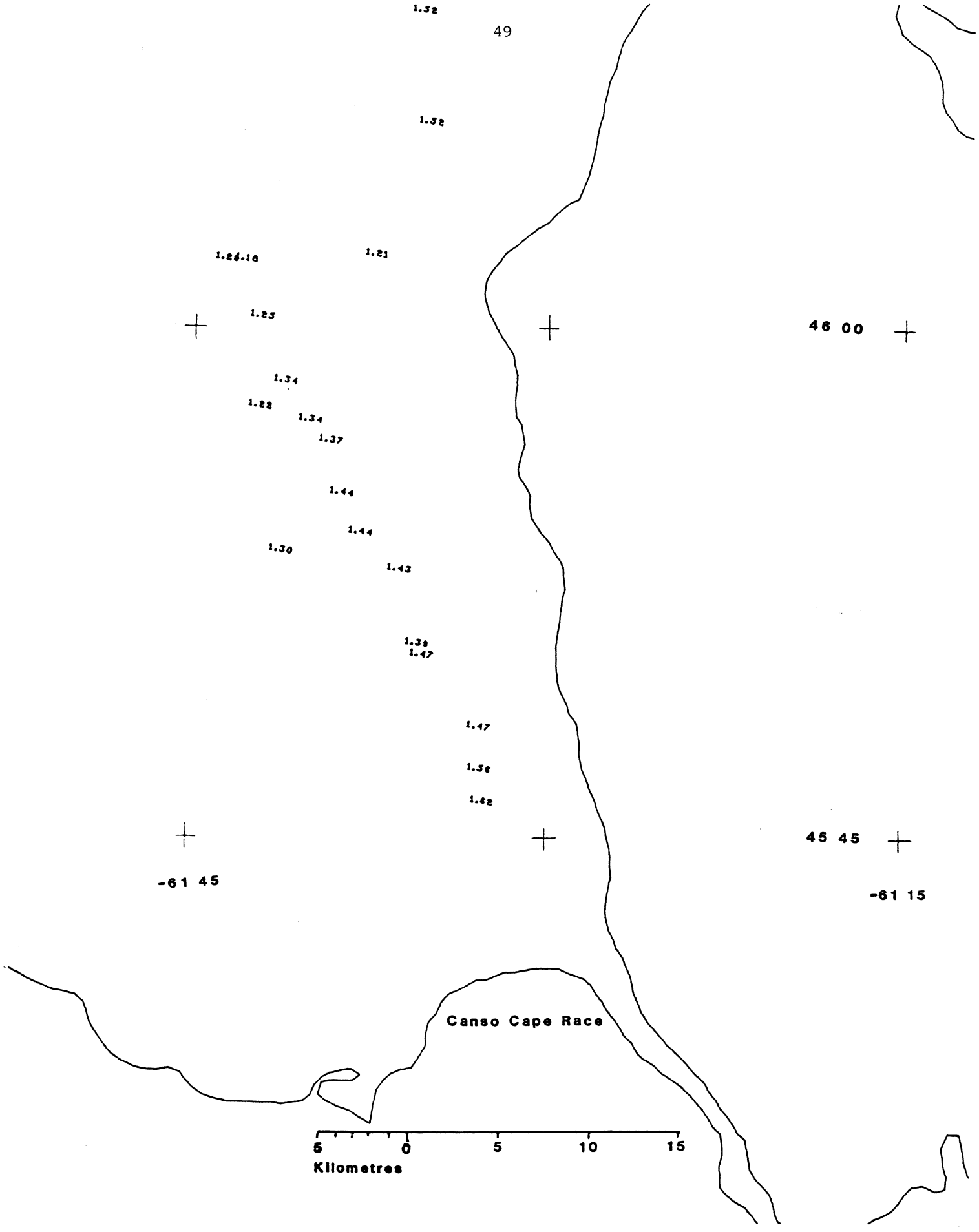
1.32
1.32
1.26
1.16
1.21
1.23
46 00
1.34
1.28
1.34
1.37
1.44
1.44
1.30
1.43
1.38
1.47
1.47
1.56
1.42
45 45
-61 45
-61 15
Canso
Cape Race
5
0
5
10
15
Kilometres

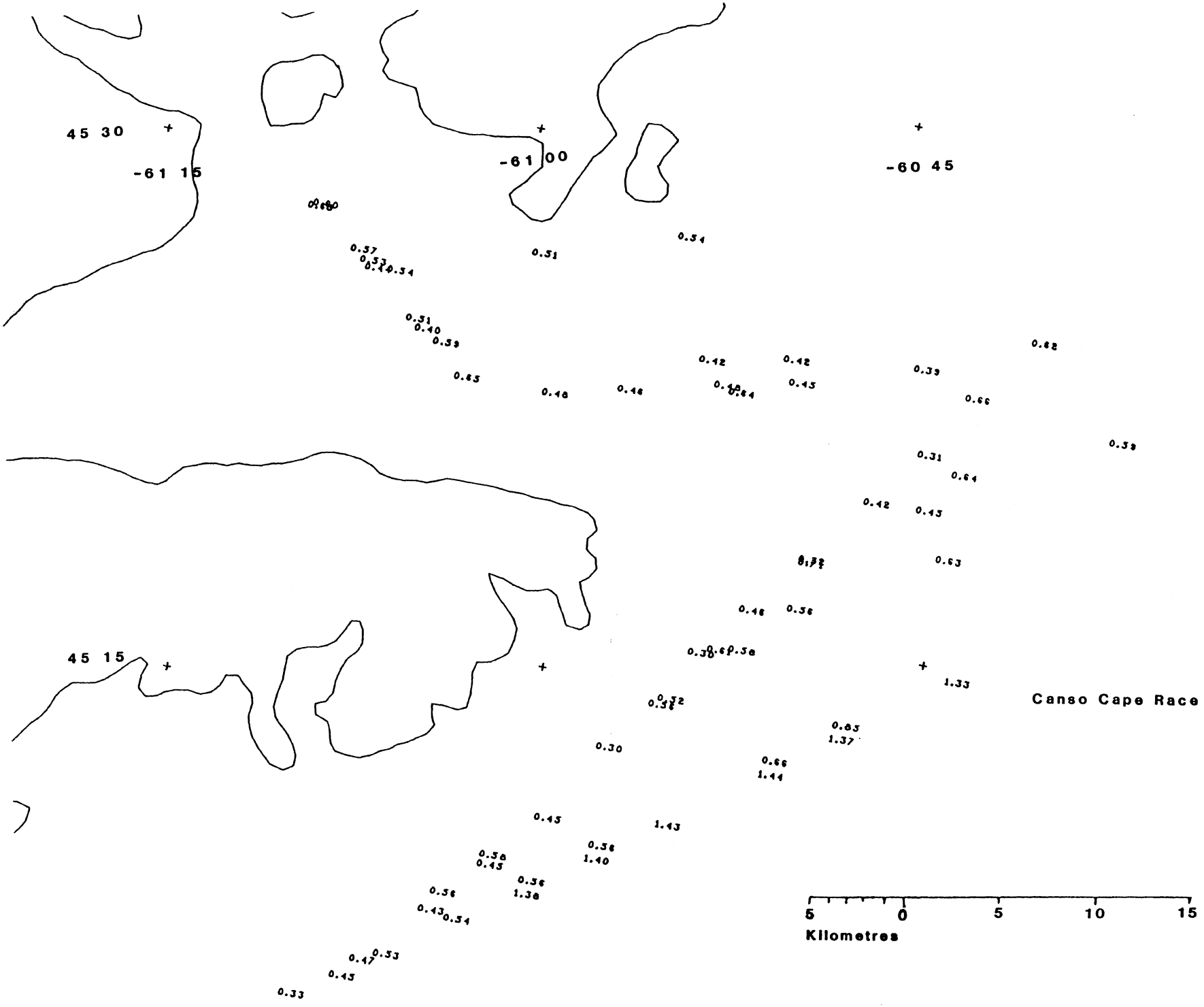
45 30
-61 15
-61 00
-60 45
45 15
Canso Cape Race
5 0 5 10 15
Kilometres

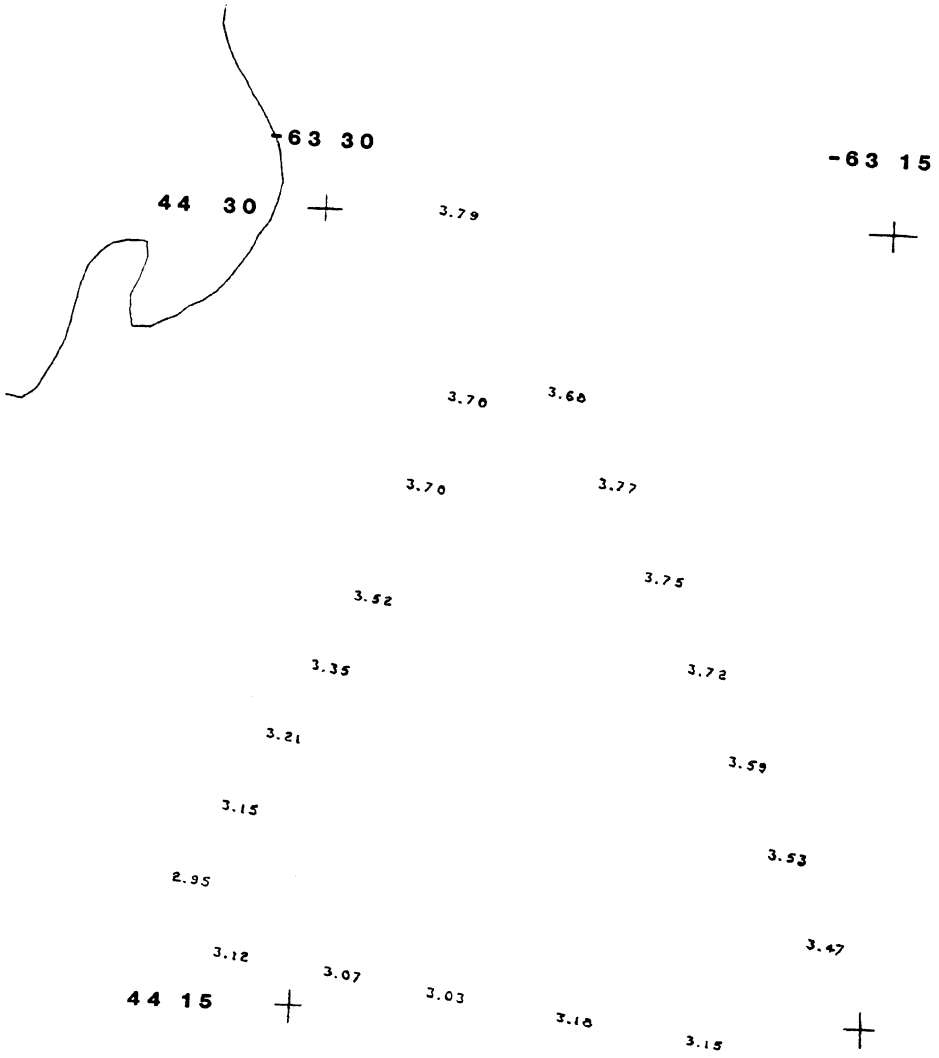

Halifax Caribou

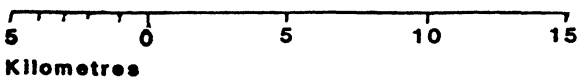

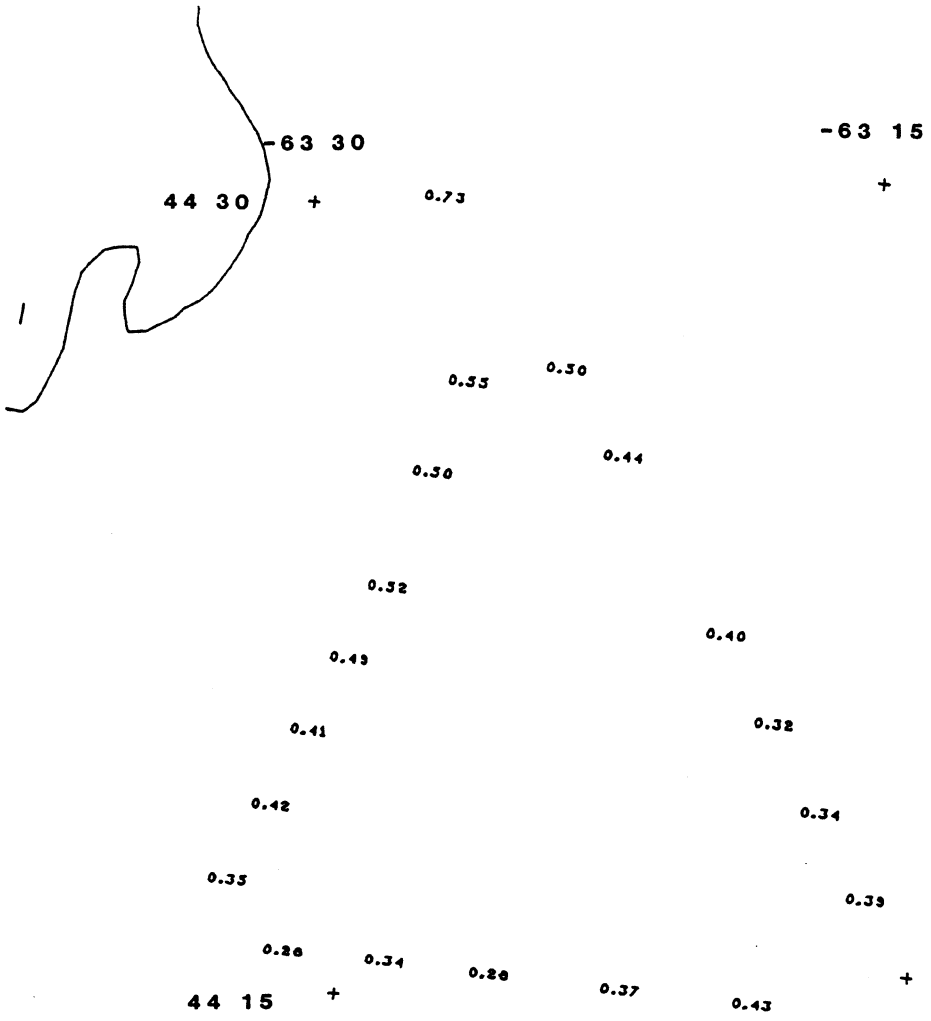
-63 30
-63 15
44 30
0.73
0.55
0.50
0.44
0.30
0.52
0.40
0.43
0.41
0.32
0.42
0.34
0.35
0.39
0.26
0.34
0.26
0.37
0.43
44 15
Halifax Nantucket
5 0 5 10 15
Kilometres

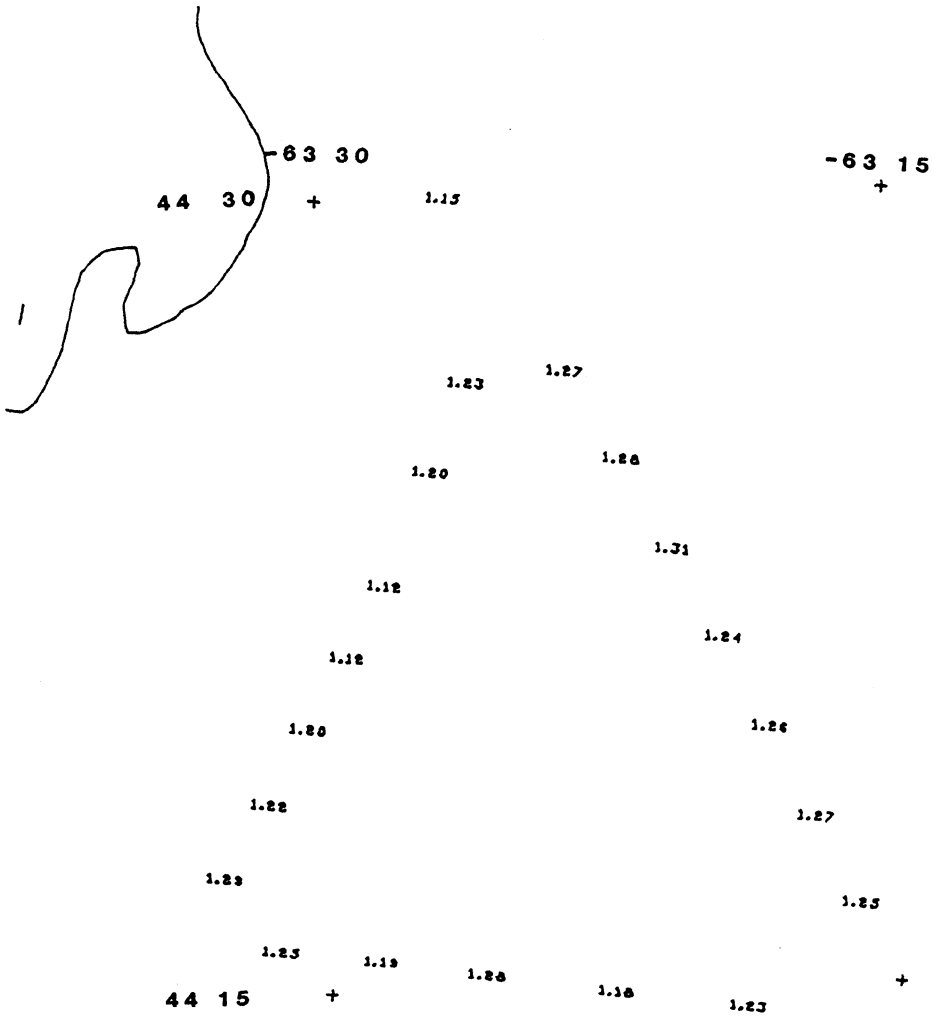
-63 30
-63 15
44 30
1.15
1.23
1.27
1.20
1.28
1.31
1.12
1.24
1.18
1.26
1.28
1.22
1.27
1.23
1.25
1.25
1.19
1.28
1.18
1.23
44 15
Halifax Cape Race
5 0 5 10 15
Kilometres

APPENDIX III

PLOTS OF RESIDUAL ASF

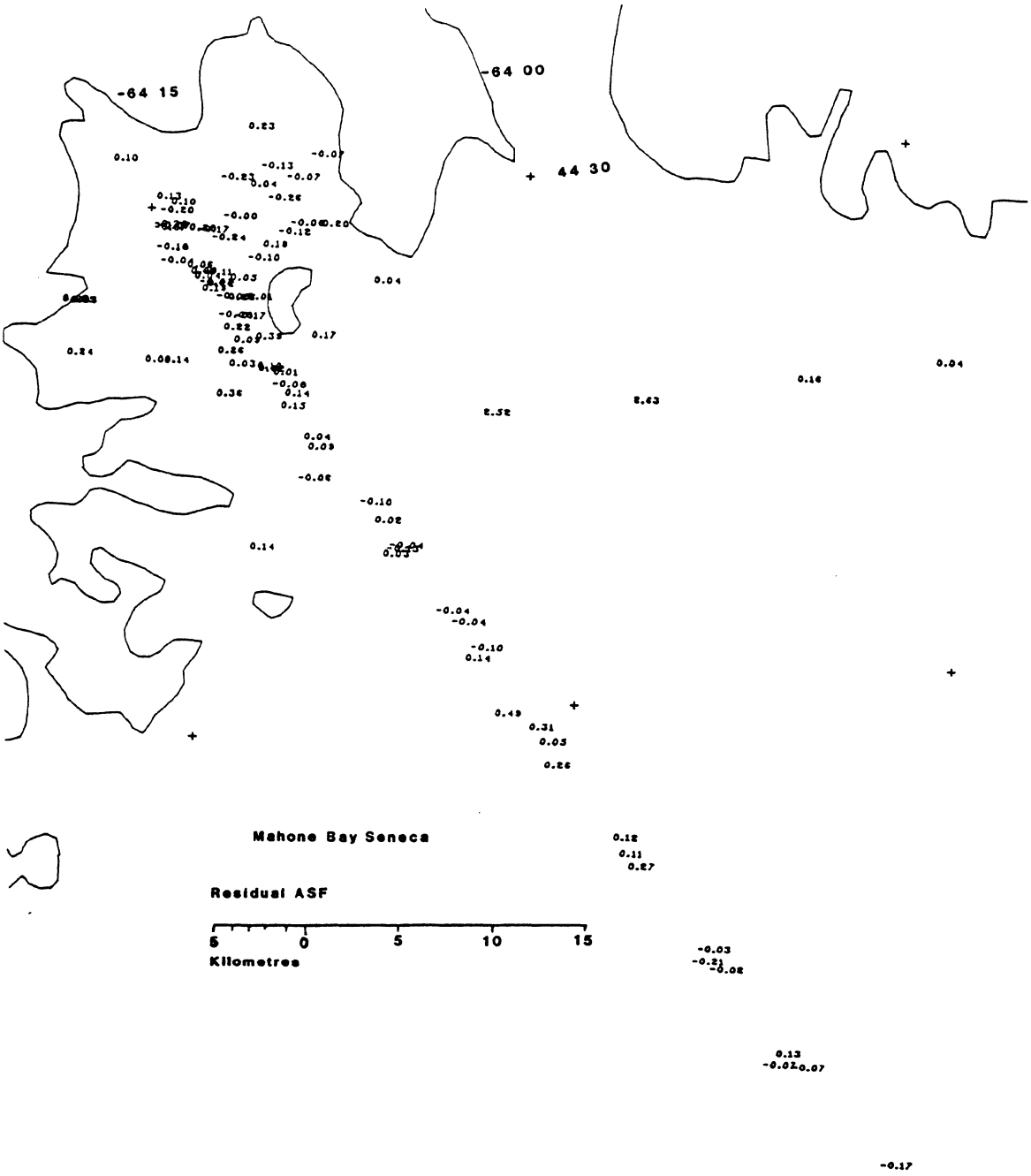
-64 15
-64 00
44 30
Mahone Bay Seneca
Residual ASF
5 0 5 10 15
Kilometres

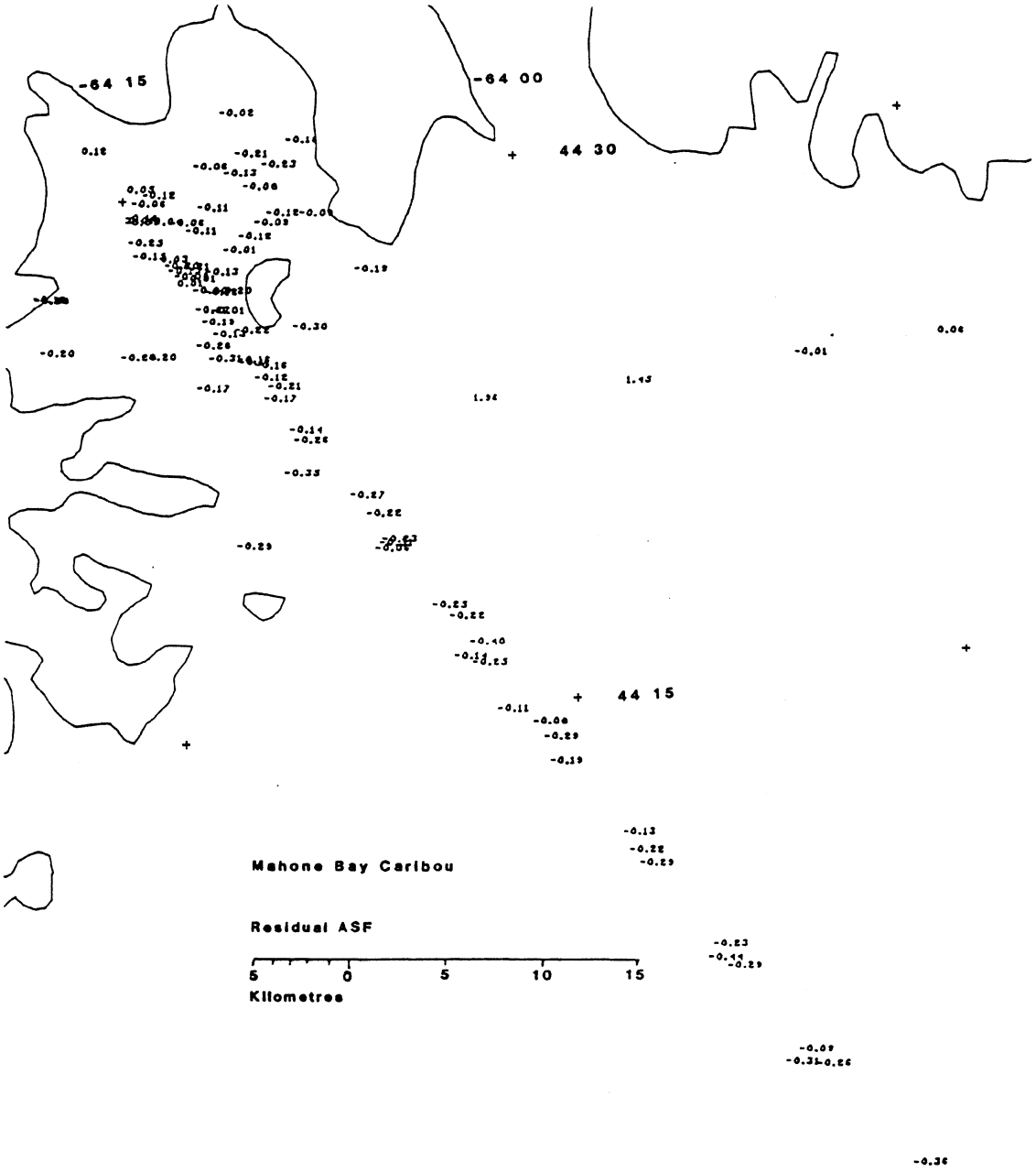
-64 15
-64 00
44 30
44 15
Mahone Bay Caribou
Residual ASF
5 0 5 10 15
Kilometres

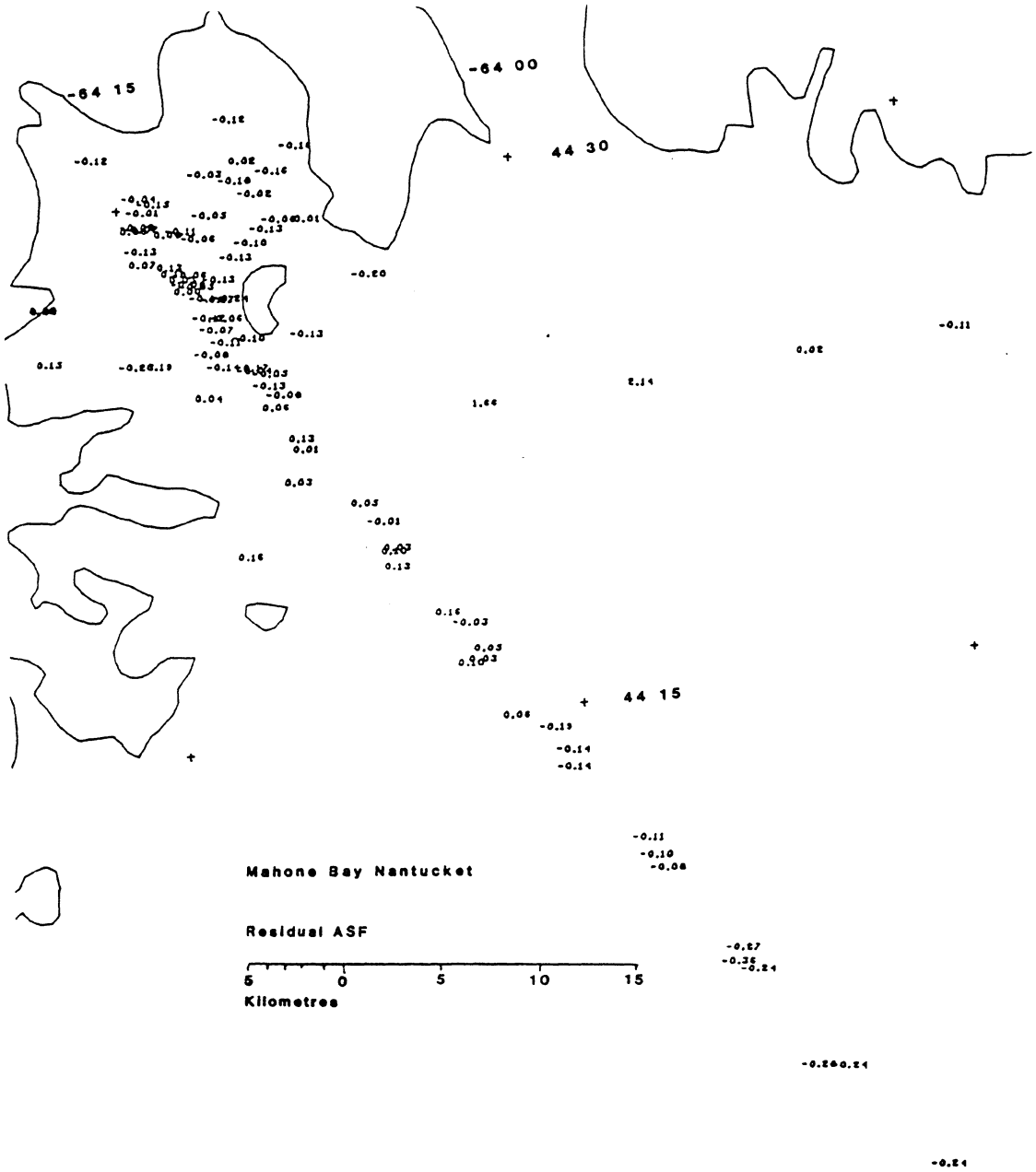
-64 15
-64 00
44 30
44 15
Mahone Bay Nantucket
Residual ASF
5 0 5 10 15
Kilometres

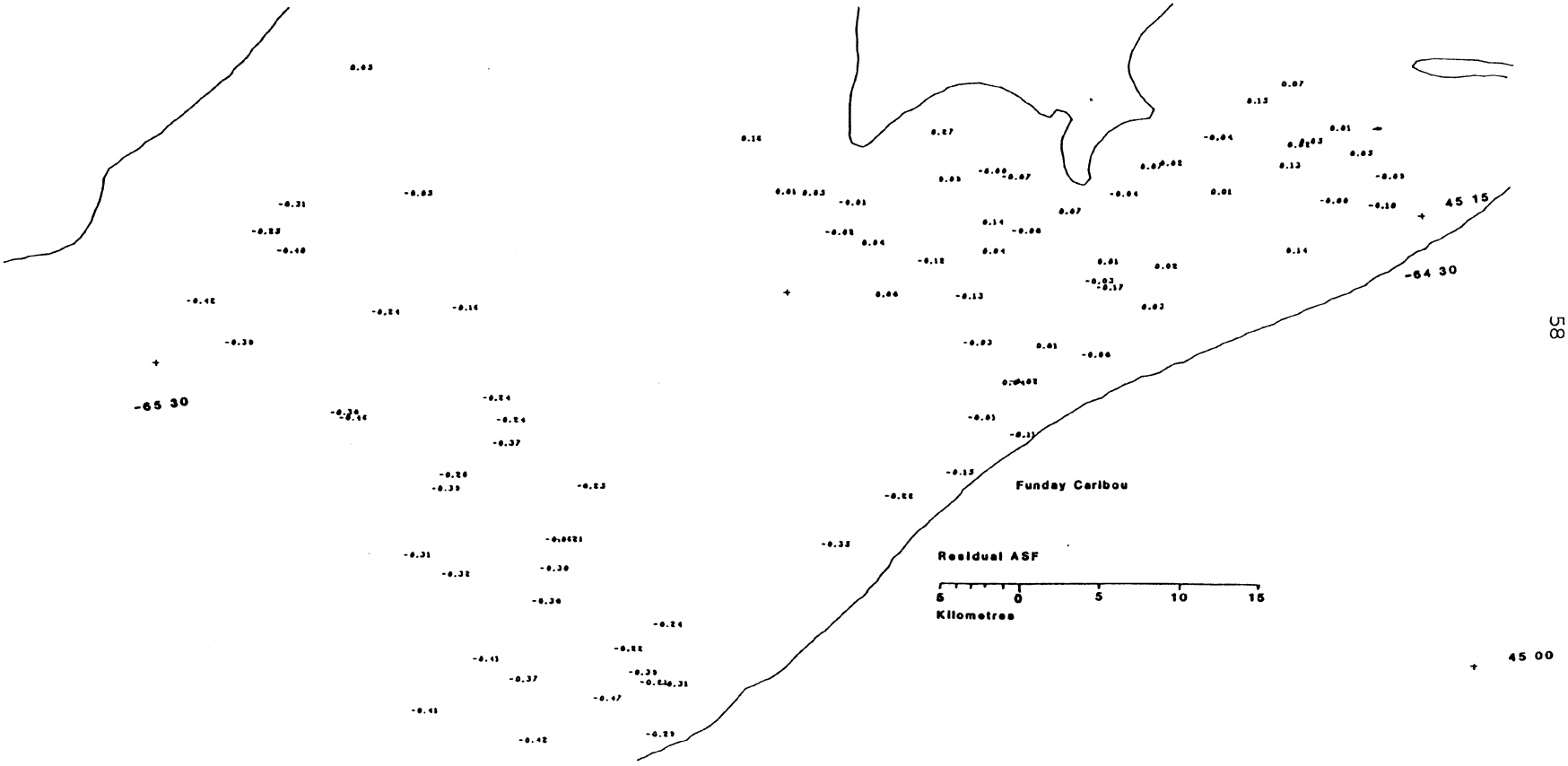
-65 30
45 15
-64 30
45 00
Funday Caribou
Residual ASF
5 0 5 10 15
Kilometres

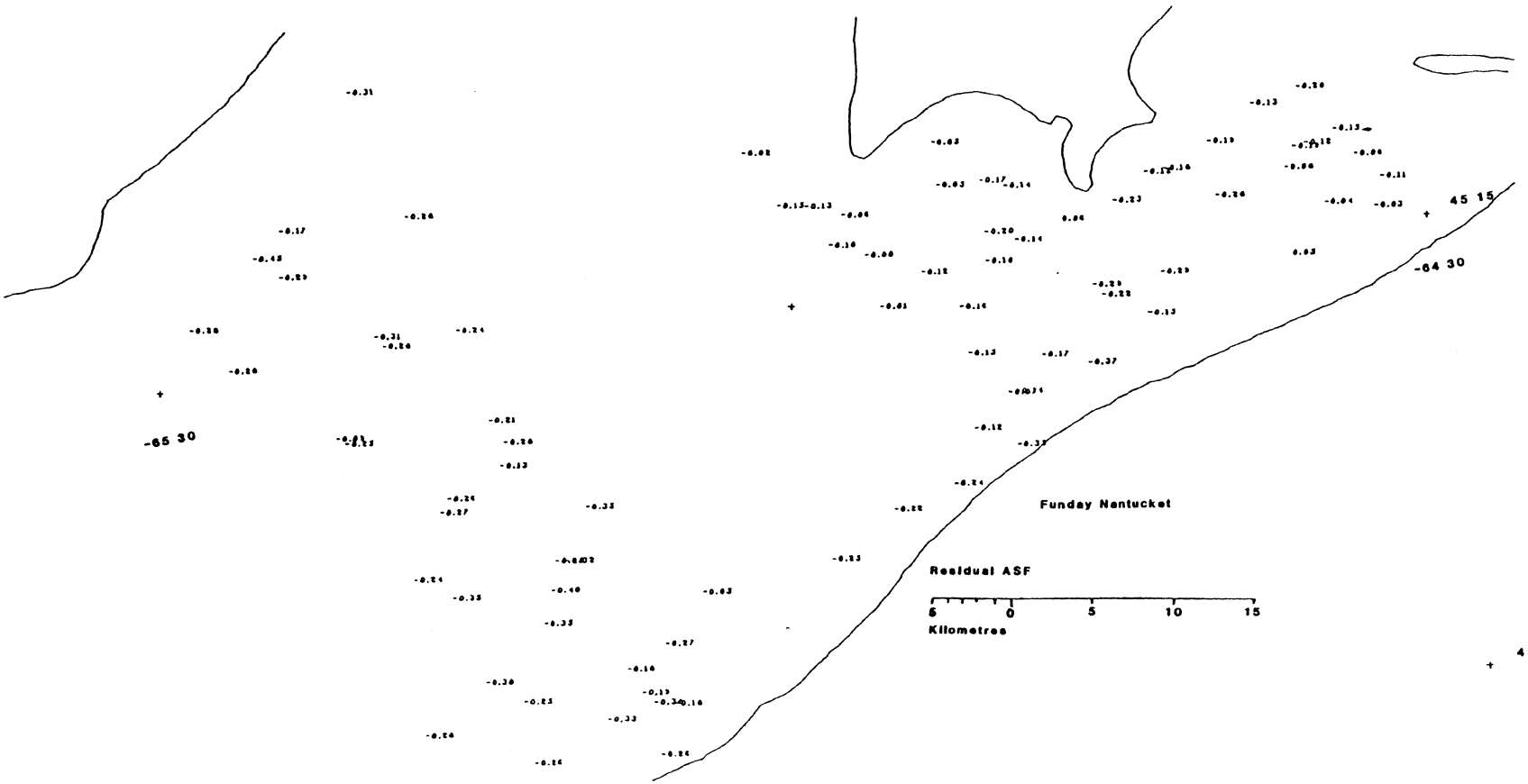
-65 30
45 15
-64 30
45 00
Funday Nantucket
Residual ASF
5 0 5 10 15
Kilometres

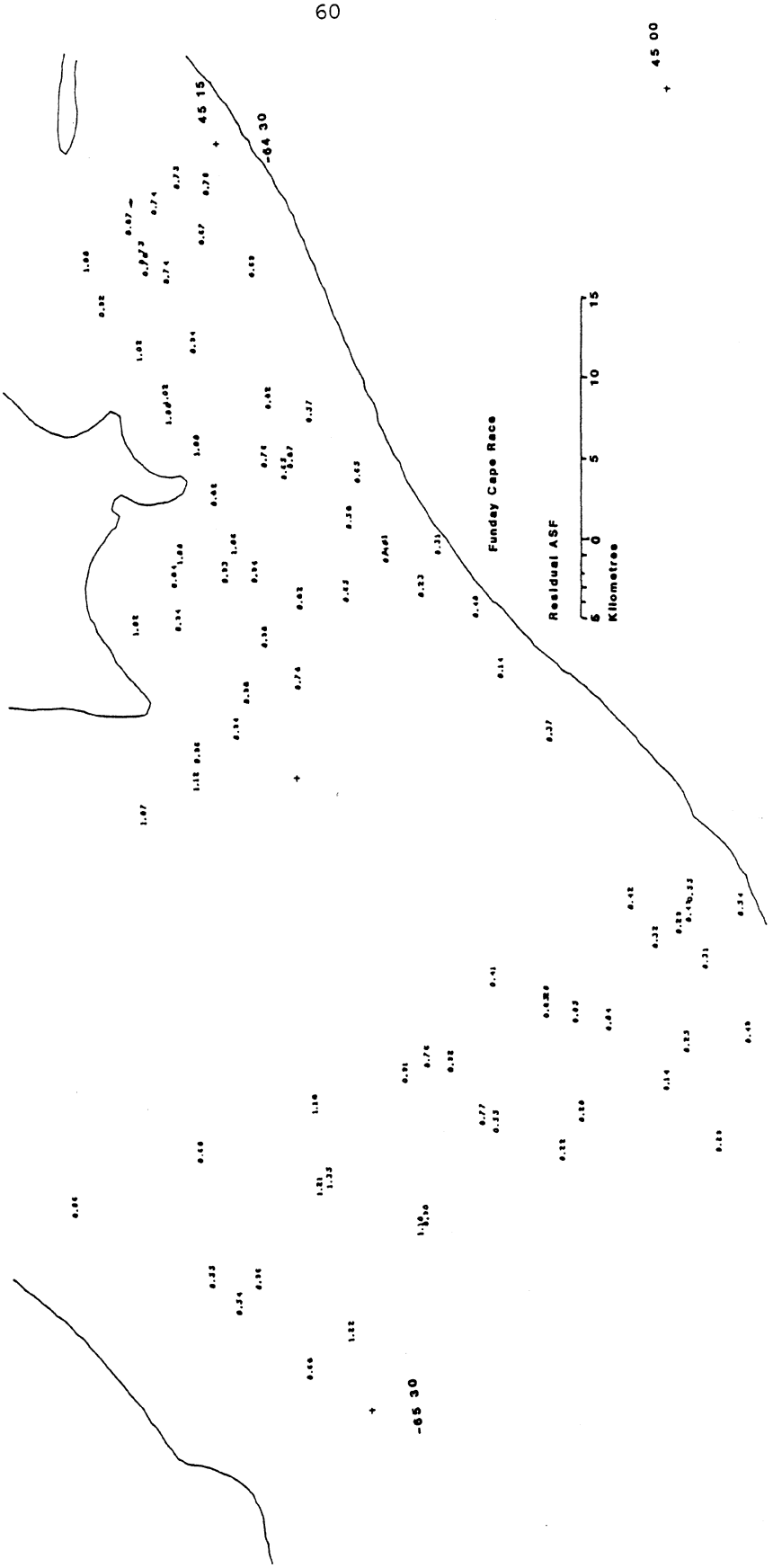
45 00
45 15
-64 30
-65 30
Fundy Cape Race
Residual ASF
0 5 10 15
Kilometres

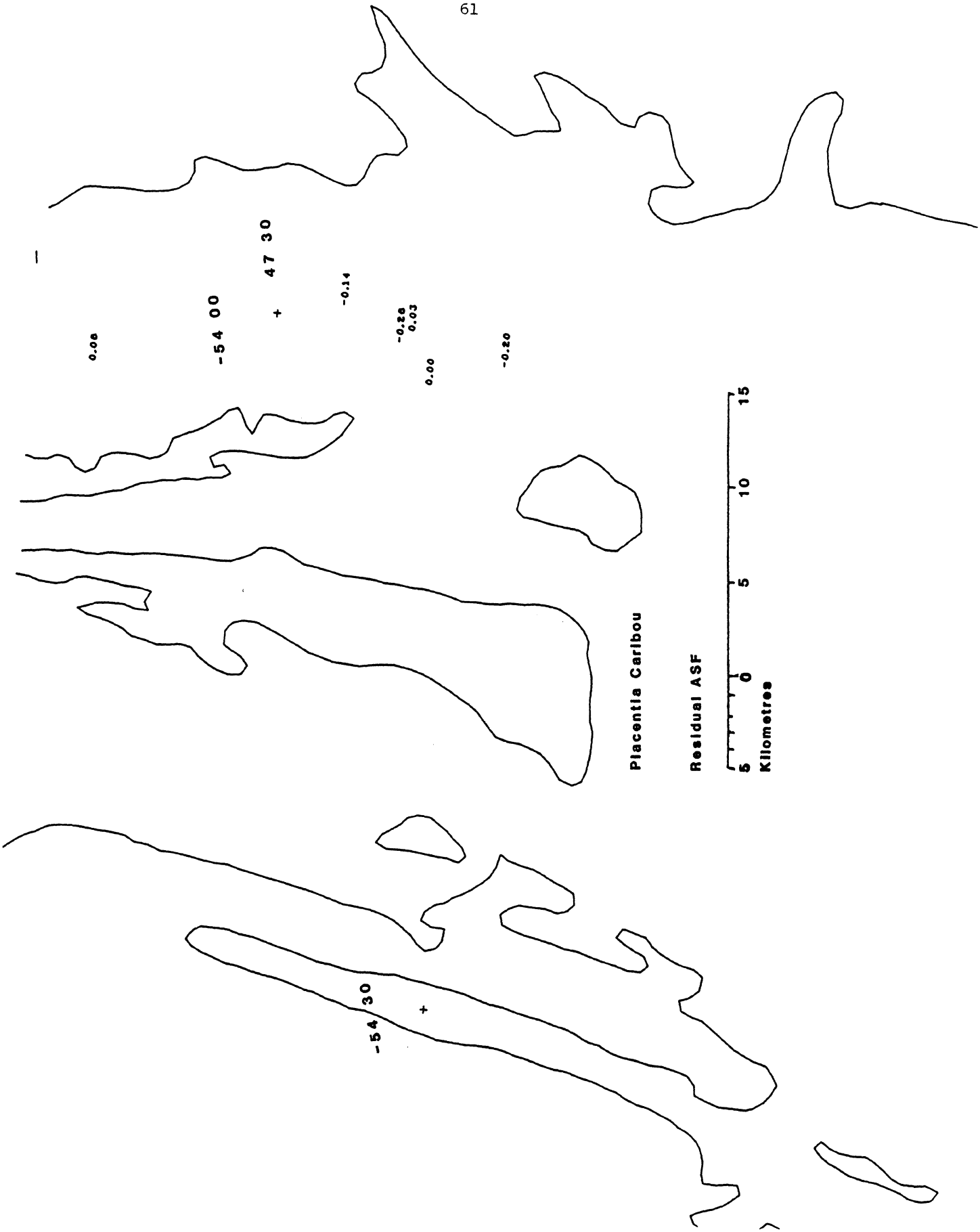
47 30
-54 00
-54 30
0.06
-0.14
-0.26
0.03
0.00
-0.20
Placentia Caribou
Residual ASF
5 0 5 10 15
Kilometres

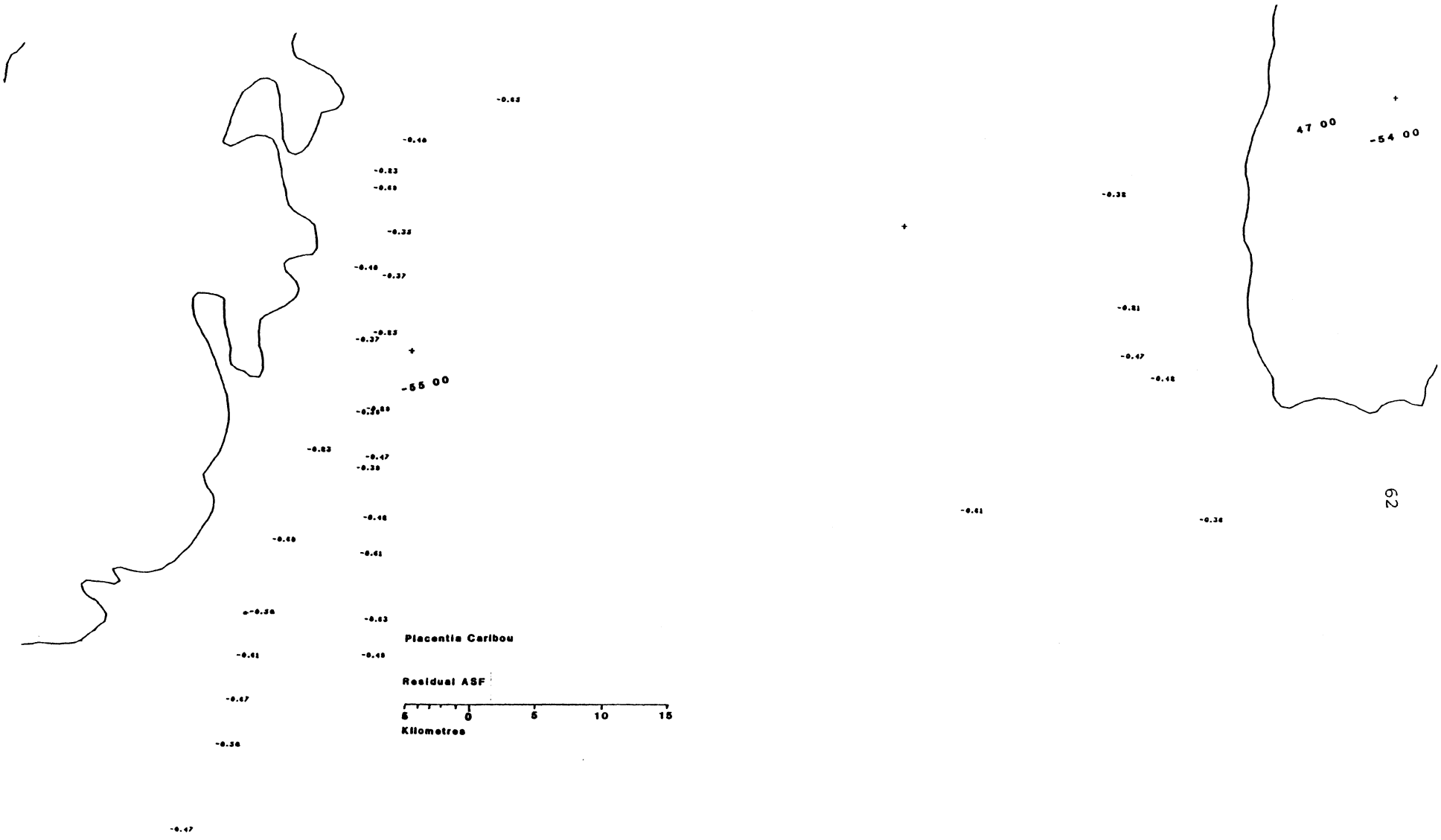
-0.63
-0.46
-0.83
-0.68
-0.35
-0.46
-0.37
-0.83
-0.37
-55 00
-0.83
-0.47
-0.38
-0.46
-0.46
-0.61
-0.38
-0.63
-0.61
-0.48
-0.47
-0.36
-0.47
Placentia Caribou
Residual ASF
5 0 5 10 15
Kilometres
47 00
-54 00
-0.38
-0.81
-0.47
-0.48
-0.61
-0.36

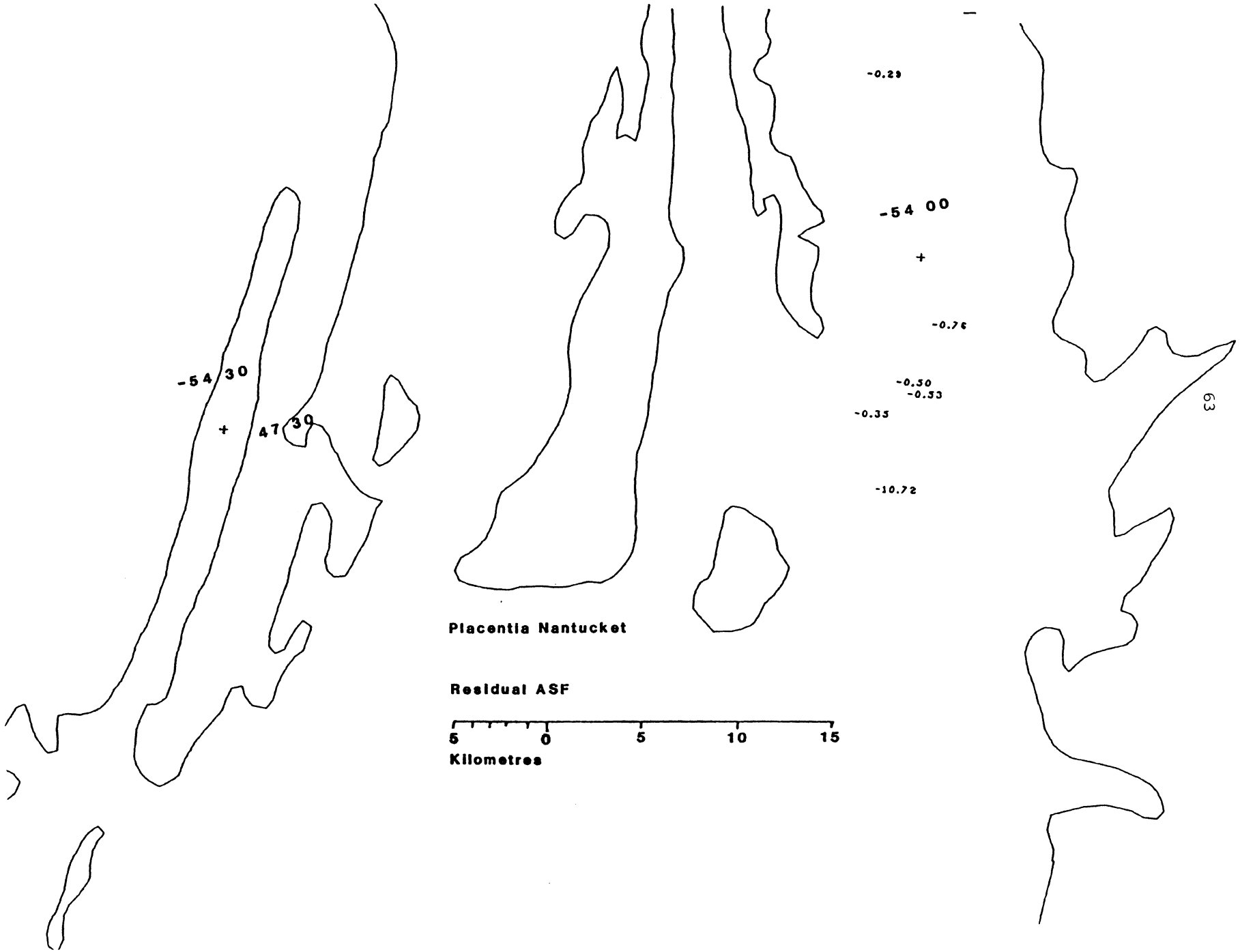
-54 30
47 30
-0.29
-54 00
-0.76
-0.50
-0.53
-0.35
-10.72
Placentia Nantucket
Residual ASF
5 0 5 10 15
Kilometres

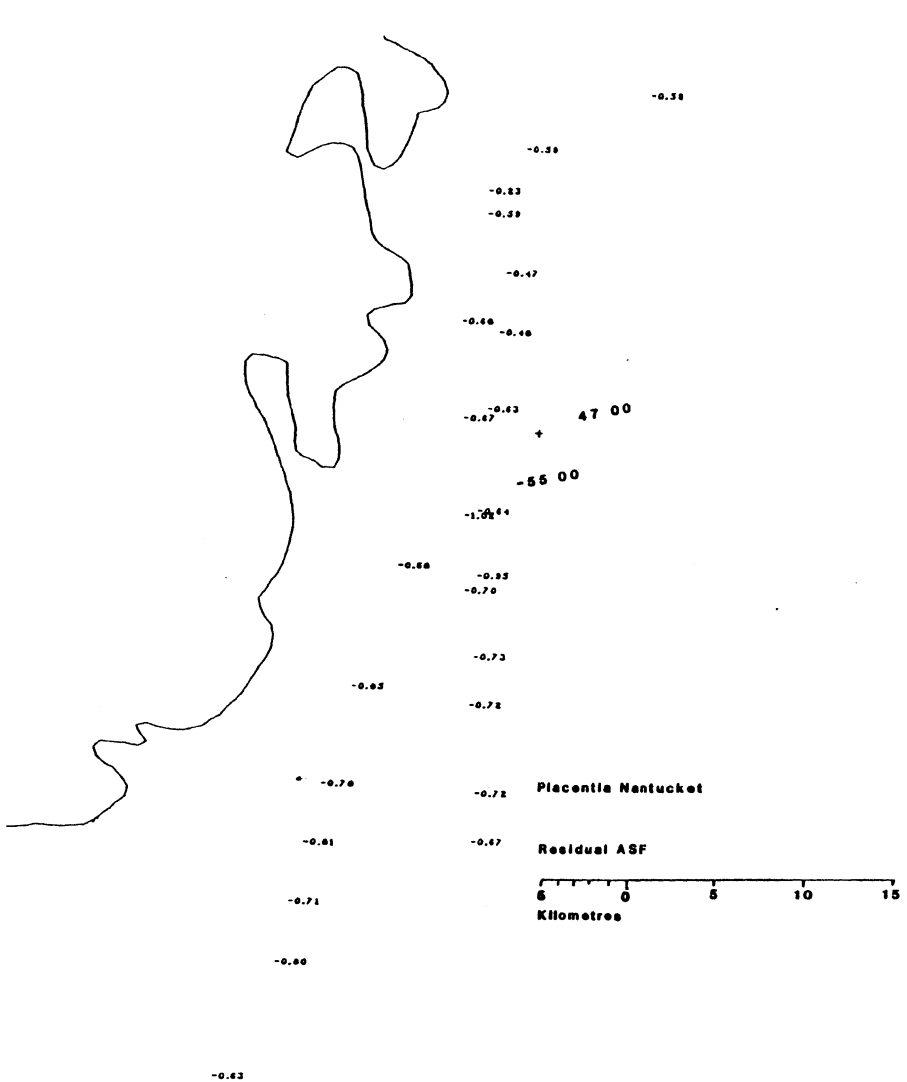
-0.58
-0.58
-0.83
-0.59
-0.47
-0.66
-0.66
-0.63
-0.67
47 00
-55 00
-1.04
-0.66
-0.85
-0.70
-0.73
-0.65
-0.72
-0.70
-0.72
-0.61
-0.67
-0.71
-0.66
-0.63
Placentia Nantucket
Residual ASF
5 0 5 10 15
Kilometres

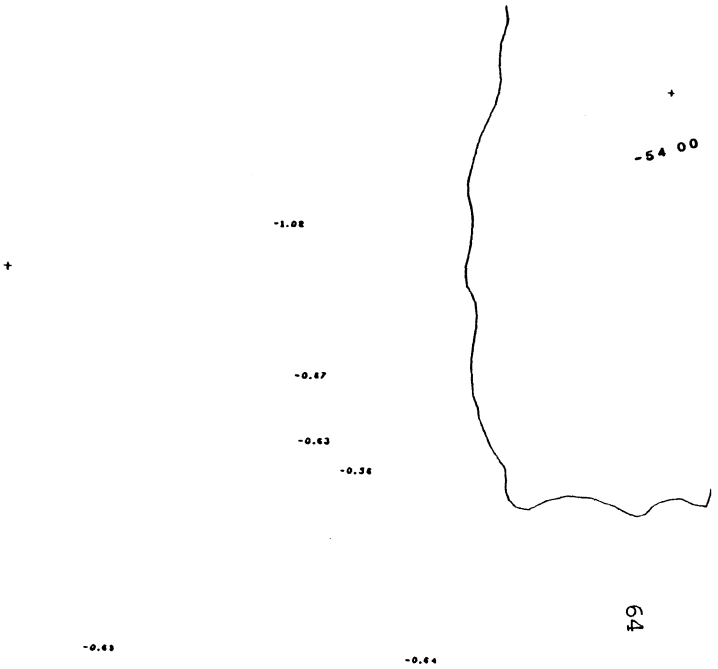
-54 00
-1.08
-0.67
-0.63
-0.36
-0.63
-0.64

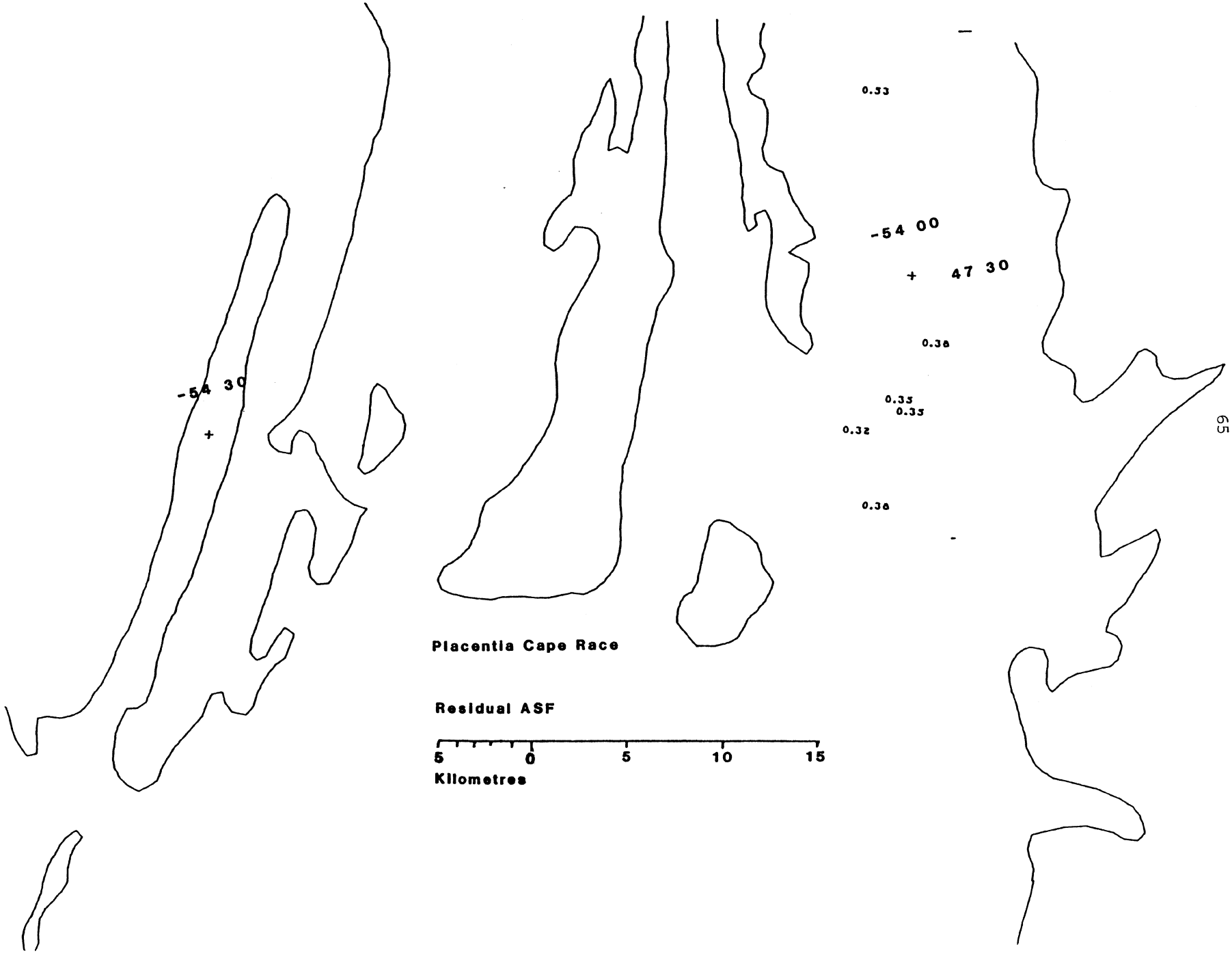
-54 30
0.33
-54 00
47 30
0.36
0.35
0.35
0.32
0.36
Placentia Cape Race
Residual ASF
5
0
5
10
15
Kilometres

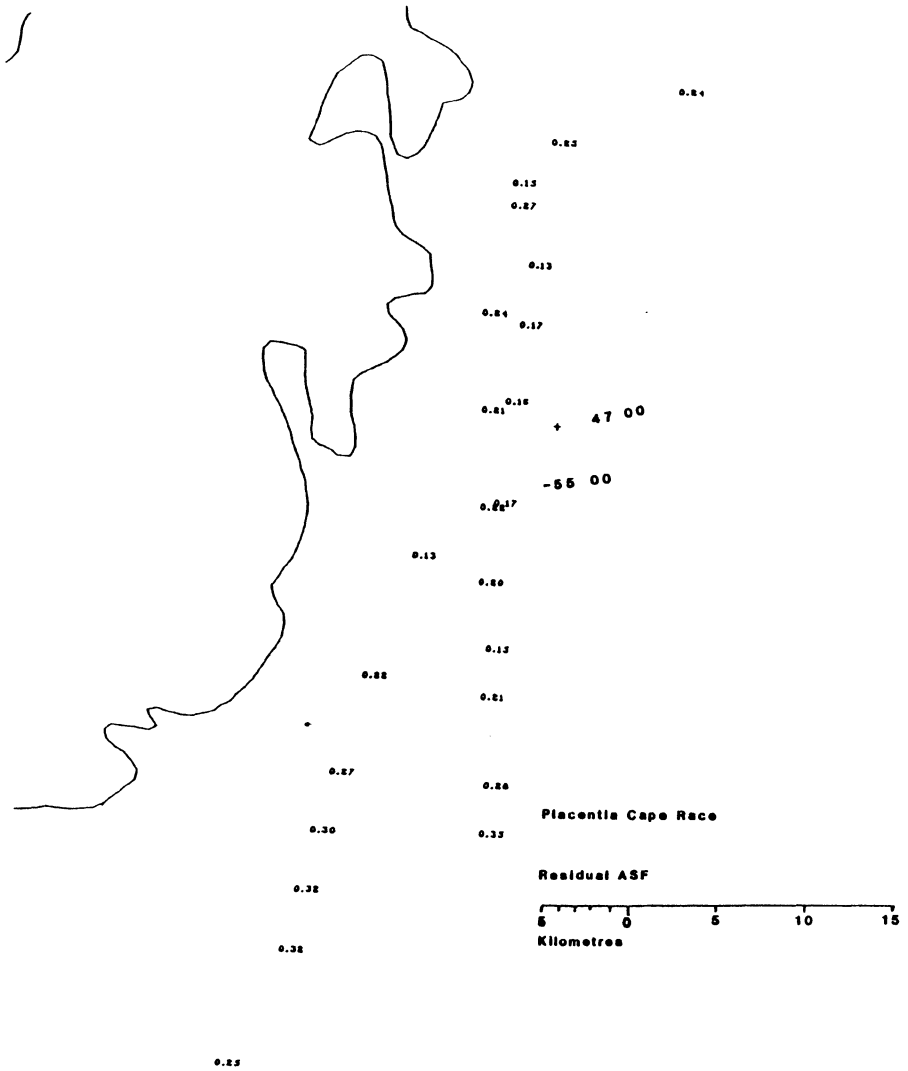
47 00
-55 00
Placentia Cape Race
Residual ASF
5 0 5 10 15
Kilometres

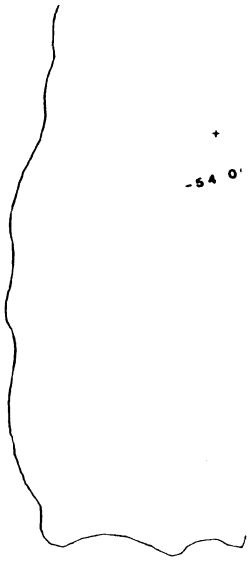
-54 0'

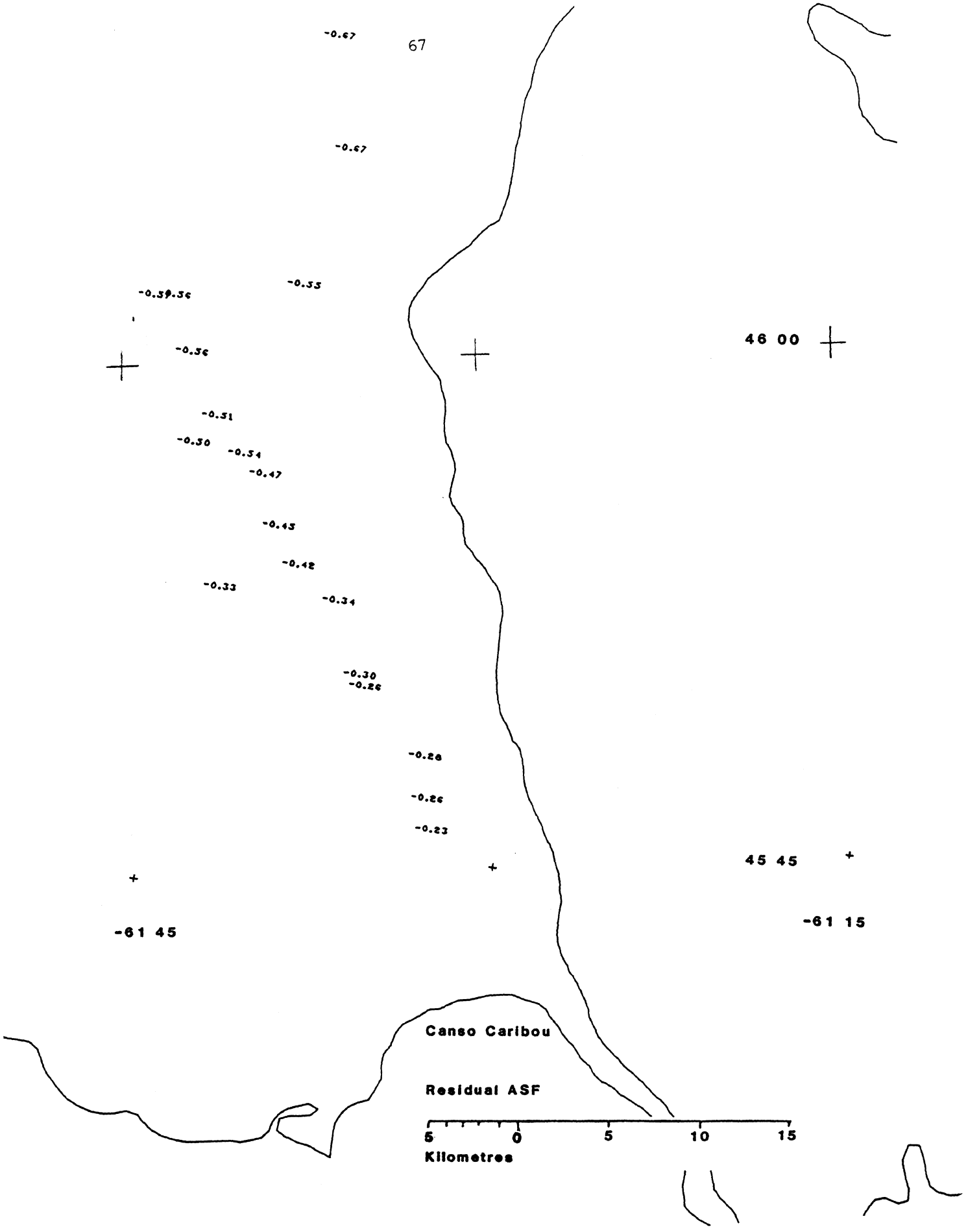
-0.67
-0.67
-0.55
-0.39
-0.36
-0.36
-0.51
-0.50
-0.54
-0.47
-0.45
-0.42
-0.33
-0.34
-0.30
-0.26
-0.28
-0.26
-0.23
46 00
45 45
-61 45
-61 15
Canso Caribou
Residual ASF
5 0 5 10 15
Kilometres

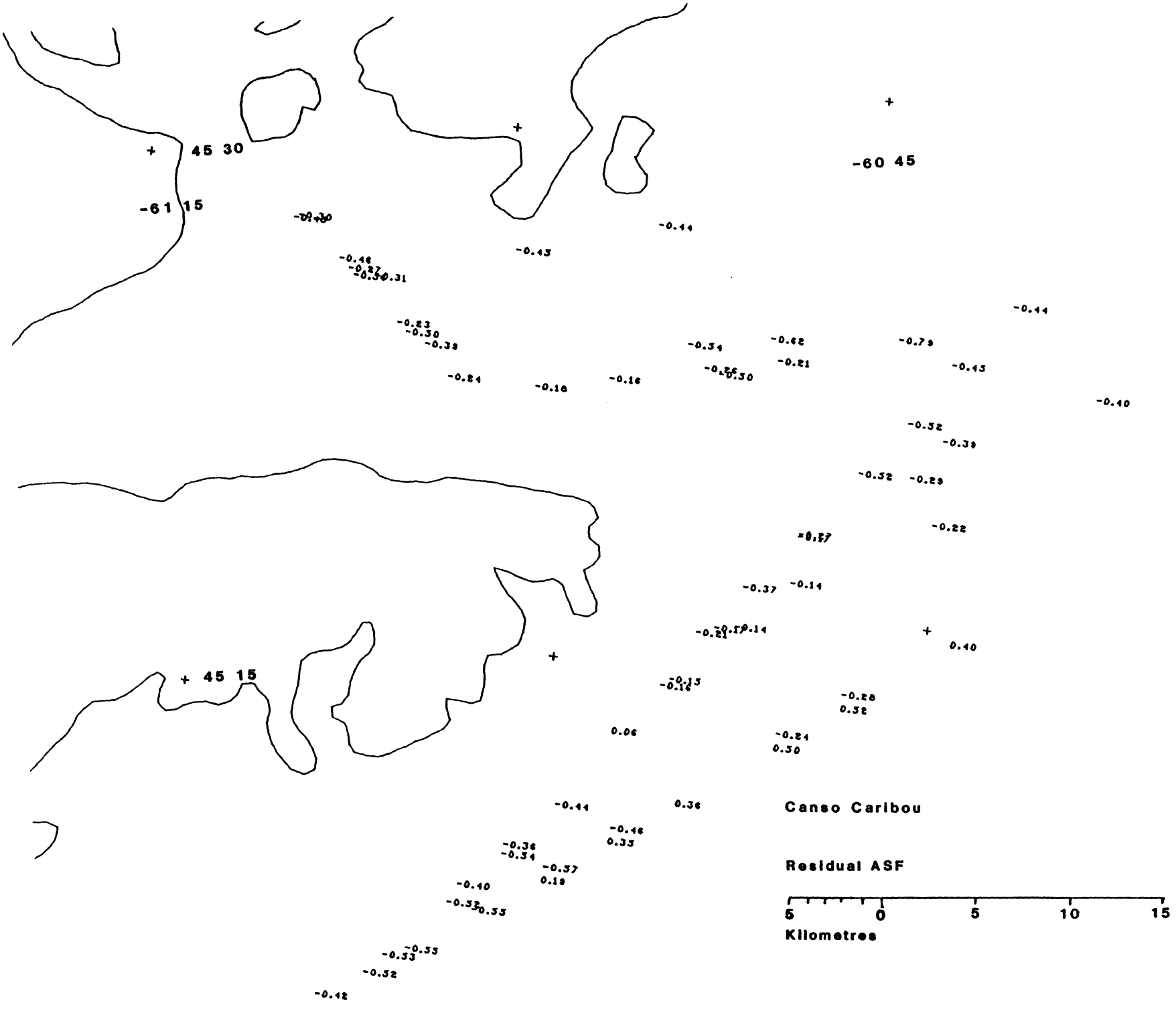
45 30
-61 15
-60 45
45 15
Canso Caribou
Residual ASF
5 0 5 10 15
Kilometres

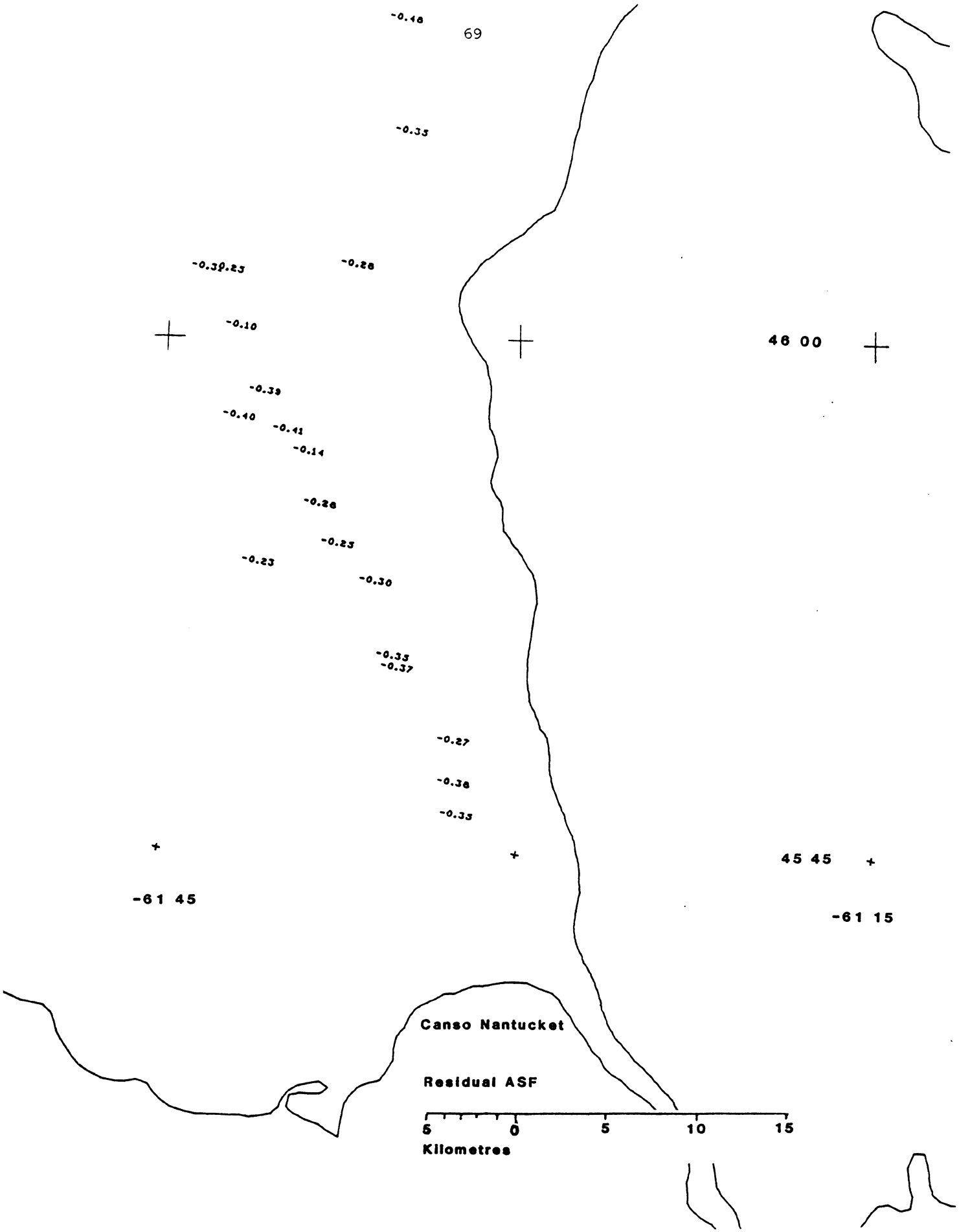
-0.48
-0.33
-0.39
-0.23
-0.28
-0.10
46 00
-0.39
-0.40
-0.41
-0.14
-0.28
-0.25
-0.23
-0.30
-0.33
-0.37
-0.27
-0.38
-0.33
45 45
-61 45
-61 15
Canso
Nantucket
Residual ASF
5
0
5
10
15
Kilometres

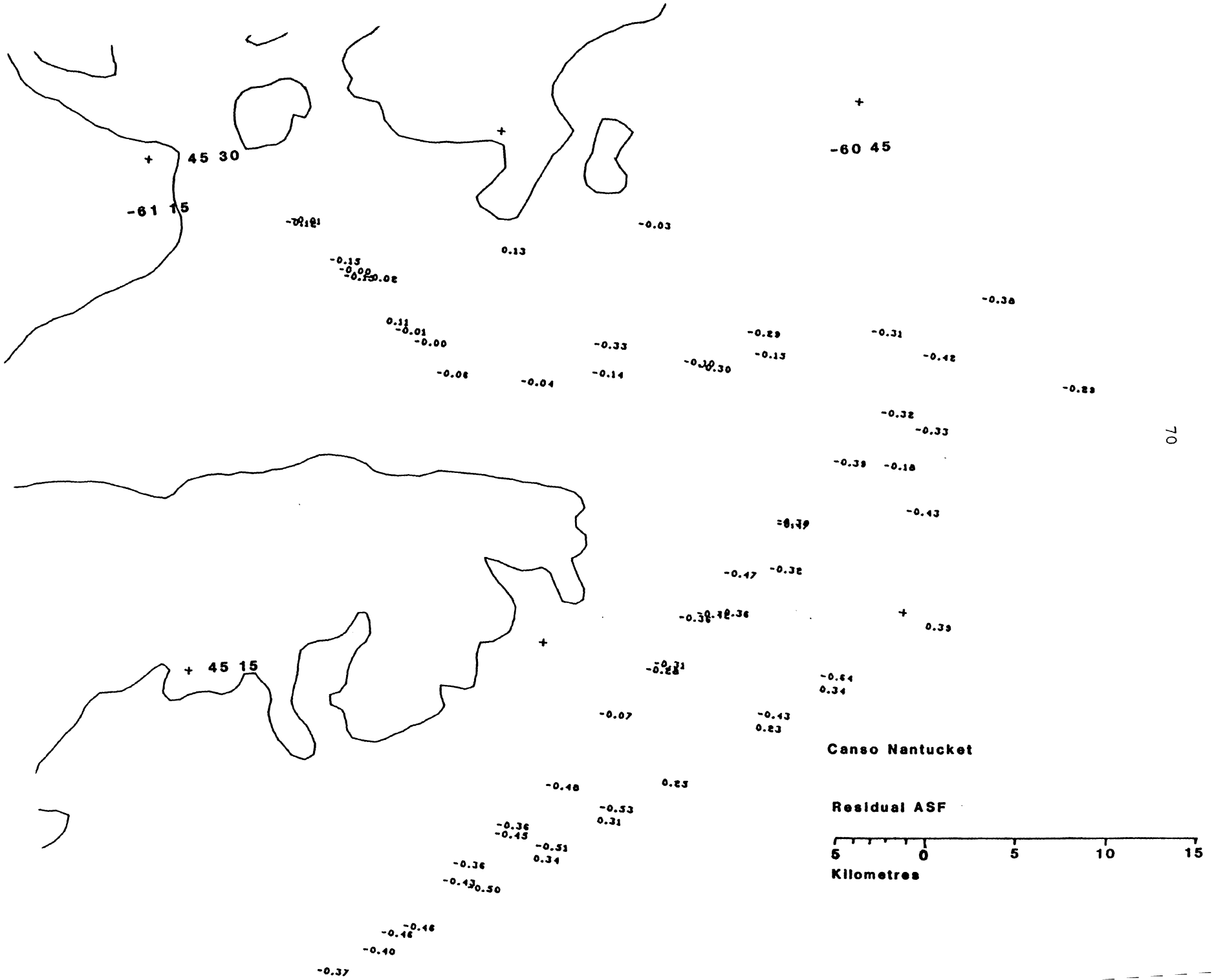
45 30
-61 15
-60 45
45 15
-0.03
0.13
-0.15
-0.33
-0.14
-0.04
-0.29
-0.31
-0.15
-0.42
-0.38
-0.28
-0.32
-0.33
-0.39
-0.18
-0.43
-0.47
-0.32
0.39
-0.64
0.34
-0.07
-0.43
0.23
-0.48
0.23
-0.53
0.31
-0.36
-0.45
-0.51
0.34
-0.36
-0.43
0.50
-0.46
-0.40
-0.37
Canso Nantucket
Residual ASF
5 0 5 10 15
Kilometres

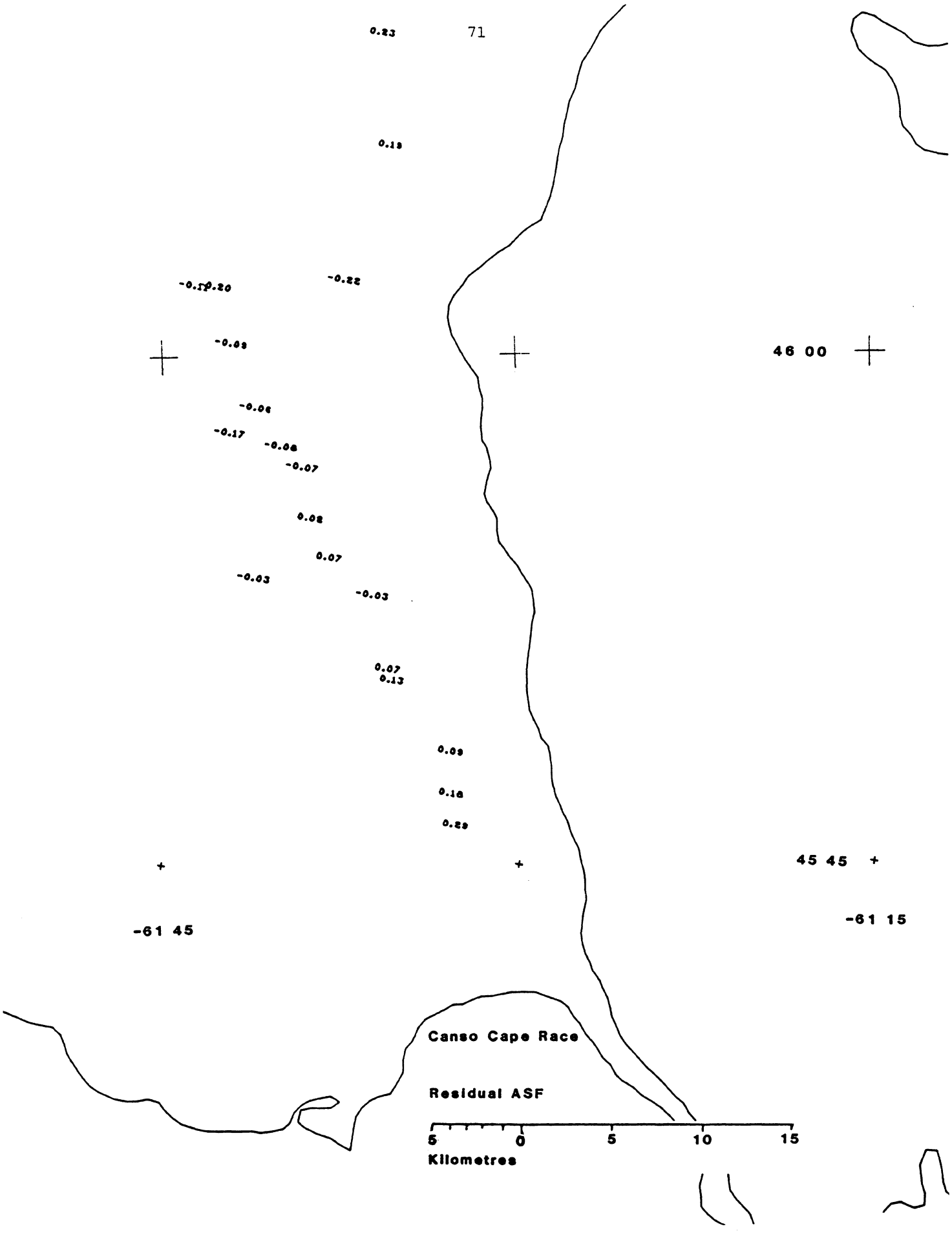
0.23
0.18
-0.22
-0.08
-0.06
-0.17
-0.08
-0.07
0.02
0.07
-0.03
-0.03
0.07
0.13
0.09
0.18
0.23
46 00
45 45
-61 45
-61 15
Canso Cape Race
Residual ASF
5 0 5 10 15
Kilometres

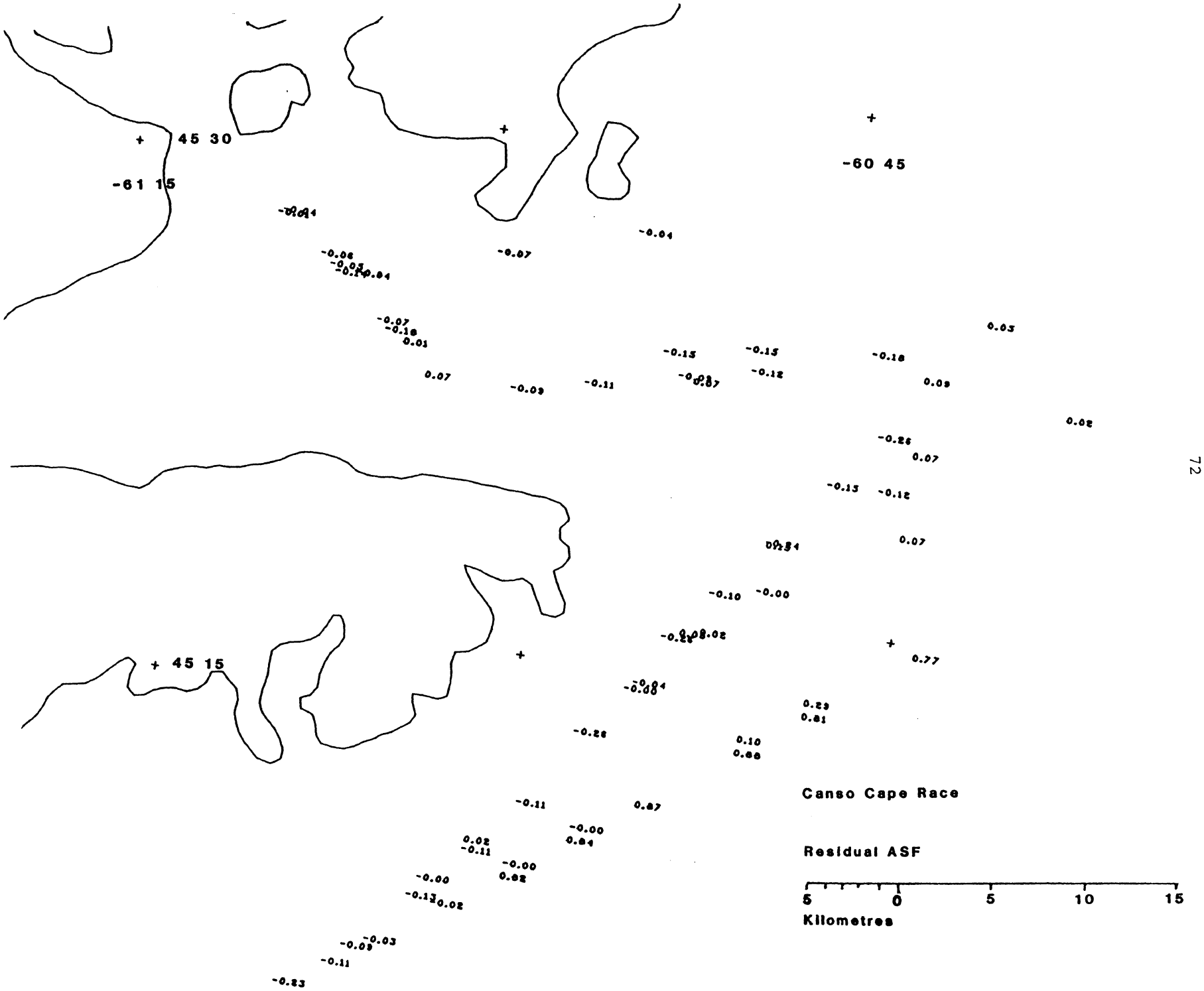
45 30
-61 15
-60 45
45 15
Canso Cape Race
Residual ASF
5 0 5 10 15
Kilometres

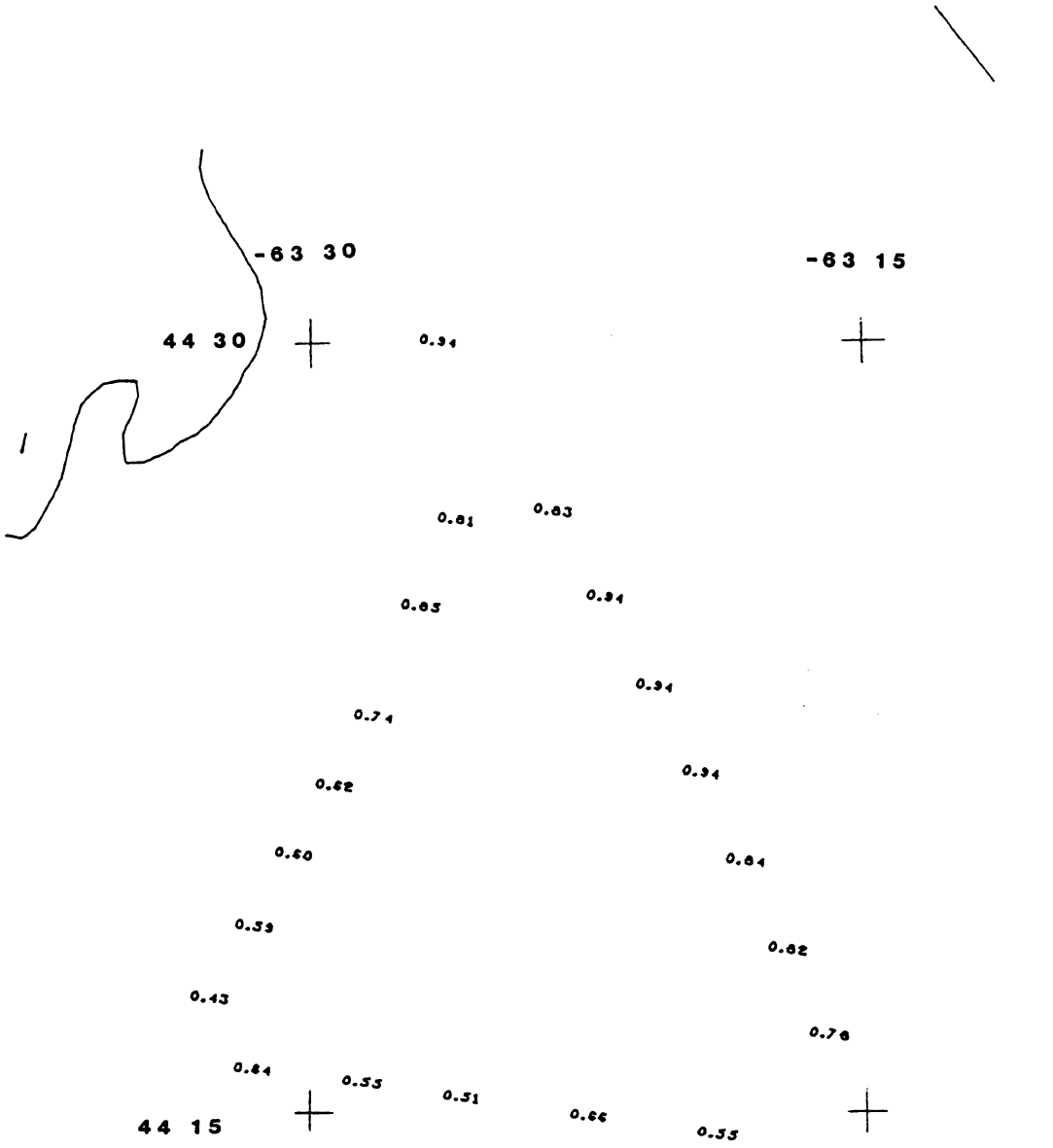
-63 30
-63 15
44 30
44 15
0.94
0.81
0.83
0.83
0.94
0.94
0.74
0.94
0.82
0.80
0.84
0.59
0.82
0.43
0.78
0.84
0.55
0.51
0.66
0.55
Halifax Caribou
Residual ASF
5
0
5
10
15
Kilometres

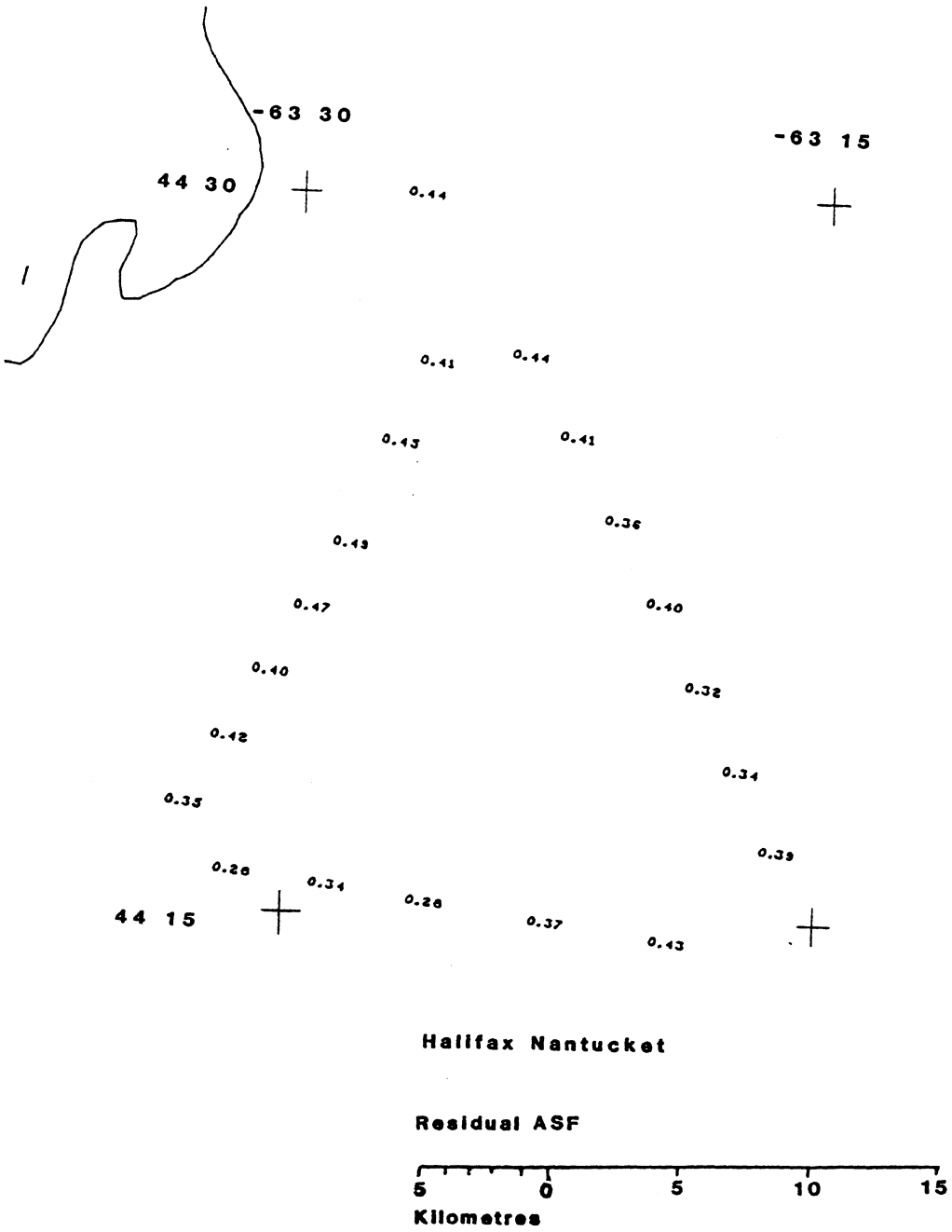
-63 30
-63 15
44 30
44 15
0.44
0.41
0.44
0.43
0.41
0.36
0.43
0.47
0.40
0.40
0.32
0.42
0.34
0.35
0.39
0.26
0.34
0.26
0.37
0.43
Halifax Nantucket
Residual ASF
5 0 5 10 15
Kilometres

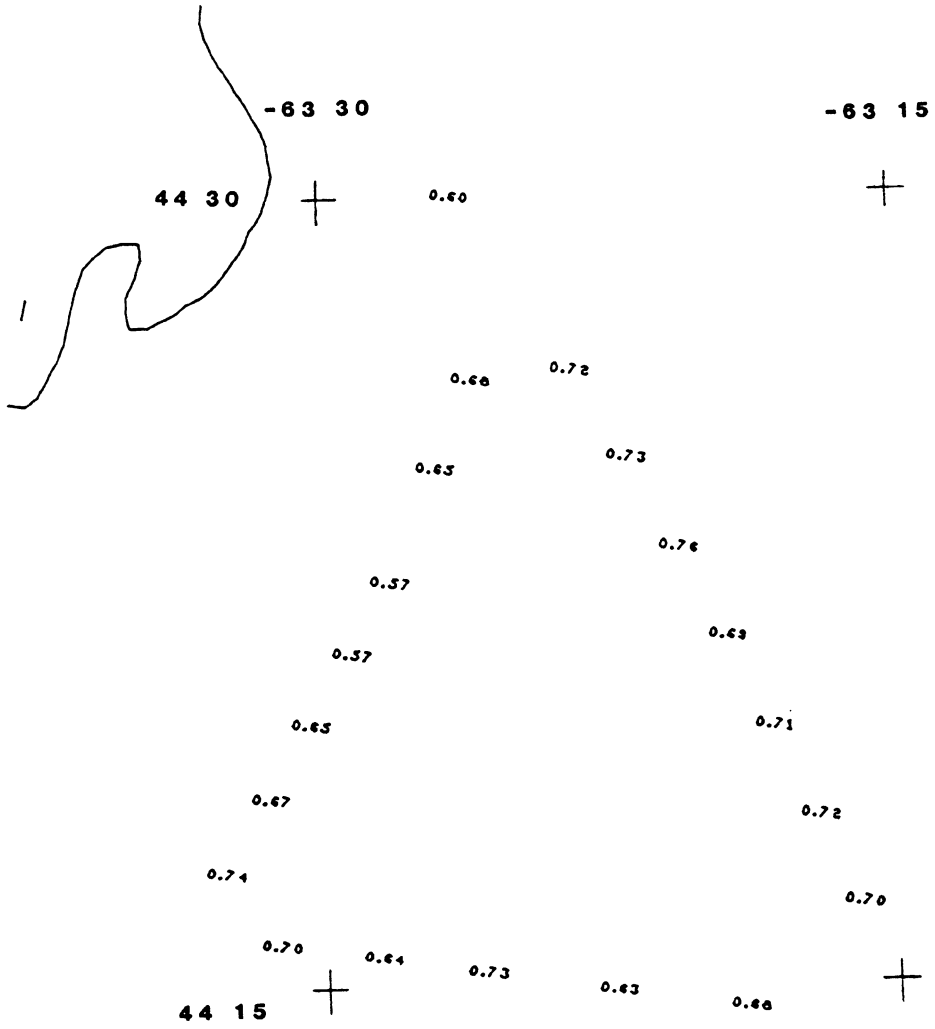

Halifax Cape Race

Residual ASF

5 0 5 10 15

Kilometres

APPENDIX IV

PLOTS OF RESIDUAL ASF
WITH LAND CONDUCTIVITY VALUES VARIED

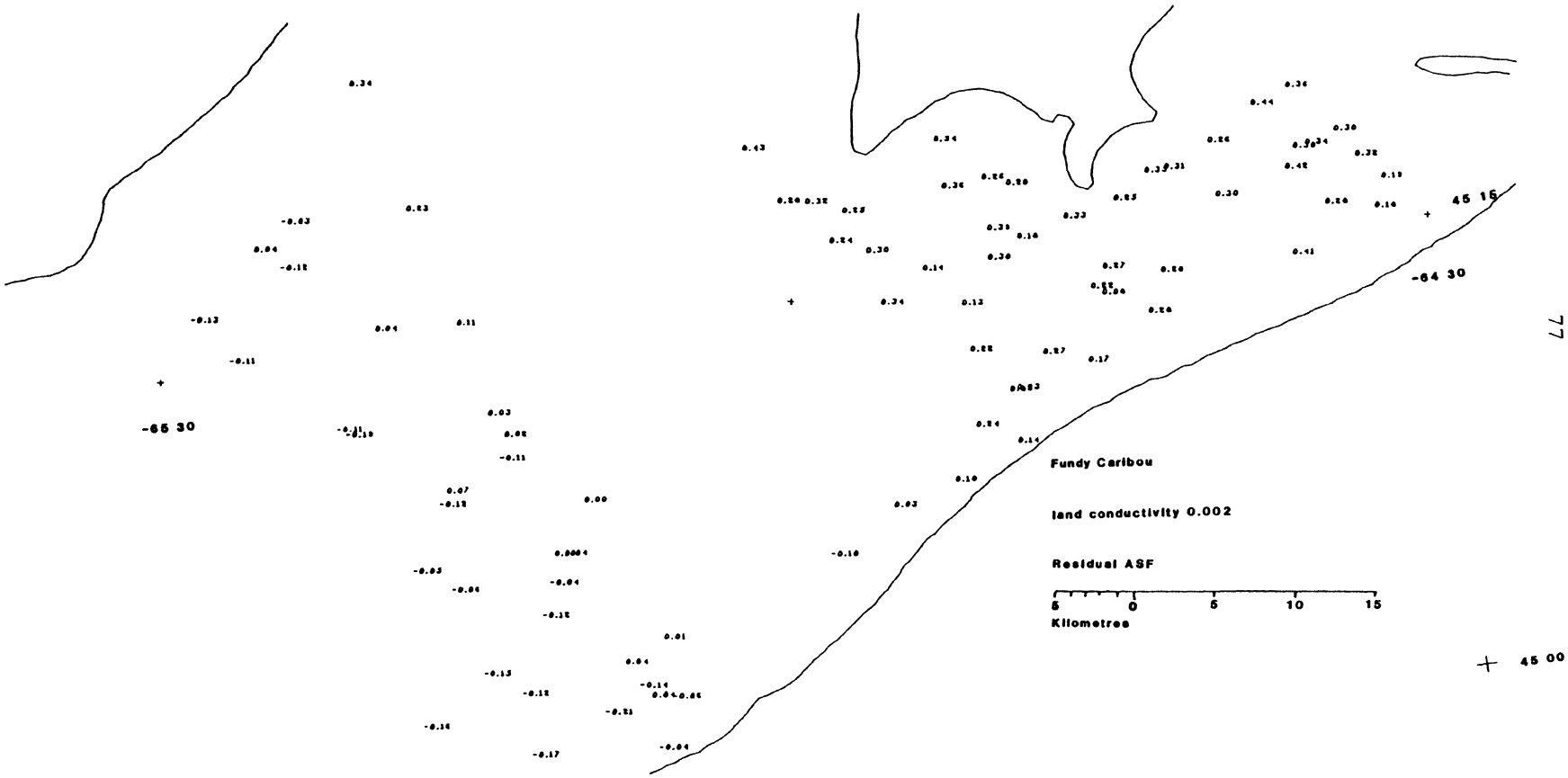
-65 30
-64 30
45 15
45 00
Fundy Caribou
land conductivity 0.002
Residual ASF
5 0 5 10 15
Kilometres

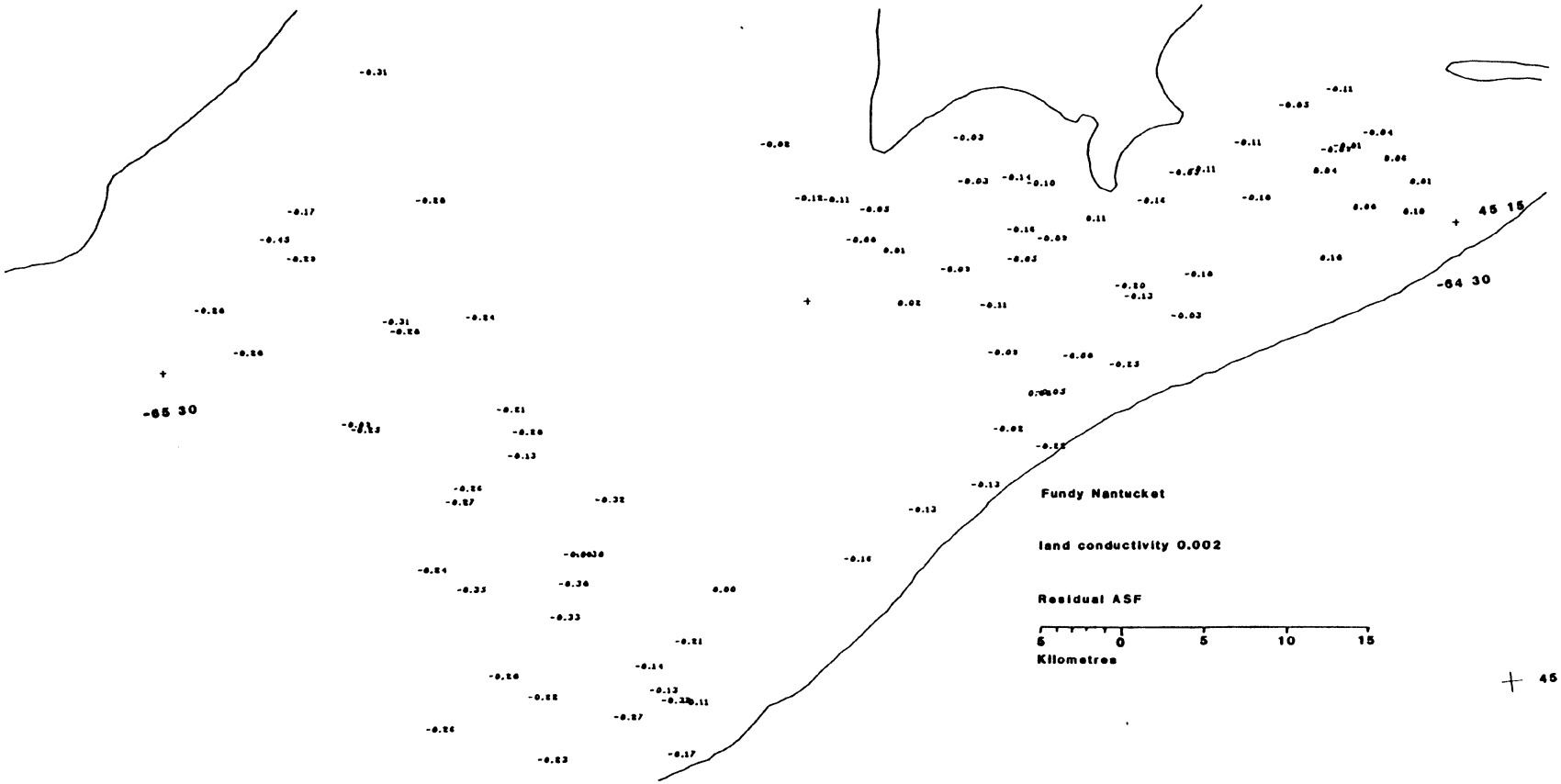
Fundy Nantucket
land conductivity 0.002
Residual ASF
5 0 5 10 15
Kilometres
-65 30
-64 30
45 15
45 00

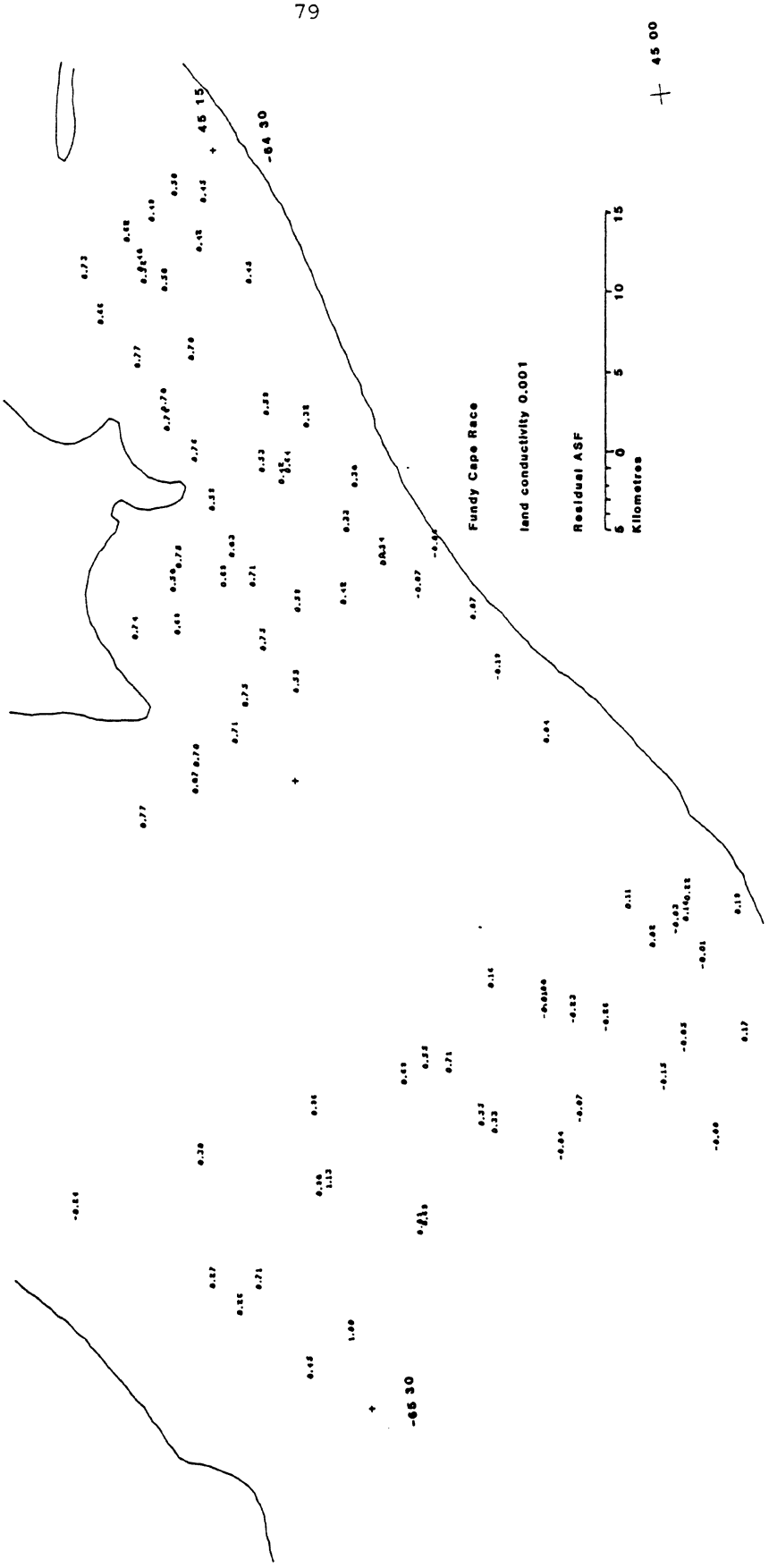
-64 30
45 15
45 00
-65 30
Fundy Cape Race
land conductivity 0.001
Residual ASF
5 0 5 10 15
Kilometres

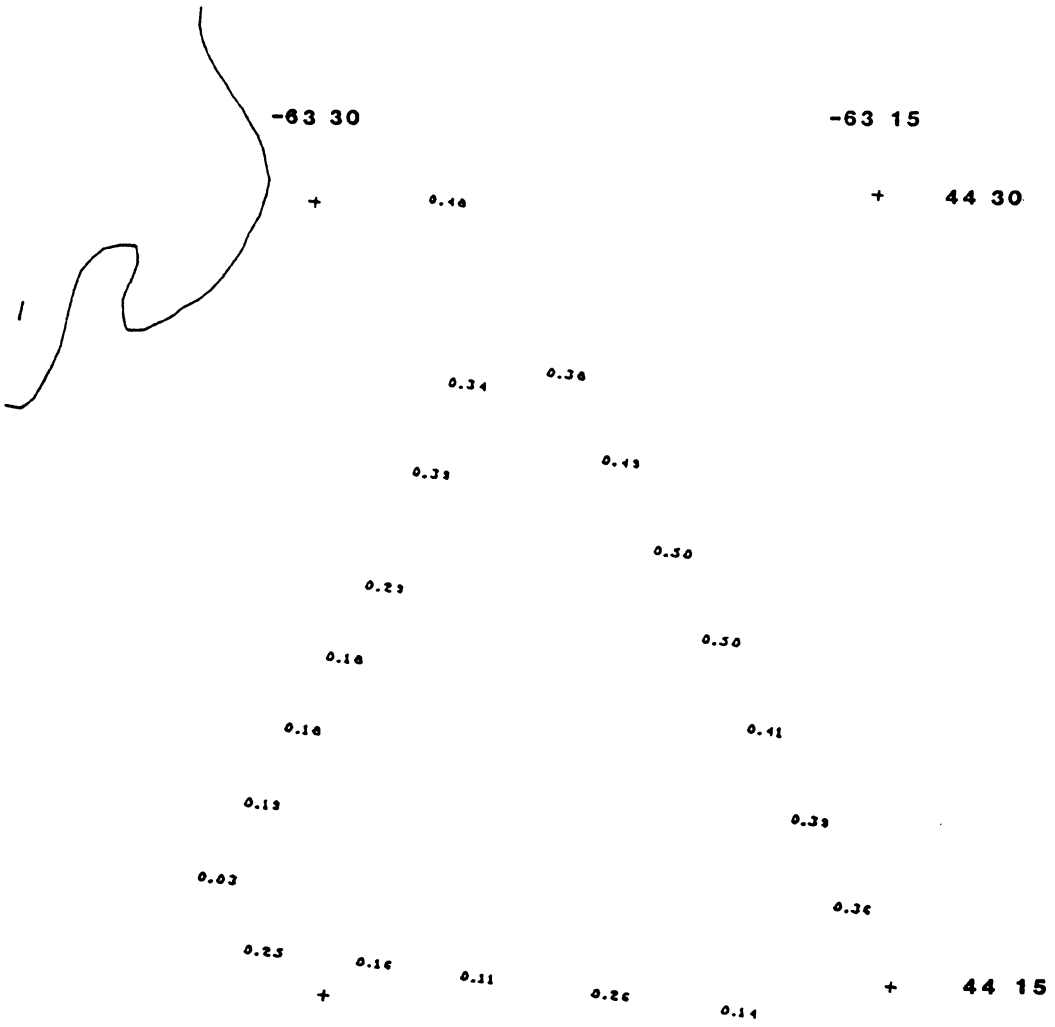

Halifax Caribou

land conductivity 0.001

Residual ASF

5 0 5 10 15

Kilometres

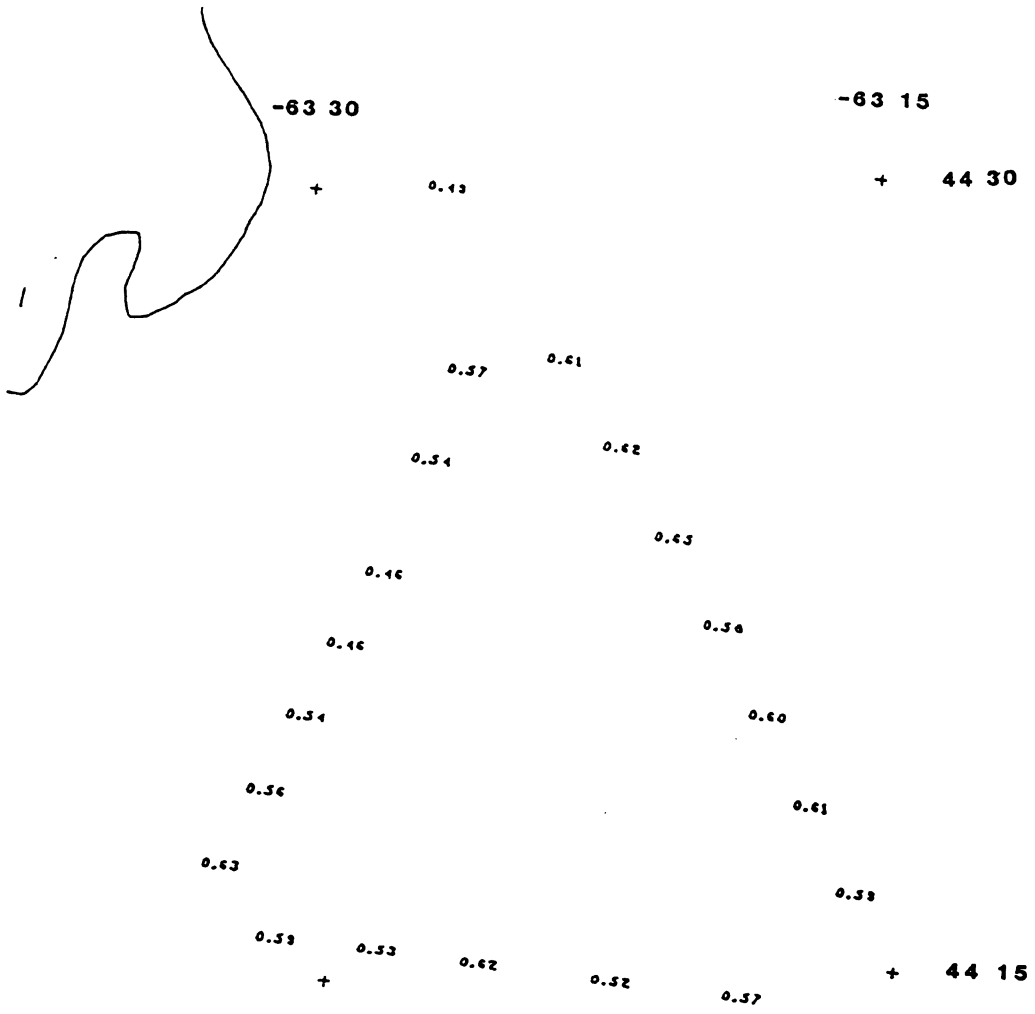

Halifax Cape Race

land conductivity 0.001

Residual ASF

5 0 5 10 15

Kilometres

APPENDIX V

82

SOME ANALYSES FOR IMPROVING LORAN-C PROPAGATION MODELLING

Heribert Kahmen

25 November 1982

1. SUMMARY

Functional and stochastic models of the total phaselag of LORAN-C signals are discussed. The parameters of these models can be determined by calibration measurements. It is shown how the calibration of LORAN-C navigation systems can be used to obtain more accurate geographic positions.

2. BASIC PRINCIPLES OF LORAN-C

LORAN-C is a pulsed, low frequency, long-range hyperbolic radio navigation system. One transmitter--the master station--transmits a group of short pulsed radio wave signals. Two or more slave stations maintain synchronization of their transmissions to the master signals. Each slave transmits a group of pulses, in a certain sequence, similar to those of the master station. Onboard the ships the signals are received and the difference in time of arrival (TOA) of the master signal and the slave signals is determined. The time difference (TD) between the received master signal and that of one of the slave signals represents a hyperbolic line of position. A LORAN-C fix can be derived from two or more time difference measurements, as the crossing point of two hyperbolic lines defines a geographical position. Special LORAN-C charts that display hyperbolic lattices are used for interpolation of the geographic position. Using specially programmed computers, the time differences can also be directly converted into geographic coordinates.

However, a LORAN-C fix can only be determined accurately if there is a mathematical model to predict the time of arrival of the signals. Different physical parameters of the earth and the atmosphere influence the propagation of the waves. Mathematical models describing the propagation effects are derived from Maxwell's equations, but there is only a rough knowledge about the physical parameters along the signal paths. Therefore, calibration measurements from independent positioning systems are used to develop some models about the behaviour of the physical parameters along the wave paths.

3. FUNCTIONAL MODELS OF THE TOTAL PHASELAG OF LORAN-C SIGNALS

The solutions of Maxwell's equations for wave propagation show propagation of LORAN-C waves is affected by the refractive index, n, its vertical gradient (represented by a parameter α), the dielectric constant, ϵ, of the earth, and the conductivity, σ, of the earth. It has been found convenient to describe the phase of the total electromagnetic field propagated by a groundwave by two terms [Johler et al. 1956]:

the primary phaselag Φ_p,

the secondary factor (SF) Φ_s.

We get the primary phaselag when we consider the field of the antenna to be in the troposphere in the absence of the earth or any other object. It is described by

$$\Phi_p = \frac{\omega}{c} n D \quad , \tag{3.1}$$

where n denotes the tropospheric refractive index; D is the distance in metres from the transmitter to the receiver; and $\omega/c = 3.3355\ 10^{-3}$ μs/m. The secondary factor [Campbell et al., 1979]

$$\Phi_s = (\frac{\omega}{c} n D)^{1/3} \alpha^{2/3} (\frac{D}{a}) \tau_o \tag{3.2}$$

accounts for the presence of the earth, with

$$\alpha = \frac{a}{a_c} = 1 + \frac{a}{n} \frac{dn}{dz}$$

where a denotes the radius of the earth, and a_c is the effective radius of the earth. The conductivity and the dielectric constant enter into τ_o through the boundary conditions at the surface of the earth. Over land the average of τ_o is of the order of and over water of the order of

The total phaselag, Φ, then can be expressed as

$$\Phi = \Phi_p + \Phi_s \quad . \tag{3.3}$$

3.1 Atmospheric Effects

The parameters n and α are a function of time and space. Maxwell's equations cannot easily be solved for propagation problems using n as a

function of the coordinates x, y, z. However, propagation problems have been solved for a few special profiles of n. Among all the possible models for LORAN-C wave propagation studies only one model is used, assuming that there is a linear variation of n with vertical height.

The surface refractive index is usually designated by the average value n = 1.000338. A change from 1.0002 to 1.0004 seems possible. Over a propagation path with a length of 1000 km that change yields a phase change of $\Delta\Phi_p$ = 0.2 μs. Normally the change over a day or during a weather change would be 0.04 μs due to a variation of 40 units of refractivity. These variations have no remarkable influence on the secondary phase correction.

There is a stronger dependence of the secondary phase correction on the lapse rate α. The graphs in Figures 3.1 and 3.2 show the importance of α.

Under extreme conditions, a change in α from 0.65 to 1.2 seems possible. Even if there is a change in α from 0.75 to 1.0, it yields a change in TOA of about 0.5 μs for travel over water and of about 1 μs for travel over land at a distance of 1000 km [Campbell et al. 1979]. Normally, however, for positioning purposes α is assumed to be a constant 0.75.

3.2 Effects of the Electrical Properties of the Earth

The electrical properties of the earth depend on the nature of the soil, its moisture content, its temperature, and the geological structure. Johler et al. [1956] developed the secondary factor to account for the disturbing influence of the earth. The electrical properties are described by the impedance being a function of the dielectric constant and the conductivity. The conductivity is the main component. Figure 3.3, derived from Johler's formulae, presents the effect of the conductivity on the phase of the secondary factor.

The value for land conductivity varies, depending on the path, from 0.0005 to 0.05. Over water normally an average value of 4.0 is assumed. Consequently paths over land are much more susceptible to propagation delay

than paths over water.

Compared with conductivity, the effects of the dielectric constant are small. Normally, one mean value over water and another over land is assumed. Figure 3.4 depicts graphically how combined land and water paths affect the secondary phaselag. There is a large increase in phaselag over land, a recovery effect beyond the land-water boundary, and a smaller increase over water.

Along composite paths, the phase distortion effect is cumulative. Empirical experiments show the phase distortion due to a composite land-water path is the average of the added phase distortions found in the forward and reverse directions. The computation method based on that knowledge is the Modified Millington's Method [Millington 1949; Bigleow 1963]. For the computation of the phase retardations formulae, described by Johler et al. [1956], approximate formulae [Brunavs 1977] or the various curves from Figure 3.3 can be used.

The use of Millington's method is hampered by several problems. The theoretical models of the phaselags have been verified for sea water paths up to distances of 500 km [Brunavs and Wells 1977]. However, some investigations show that there are larger discrepancies between the predicted and measured phase recovery near the shore when there are high mountains along the land-water boundary [Eaton et al. 1979]. There are no extensive investigations testing the theories over land. Testing over land is a difficult task, because the soil is a heterogeneous and stratified medium with an irregular surface and irregular pockets and layers of differing conductivities. In general, only rough conductivity models are known for paths over land. Besides, for very low ground conductivites the theories show a curious phenomenon: the phaselags start to decrease when conductivity tends to zero. It has not been verified whether this is a true fact or a deficiency in the presently accepted theories.

3.3 Temporal Variations of LORAN-C Propagation

Recent studies have shown that the time of arrival of LORAN-C signals varies with periods from less than a day to more than a year [Samaddar

1979; 1980; Mungall et al. 1981]. A significant degree of correlation between fluctuations in TOA or TOA differences and temperature variations could be experimentally proved. Figures 3.6, 3.7, and 3.8 show the results of some experiments of the Division of Physics, National Research Council, Ottawa [Mungall et al. 1981]. Figure 3.5 depicts the location of the LORAN-C transmitters and the observation station at Ottawa. Figure 3.6 shows the difference between two TOA signals depending on time. A change in amplitude of the fluctuations from summer to winter and an annual variation is visible. The variations correlate very closely with the air temperature, measured at Ottawa. In Figures 3.7 and 3.8 another horizontal scale is chosen to demonstrate the short periodic effects in more detail. The series of measurements verify that there are strong day-to-day correlations between TOA and temperature during freeze-up in winter. There is a zero correlation when the freeze-up period is over. These effects are larger only for paths over land.

In winter freezing of the ground is the main cause for larger changes in its dielectric and conductivity properties. During this time the refractive index of the atmosphere too will be more susceptible to fluctuations of the atmospheric parameters. Consequently the dry term of the index, being primarily temperature dependent, gets larger variations whereas the water vapour term is nearly zero due to the absolute humidity of cold air masses. During summer the dry and water vapour terms of the refractive index get temperature dependent variations of similar magnitude but opposite sign. Consequently the net change of the refractive index is approaching zero.

There have been some investigations to improve TOA measurements using the correlations between temperature and TOA fluctuations [Dean 1978; Samaddar 1980]. As a result some fundamental theories have been offered using surface weather data for additional information. At present however there is no verified general propagation model incorporating weather parameters in a realistic manner.

4. STOCHASTIC MODELS OF THE TOTAL PHASELAG OF LORAN-C SIGNALS

The refractive index, n, it's lapse rate, α, the dielectric constant, ε, and the conductivity, σ, of the ground are a function of time and space. Normally within LORAN-C theories, n, α, and ε are assumed to be constant in space and time. For σ one mean value over water and another over land is chosen. The fluctuations of the parameters around these mean values describe a stochastic process depending on space and time. Consequently the changes in Φ describe a stochastic process, depending on space and time.

4.1 Dependence of the Stochastic Models on the Parameter Time

As previously shown in Section 3.3, the time-dependent variations of LORAN-C have a diurnal as well as a seasonal character. The structure of this process is depicted in Figure 4.1. The process can be described by the linear model

$$\Delta\underline{\Phi}(\underline{t}) = \underline{s}_1(\underline{t}) + \underline{s}_2(\underline{t}) + \underline{f}_1(\underline{t}) + \underline{f}_2(\underline{t}) \quad , \tag{4.1}$$

where $\underline{s}_1(\underline{t})$ and $\underline{s}_2(\underline{t})$ denote the non-deterministic part of the process, and $\underline{f}_1(\underline{t})$ and $\underline{f}_2(\underline{t})$ the deterministic part.

$\underline{s}_1(\underline{t})$ is a short-periodic process influenced by the diurnal variations of the parameters and the changes caused by weather fronts. $\underline{s}_2(\underline{t})$ is a long-periodic random process, affected by the seasonal changes of the parameters. For one signal $\underline{s}_1(\underline{t}) \equiv \underline{s}_1$ we can assume:

$$E\{\underline{s}_1\} = 0 \quad , \tag{4.2}$$

$$E\{\underline{s}_1\ \underline{s}_1^T\} = \sigma_d \exp(-a_d^2\tau^2) \cos \omega_d\tau = r_d(\tau) \quad , \tag{4.3}$$

where σ_d^2 is the variance, τ describes the time difference between the individual measurements, a_d is a constant, and ω_d equals 1 cycle a day. For one signal $\underline{s}_2(\underline{t}) \equiv \underline{s}_2$ we can assume:

$$E\{\underline{s}_2\} = 0 \quad , \tag{4.4}$$

$$E\{\underline{s}_2\ \underline{s}_2^T\} = \sigma_s \exp(-a_s^2\tau^2) \cos \omega_s\tau = r_s(\tau) \quad , \tag{4.5}$$

where σ_s is the variance, a_s is a constant, and ω_s equals 1 cycle a year.

Assuming the two random signals, $\underline{s}_1$ and $\underline{s}_2$ to be independent, and neglecting that σ_d has different magnitudes during summer and winter, we find (see Figure 4.2):

$$r(\tau) = r_d(\tau) + r_s(\tau) \quad . \tag{4.6}$$

We get further insight into the estimation of variances when we consider variances as a function of their frequencies. The variance spectrum s(f) of fluctuations is given by the transformation

$$s(f) = \int_{-\infty}^{+\infty} r(\tau)\, e^{-2\pi i f\tau}\, d\tau \quad , \tag{4.7}$$

where f is the frequency of the fluctuations. s(f) has the dimension of a variance per frequency. When calculating the ordinates by $f \cdot s(f)$ and the abscissa by lnf, we get a graph which shows the variances as a function of the frequencies

$$\sigma^2 = \int_{-\infty}^{+\infty} s(f)\, df = \int_{-\infty}^{+\infty} f \cdot s(f)\, d\,\mathrm{ln}f \quad , \tag{4.8}$$

where

$$\frac{d\mathrm{ln}f}{df} \cdot df = \frac{1}{f}\, df \quad . \tag{4.9}$$

Figure 4.3 shows a $f \cdot s(f)$ - lnf graph, calculated by (4.6). Furthermore, (4.8) demonstrates that we cannot get the total variance when measurements are made over a limited period of time. At least a series of measurements for several years should be available.

4.2 Dependence of the Stochastic Models on Distance

The secondary factor (SF) of the LORAN-C ground waves mainly depends on the parameter τ_o, representing the impedance of the surface.

Consequently with (3.2) and the laws of error propagation [Dreszer 1975], the variance of the SF can be estimated by

$$\sigma^2_{SF}(D) = [(\frac{\omega}{c} n D)^{1/3} \alpha^{2/3} (\frac{D}{a})]^2 \int_0^s \int_0^s r_{\tau_o \tau_o}(D' D'') \, dD' \, dD'' \qquad (4.10)$$

where $r_{\tau_o \tau_o}$ is the covariance function of τ_o depending on distance.

Equation (4.10) shows we could estimate the variance if the covariance function $r_{\tau_o \tau_o}$ were known.

5. TOA AND TD CALIBRATION

A LORAN-C fix is obtained from two or more time difference readings. The time differences can be converted into geographic coordinates when plotted on a special LORAN-C chart. In recent years, besides charts, specially programmed computers have been used to obtain the LORAN-C fixes directly. The methods are based on (3.1) and (3.2) and Millington's method. The signals are assumed to propagate only over water paths with an assumed constant conductivity.

The plotted or computed values will differ from the observed ones because of the mixed propagation path of the transmitted signal. Water masses and various types of land masses influence the propagation of the signals. Therefore calibration measurements should be done.

The calibrations are based on LORAN-C TOA measurements and position fixing using SATNAV and other high precision range-range systems as the position reference. From position fixing the geodetic distances between the observation points and the transmitter are obtained. With these, TOA values can be predicted. Then each measured TOA can be judged against the predicted value and a chain can be analysed prior to the stations which are transmitting.

Comparing computed and observed values and using geological information, mean conductivity values can be assigned to the different land segments [Brunavs 1980]. In general, the conductivity model of a LORAN-C chain is derived from about 15 to 20 calibration measurements.

Using those conductivity models, corrections (additional secondary factors (ASF)) can be computed for one station from the forward and reverse solution of Millington's method. Finally $(ASF)_{diff}$ corrections for the time difference for a master-slave transmitting station have to be computed:

$(ASF)_{diff}$ - corrections = (master correction) - (slave correction).

The corrections for the time differences can be computed if the ASF corrections of each transmitter are arranged into a matrix with regularly spaced intervals of latitude, ϕ, and longitude, λ. As well these grids can be easily used to contour corrected hyperbolic lattices.

There are two ways to compute these gridded ASF. First, Millington's method can be directly used to get the corrections along the regularly spaced ϕ- and λ-intervals. The second method is more computer-compatible and has to be done in two steps. The first step would be to compute corrections in an azimuthal array. This array consists of a series of geodetic azimuths, where the corrections are computed at incremented distances along each azimuth. Then in a second step this array has to be rearranged by interpolation into a matrix with regularly spaced intervals of latitude and longitude.

For interpolation, different methods can be used. A very efficient method is given when least squares collocation is used to interpolate the grid points. However, this method is very expensive in computation time.

The physical model, however, describing the conductivity values over land is only a very general one. Therefore a simpler model should be used to interpolate the grid points. An equally spaced grid of the ASF can easily be interpolated by a moving surface-modelling function. This method is computer-compatible and leads to simple methods to analyse for erroneous data. The following function in longitude and latiitude may be chosen:

$$c = \sum_{k=0}^{n} \sum_{i+j=k} a_{ij} \lambda^i \phi^j \qquad (5.1)$$

where

a_{ij} = coefficients of the polynomial,
n = degree of the polynomial.

If n=0, we get a horizontal plane; with n=1 we get a tilted plane, and finally n=2 leads to a surface of degree 2 and so forth. Using least squares methods we get the observation equations:

$$\sum_{k=0}^{n} \sum_{i+j=k} a_{ij} \lambda^i \phi^i = c + v \qquad (5.2)$$

with the weighting function

$$p = \frac{1}{s^m} \quad , \qquad (5.3)$$

where

s = distance between the position of the interpolated point and the position of the correction value,

m = 0, 1, 2,....

In matrix notation the error equations have the form

$$\underline{Ax} = \underline{\ell} + \underline{v} \quad . \qquad (5.4)$$

Then, as is generally known, the normal equations are described by

$$\underline{A}^T \underline{C}_{\ell}^{-1} \underline{Ax} = \underline{A}^T \underline{C}_{\ell}^{-1} \underline{\ell} \quad . \qquad (5.5)$$

As (5.3) shows, the covariance matrix is a diagonal matrix. p becomes infinite if the interpolated point has the same position as the correction value. Then the surface of the modelling function goes through the correction value.

It has to be determined which data points are to be included in the determination of the surface-modelling function. A radius can be defined so that all data within this radius about each grid point have been included. Trial computations with a given array of data will finally show which radius has to be chosen. Probably only the nearest correction values around the interpolation point are needed. Then a moving pattern consisting of eight octogons (Figure 5.1) can help to select these points.

There are test criteria available to decide which degree of the surface-modelling function is suitable. The first criterion is the standard deviation of the estimated corrections at the grid points, and the

second is the correlation coefficient which describes the distribution of the data points with respect to the reference grid points.

To verify that the gridded ASF represent the data, the data have to be compared back to the grid. To accomplish this the moving surface-modelling function can also be used to interpolate ASF at the data points. Then the differences can be used to compute two-dimensional signal covariance functions in order to study the stochastic characteristics of the residuals.

6. ASF CORRECTED CHARTS

If instead of ASF corrections, TOA grids and finally TD grids are predicted using the models described in Chapter 5, then ASF corrected hyperbolic lattices can be contoured on charts. Data points of the corrected lattices have to be interpolated along the grid lines. Then, finally, corrected hyperbolic lattices can be plotted using cubic splines or polynomial approximations.

7. REFERENCES

Bigelow, H.W. (1963). "Electronic surveying: Accuracy of electronic positioning systems." Proceedings of the American Society of Civil Engineers, Journal of the Surveying and Mapping Division, October, p. 37-76. Reprinted in a supplement to the International Hydrographic Review, Vol. 6, pp. 77-112, September 1965.

Brunavs, P. (1977). "Phase lags of 100 GHz radiofrequency ground wave and approximate formulas for computation." Unpublished paper, Canadian Hydrographic Service, Ottawa.

Brunavs, P. (1980). "Predicted versus observed phase lags of LORAN-C maritime inshore areas." Contract report, Canadian Hydrographic Service, Ottawa, March.

Brunavs, P. and D.E. Wells (1971). "Accurate phase lag measurements over seawater using Decca Lambda." Department of Energy, Mines and Resources, Marine Sciences Branch, Report No. AOL 1971-2.

Campbell, L.W., R.H. Doherty and J.R. Johler (1979). "LORAN-C system dynamic model temporal propagation variation study." U.S. Department of Transportation, Report No. DOT-CG-D57-79, Washington.

Dean, W.N. (1978). "Diurnal variations in LORAN-C groundwave propagation." Proceedings of the Ninth Annual Precise Time and Time Interval (PTTI) Applications and Planning Meeting, Goddard Space Flight Center, Nov-Dec 1977. NASA Technical Memorandum 78104.

Dreszer, J. (1975). Mathematik-Handbuch fur Technik und Naturwissenschaft. Leipzig VEB-Fachbushverlag.

Eaton, R.M., A.R. Mortimer and D.H. Gray (1979). "Accurate chart latticing for LORAN-C." International Hydrographic Review, LVI(1):

Johler, J.R., W.J. Kellar and L.C. Walters (1956). "Phase of the low radio frequency ground wave." U.S. National Bureau of Standards, Circular 573, Washington.

Millington, G. (1949). "Groundwave propagation over an inhomogeneous smooth earth." Proceedings of the IEE, 96, Part III.

Mungall, A.G., C.C. Costain and W.A. Ekholm (1981). "Influence of temperature-correlated Loran-C signal propagation delays on international timescale comparisons. Metrologia, Vol. 17, pp. 91-96.

Samaddar, S.N. (1979). "The theory of LORAN-C groundwave propatation--A review." Navigation, Vol. 26, No. 3, Fall.

Samaddar, S.N. (1980). "Weather effect on LORAN-C propagation." Journal of the (U.S.) Institute of Navigation, Vol. 27, No. 1, pp. 39-53.

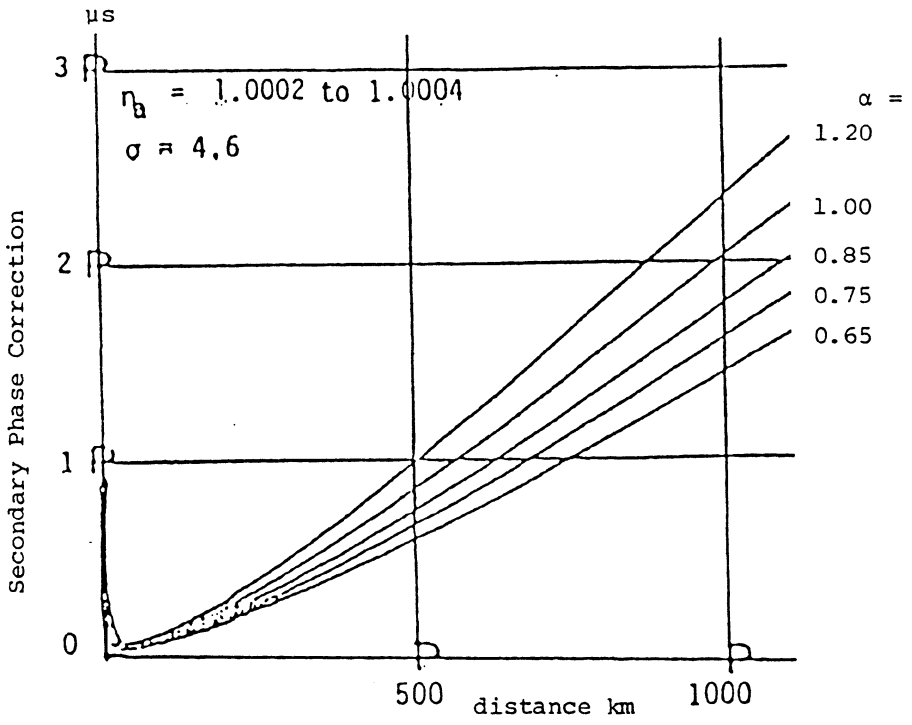

FIGURE 3.1

Secondary Phase Correction as a Function of Distance for Various Atmospheric Lapse Factors α and Ground Conductivity σ = 4.6 [Campbell et al.]979].

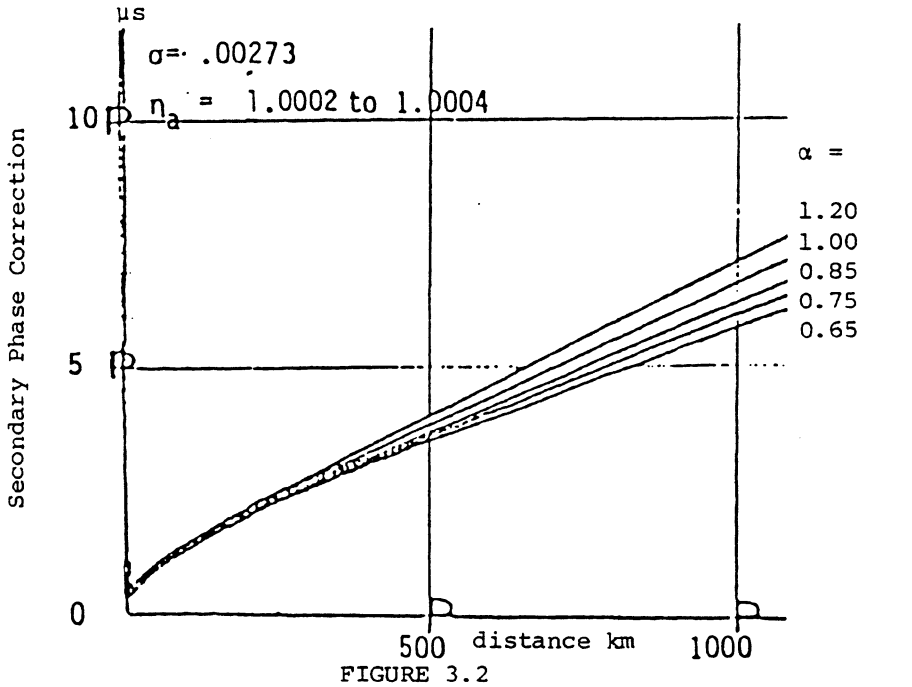

FIGURE 3.2

Secondary Phase Correction as a Function of Distance for Various Atmospheric Lapse Factors α and Ground Conductivity σ = .00273 [Campbell et al.]979].

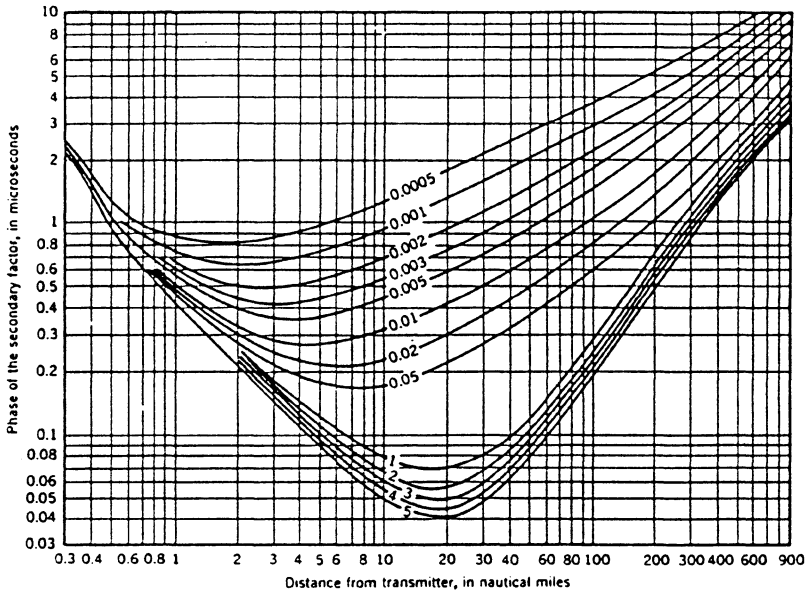

FIGURE 3.3

Phase of Secondary Factor for Selected Conductivities.

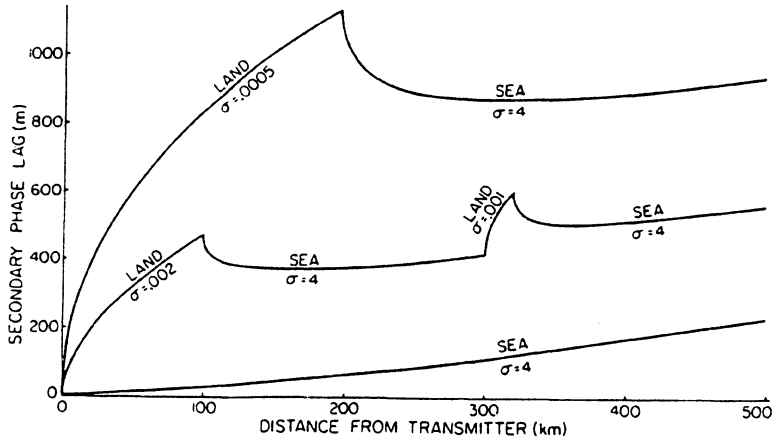

FIGURE 3.4

Phase of Secondary Factor for Mixed Land-Sea Paths.

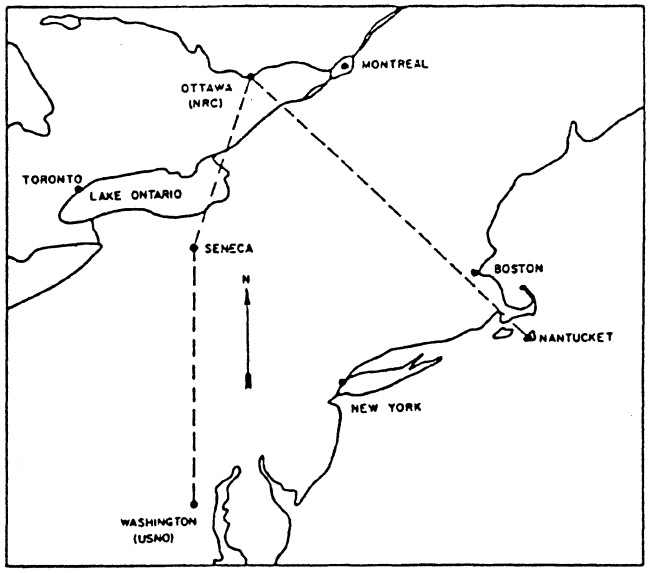

FIGURE 3.5

Map Showing Locations of Ottawa, Washington, and the LORAN-C Stations at Seneca and Nantucket [Mungall et al.1981].

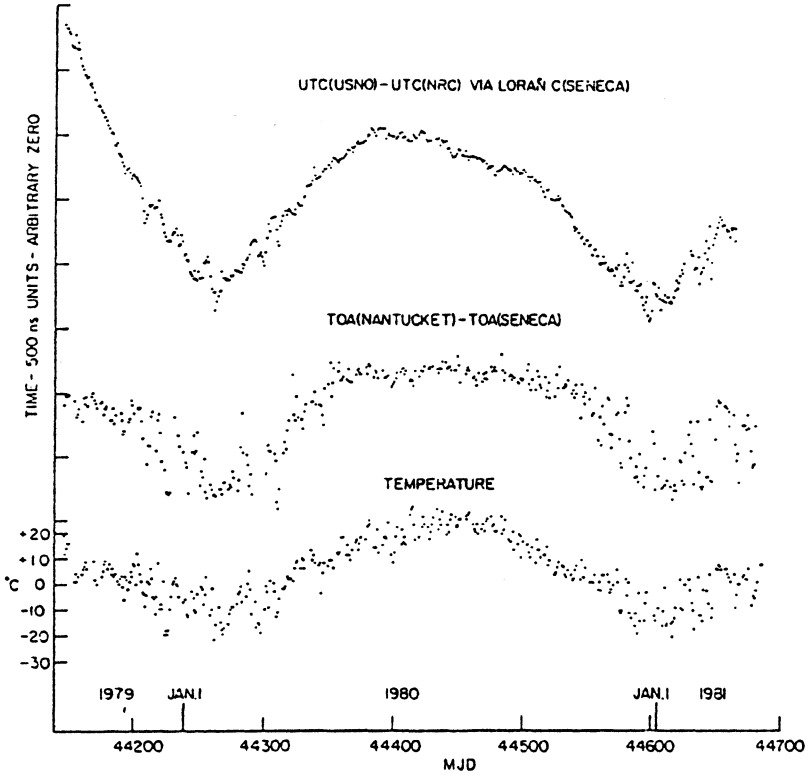

FIGURE 3.6

Correlation with Temperature of the Difference in TOA for LORAN-C Signals Received at Ottawa (NRC) from Nantucket and Seneca [Mungall et al.1981].

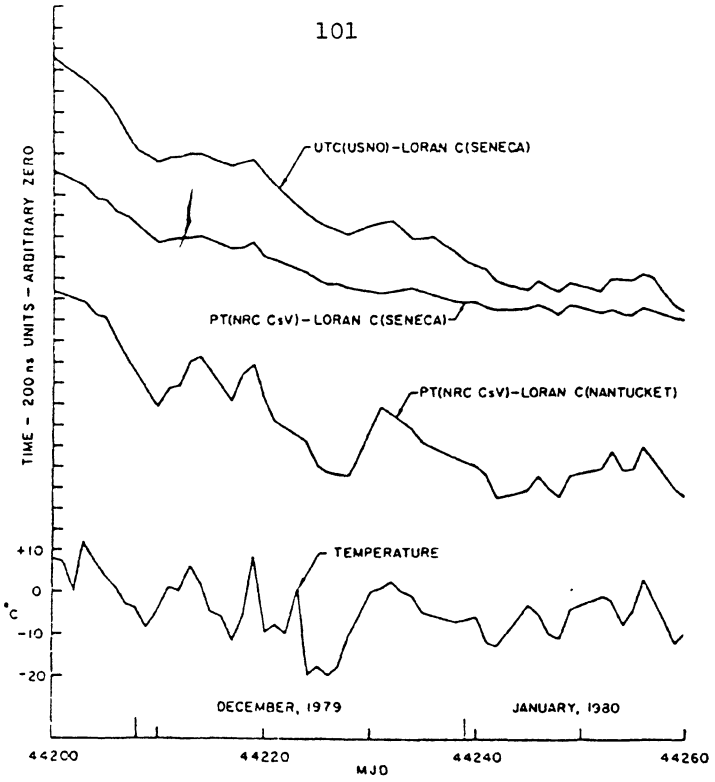

FIGURE 3.7

Correlation with Temperature During Freeze-up, 1979, of Ottawa (NRC) Measurements of the LORAN-C Signals from Seneca and Nantucket and of Washington (USNO) Measurements of those from Seneca [Mungall et al. 1981].

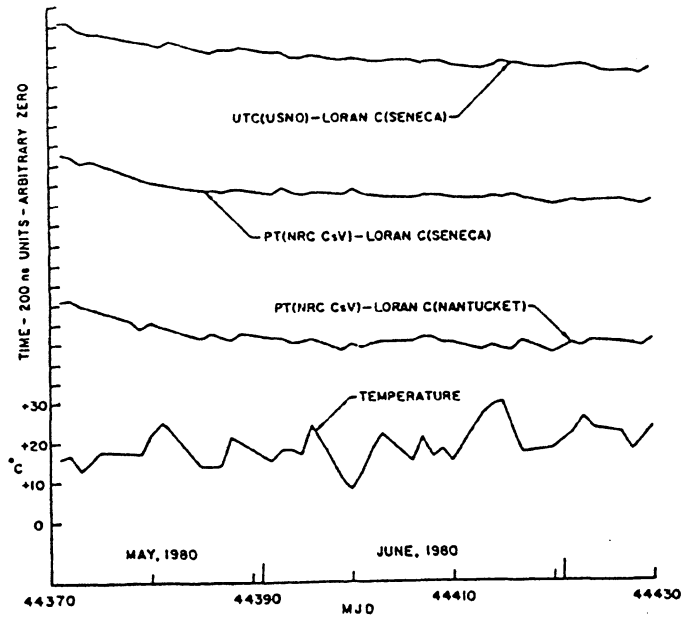

FIGURE 3.8

Correlation with Temperature During Summer, 1980, of Ottawa (NRC) Measurements of the LORAN-C Signals from Seneca and Nantucket, and of Washington (USNO) measurements of those from Seneca [Mungall et al. 1981].

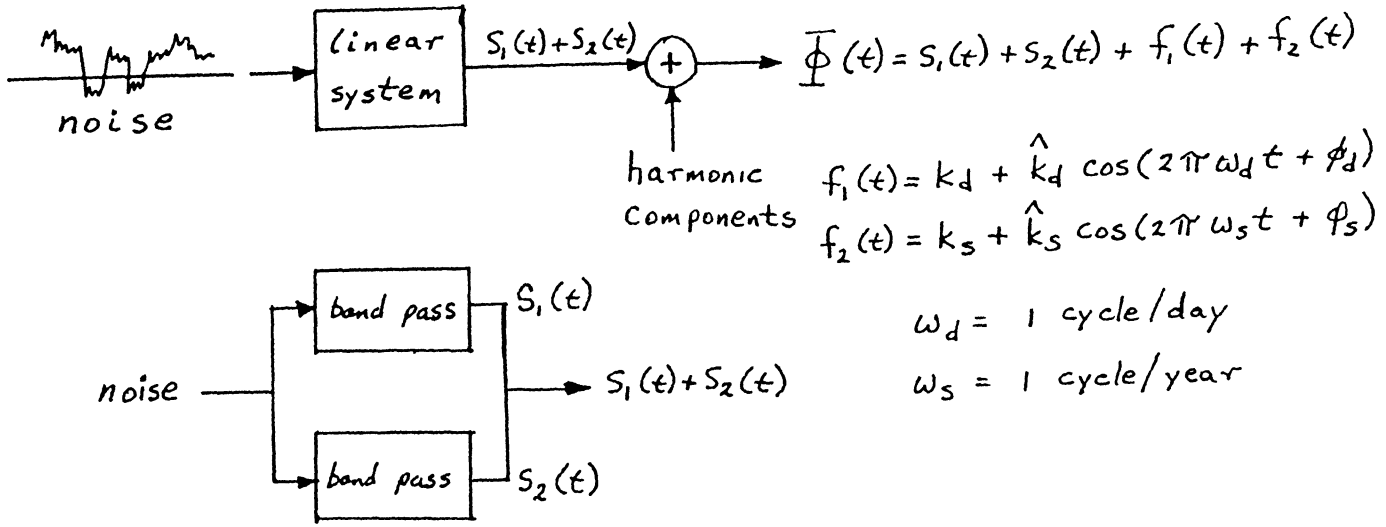

FIGURE 4.1

Structure of the Process of the Total Phaselags of LORAN-C Signals.

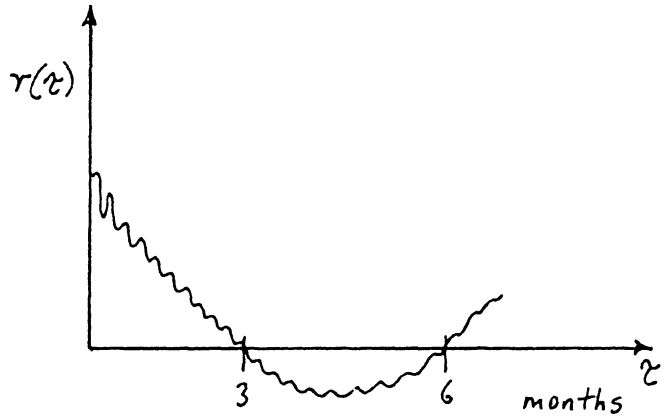

FIGURE 4.2

Correlation Function of the Process of the Total Phaselags of LORAN-C Signal.

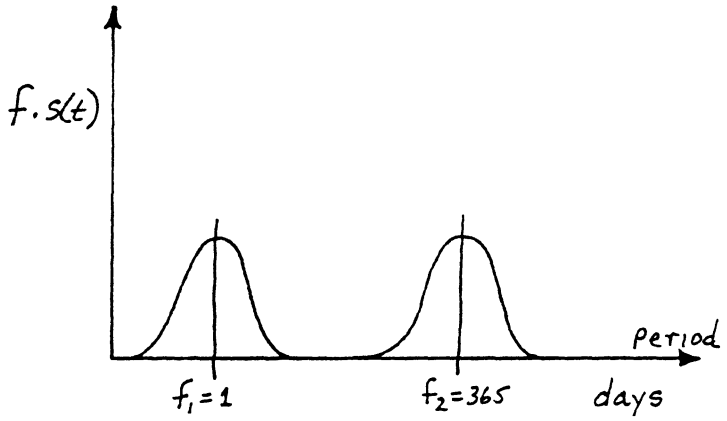

FIGURE 4.3

Variances of the Total Phaselags of LORAN-C Signals as a Function of the Frequencies.

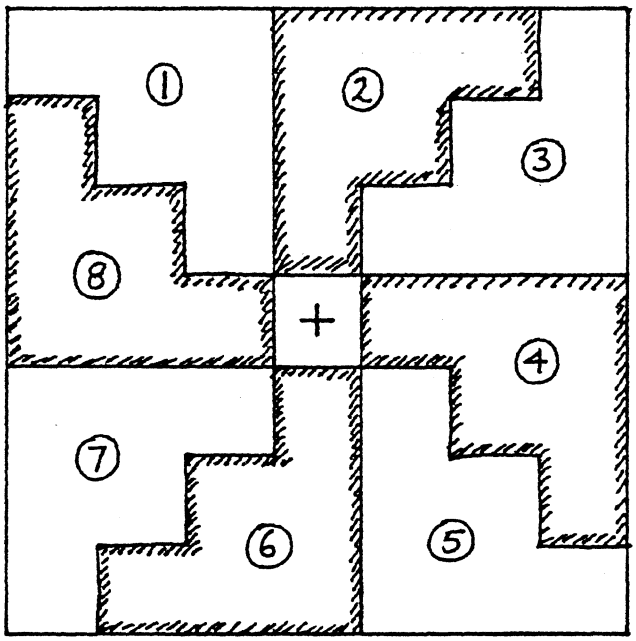

FIGURE 5.1

Moving Octogons.